INFORMATION TO USERS

This manuscript has been reproduced from the microfilm master. UMi films the text directly from the original or copy submitted. Thus, some thesis and dissertation copies are in typewriter face, while others may be from any type of computer printer.

The quality of this reproduction is dependent upon the quality of the copy submitted. Broken or indistinct print, colored or poor quality illustrations and photographs, print bleedthrough, substandard margins, and improper alignment can adversely affect reproduction.

In the unlikely event that the author did not send UMI a complete manuscript and there are missing pages, these will be noted. Also, if unauthorized copyright material had to be removed, a note will indicate the deletion.

Oversize materials (e.g., maps, drawings, charts) are reproduced by sectioning the original, beginning at the upper left-hand corner and continuing from left to right in equal sections with small overlaps.

Photographs included in the original manuscript have been reproduced xerographically in this copy. Higher quality 6" x 9" black and white photographic prints are available for any photographs or illustrations appearing in this copy for an additional charge. Contact UMI directly to order.

UMI®

University of Alberta

Interactions of Human Skin Fibroblasts with Titanium

By

Kalal Derhami　ⓒ

A thesis submitted to the Faculty of Graduate Studies and Research in partial fulfillment
of the requirements for the degree of Doctor of Philosophy

Medical Sciences-Oral Health Sciences

Edmonton, Alberta

Fall 2000

The author has granted a non-exclusive licence allowing the National Library of Canada to reproduce, loan, distribute or sell copies of this thesis in microform, paper or electronic formats.

The author retains ownership of the copyright in this thesis. Neither the thesis nor substantial extracts from it may be printed or otherwise reproduced without the author's permission.

L'auteur a accordé une licence non exclusive permettant à la Bibliothèque nationale du Canada de reproduire, prêter, distribuer ou vendre des copies de cette thèse sous la forme de microfiche/film, de reproduction sur papier ou sur format électronique.

L'auteur conserve la propriété du droit d'auteur qui protège cette thèse. Ni la thèse ni des extraits substantiels de celle-ci ne doivent être imprimés ou autrement reproduits sans son autorisation.

0-612-59577-3

Canadä

University of Alberta

Library Release Form

Name of Author: Kalal Derhami

Degree: Doctor of Philosophy

Year this Degree Granted: 2000

Permission is hereby granted to the University of Alberta Library to reproduce single copies of this thesis and to lend or sell such copies for private, scholarly or scientific research purposes only.

The author reserves all other publication and other rights in association with the copyright in the thesis, and except as herein before provided, neither the thesis nor any substantial portion thereof may be printed or otherwise reproduced in any material form whatever without the author's prior written permission.

Kalal Derhami,
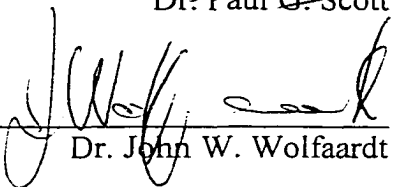#420-5125 Riverbend Rd.
T6H 5K5, Edmonton, AB.

September 27, 2000

University of Alberta
Faculty of Graduate Studies and Research

The undersigned certify that they have read, and recommended to the Faculty of Graduate Studies and Research for acceptance, a thesis entitled Interactions of Human Skin Fibroblasts with Titanium submitted by Kalal Derhami in partial fulfillment of the requirements for the degree of Doctor of Philosophy in Medical Sciences. -Oral Health Sciences.
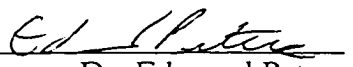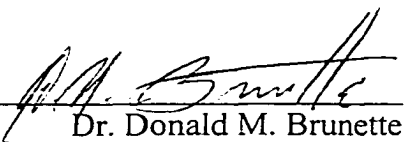
_____
Dr. Paul G. Scott

_____
Dr. John W. Wolfaardt

_____
Dr. Walter Dixon

_____
Dr. Edmund Peters

_____
Dr. Andrew Shaw

_____
Dr. Donald M. Brunette

ABSTRACT

A better understanding of the physical and biochemical events that occur during the interaction of cells with titanium will facilitate development of tissue-specific biomaterials. In the present study we examined the adhesion of normal human skin fibroblasts to two different growth supporting surfaces, namely commercially pure titanium (cpTi) and tissue culture polystyrene (TPS). We compared the composition of the total protein pools synthesised by fibroblasts on both surfaces and in the "substrate-attached material" (SAM) that remained on the surfaces following detachment of fibroblasts with a chelating agent. In addition, we studied the adhesion-promoting property of coating cpTi with SAM.

The results show that fibroblasts adhere less strongly to cpTi. Coating of cpTi with SAM enhanced adhesion of cells. The results of immunofluorescence staining of fibronectin and its receptor suggest that the nature of the interaction between this extracellular matrix ligand and the substrate may be important in determining cellular stiffness at the cell-extracellular matrix interface.

Proteins from extracts of whole cells, adsorbed serum, SAM and whole cells grown on cpTi coated with SAM were separated and identified by two-dimensional gel electrophoresis. In all, 45 proteins were identified by matrix-assisted laser desorption/ionisation mass spectrometry, database searching, immunoblotting, comparing to a standard-gel or by a combination of these techniques. Many of the proteins collected from the two surfaces were found to derive from the serum used in the culture medium. Surface properties of titanium appear to promote the formation of a more concentrated

carpet of serum proteins.Many proteins from bovine or human serum were found to adsorb in comparatively high concentrations onto cpTi. We found that among the major cellular proteins, fibronectin and a cytoskeletal protein: non-muscle myosin heavy chain type A (NMMHC-A), were expressed at lower levels by fibroblasts grown on cpTi compared to TPS. Coating of titanium with SAM also enhanced the expression of NMMHC-A. By analysing the changes in the composition of the entire protein pool of cells in response to different growth substrates and/or treatments we may find possible molecular markers of biocompatibility.

Dedication

To my parents who gave me life
To my wife for whom I live
To my future children, may they live with honor

ACKNOWLEDGMENTS

Since the earliest stage of this program, I have often thought how good it must feel to be writing this section. Little did I know that "good" does not begin to describe my present feelings. There is no doubt in my mind that I could not experience these intoxicating emotions of pride and joy, were it not for the people I am about to thank.

My supervisors, Dr. Paul Scott and Dr. John Wolfaardt, have thought me the importance of hard work, persistence, logical reasoning, curiosity, independent thinking, effective communications and,... The complete list would possibly add another volume to this work. But most of all I am thankful to both my mentors for giving me the ability to combine clinical experience with scientific insights. I hope that I can live-up to their teachings.

I am genuinely proud to have been a student of Dr. Walter Dixon and Edmund Peters who were members of my supervisory committee from the beginning of my Ph.D. program. To me, they are both true examples of how academicians should be, open-minded and always having the best interest of their student at heart. I am grateful for their trust and wisdom.

A large part of this dissertation was made possible by collaborating with other scientists or scientific groups. Perhaps, the most crucial results were provided by mass spectrometry. Dr. Liang Li and his group including Dr. Brend Keller and Ms. Jing Zheng in the Department of Chemistry provided me with their rare expertise and equipments. Dr. Anne Wennerberg, from the Department of Biomaterials at the University of Göteborg conducted the profilometric analysis of the substrates used in our studies. This

also be appropriate to thank Nobel Biocare (Göteborg, Sweden) for furnishing the implant-grade titanium discs that were used in this study.

I was lucky to have been associated with so many people who, in one way or another, worked in our laboratories. My dear friend and mentor, Dr. Aziz Ghahary, who cared for me as only a brother could. Dr. Takuo Nakano, from whom I learned my first lessons in cell culture, is a most modest and hard-working scientist I have ever had the pleasure of knowing. Ms. Carol Dodd, our skilled laboratory-assistant, thought me the "do's" and the "don'ts" of the lab, which I tried so desperately to imitate. I also like to thank Neda Assadi, Karim seyani, Chris Sikora, Dr. Bernadett Nedelec and Dr. Itaru Mizoguchi for sharing with me their ideas and lifting my spirit.

As an Old Persian saying goes, "If you want to get to know a person, travel with him". The past six years has been an incredible journey and I have found life-time friendships that I will cherish for the rest of my days. The late Dr. Imad Akram, was my first friend in Edmonton. My laboratory-book is still filled with his suggestions of how to design my first experiments. I am sure he is happy to see me finish my studies. Dr. Mehran Pooladi-Darvish who is now a professor in the University of Calgary, helped me with understanding the physics of centrifugation but more importantly he has been a devoted friend. I am deeply in debt to Dr. Hossein Ahmadzadeh for his unconditional friendship and mentoring during some of the most difficult stages of my work and also for introducing me to Dr. Liang Li's group. I also like to thank Dr. Sumonta Chaisomchit for many hours of discussion and sincere talks.

Words are helpless in describing my gratitude toward my beloved family for their continual support and encouragement throughout my life, pushing me to reach new

heights. During a time when I should have been supporting her, my dearest wife, Shiva, held me up, gave me hope and carried me through the roughest miles of this race. My gentle mother, Mrs. Shokooh Khozooei, has tirelessly supported me throughout my life and followed me every step of the way to the farthest corners of the globe. My Father, Dr. Mohammad Derhami, has always inspired me to become a better person than he is, a task that I do not believe I will ever accomplish. My kind-hearted sister, Mehrazar, has so generously given of herself to protect me at all costs, and my wise brother, Mehrdad, whose encouragement and advice gave me strength to continue.

They say, "money isn't everything".... well, neither is "devotion" but both are necessary to conduct research. I am grateful for the generous contributions that were provided by Craniofacial Osseointegration Maxillofacial Prosthetic rehabilitation Unit (COMPRU), Caritas Foundation for Medical Research, Fund for Dentistry and the Department of Dentistry at the University of Alberta.

TABLE OF CONTENTS

III. RESULTS

IV. DISCUSSION

LIST OF FIGURES

LIST OF TABLES

Interaction of Human Skin Fibroblasts with Titanium

Kalal Derhami

CHAPTER 1: INTRODUCTION

1.1. Rationale

The percutaneous or permucosal titanium implant system for extra- and intra-oral implants developed by Brånemark and co-workers (Brånemark and Albrektsson, 1982) has proved to be a very promising tool in craniofacial rehabilitation. A high degree of success has been reported for fixation of dental implants (Adell et al., 1990), bone-conduction hearing aids (Hakansson et al., 1990) and external ear and facial prostheses (Tjellstrom et al., 1985; Parel et al., 1986). These fixtures have also found applications in orthopedic replacement of digits and limbs (Hagert et al., 1986). The secure attachment of various prosthetic or hearing devices to these implants has provided a definite improvement in the quality of life for the patients requiring such devices (Fig. 1.1.).

The clinical success of craniofacial implants has been primarily estimated on the assessment of hard tissue response (Bonding et al., 1992) It is difficult to evaluate the success of soft tissue reaction to the implants. The presence of varying degrees of skin reaction is observed in a large number of patients. It is shown that approximately 31.3 % of patients with auricular prostheses (Holgers et al., 1987) and 23.3 % of patients with hearing aids (Holgers et al., 1988) develop some degree of skin reaction around their implant(s). In general inflammatory cells are present in the connective tissue around the implants (Holgers, 1994). Fixtures with an attached soft tissue-implant junction appear to exhibit a reduced inflammatory reaction. These observations are supported by our clinical experience with craniofacial implants at Craniofacial Osseointegration Maxillofacial

Fig. 1.1. The quality of rehabilitation of disfigurments in the craniofacial region has been markedly improved by using osseointegrated percutaneous implants

Prosthetic Rehabilitation Unit (COMPRU) in Edmonton, Canada (Wolfaardt JF, personal communication).

The soft tissue acts as a barrier and protectss the underlying structures surrounding the fixture. Successful integration of the soft tissue and accomplishment of an optimal interface at this level to the implant surface would reduce failures due to insults from the external environment. Numerous reports (James, 1976; McKinney et al., 1985; McKinney et al., 1988; Gould et al., 1990) have suggested that in dental implants the epithelial cells attach to the abutment surface in much the same manner as they attach to natural tooth surfaces with a gingival junction consisting of keratinized and non-keratinized epithelium and a dermal junction consisting of gingival fibroblasts in a connective tissue network. It is believed that in dental implants hemidesmosomes attach gingival keratinocytes to the basal lamina over the abutment surface (Donely and Gillette, 1991). In contrast to intraoral implants, there is no evidence of attachment at the interface of titanium implants and skin (Fig. 1.2.) (Holgers, 1994). This is also consistent with our clinical observations. It appears that a failure to seal at the dermal junction allows the down-growth of keratinocytes around percutaneous implants. This is considered to be a major cause of implant failure that may eventually result in deep pocket formation and marsupialization of the implant (Chehroudi and Brunette, 1991). A physical approach to resolve this problem advocates altering implant surface topography to modify epithelial migratory behavior and inhibit downward migration (Chehroudi and Brunette, 1991). Alternatively, it may be possible to improve the attachment of connective tissues to the implant at the dermal junction. This would require a more precise understanding of the
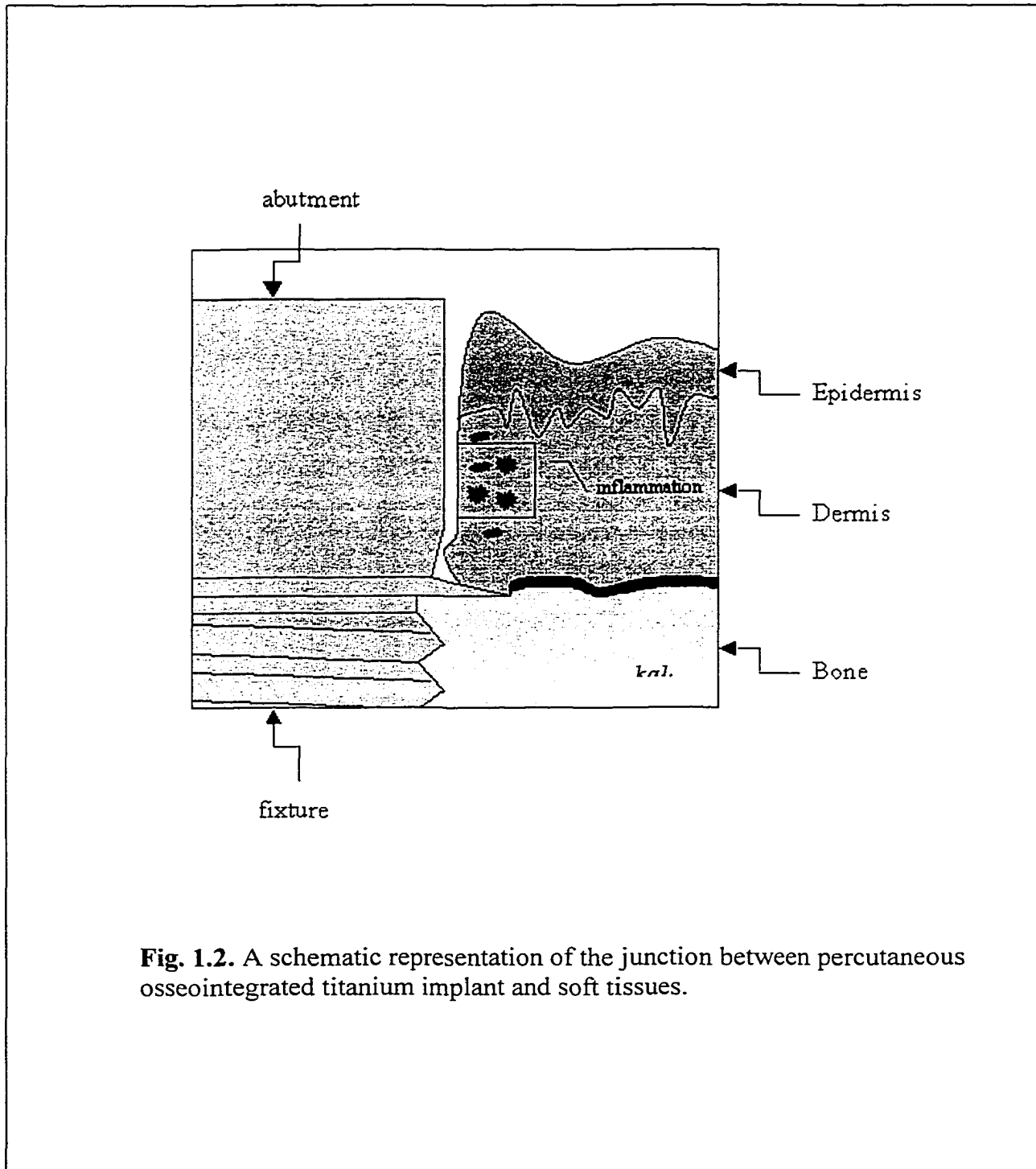
Fig. 1.2. A schematic representation of the junction between percutaneous osseointegrated titanium implant and soft tissues.

nature of biochemical and physical interactions between connective tissue cells and implants.

1.2. Background

1.2.1. Titanium as a metal for implantation: from myth to mystery to metal

"Never has there been, as in the case of titanium, the concentration of scientific and technical devotion to a single metal...never has metal, normally considered so mundane, been so extravagantly described as the wonder metal and the metal of promise" (Williams, 1977).

In 1795, the German chemist Martin Heinrich Klaproth discovered the element in the mineral rutile and named it titanium in allusion to the strength of the mythological Greek Titans. Titanium ranks ninth in abundance among the elements in the crust of the earth but it is never found in the pure state occurring as an oxide in the minerals ilmenite, $FeTiO_3$; rutile, TiO_2; and sphene, $CaO \cdot TiO_2 \cdot SiO_2$. The pure metal was isolated in 1910 (Microsoft Encarta, 1999) and became commercially available in 1940's. In fact, it was in 1940 that the first surgical implantation of titanium was reported in the United States and studies by Leventhal, Clarke and Hickman showed outstanding corrosion resistance *in vivo* (Williams, 1977). Even though the suggestion for clinical use originated in the US, for unknown reasons it went unnoticed in that country and instead two British manufacturers of orthopedic devices became interested in its use in the 1950s. By mid 1960's the American manufacturers also started to take interest and an ASTM specification for titanium for surgical implants was published (Williams, 1977).

A Swedish group lead by Professor Brånemark introduced titanium as dental implants in the late 1960's (Brånemark et al., 1977). The combination of proper surgical protocol, implant design and good clinical follow-up techniques made the Brånemark fixtures the standard choice for dental and craniofacial implantation. Based on their work with bone anchored titanium implants, Brånemark and co-workers coined the term "osseointegration". It describes the phenomenon whereby bone is integrated with commercially pure titanium (cpTi). The presumed "direct connection" of bone to titanium observed at the light microscopic level, only added a new mystical dimension to the already mythical status of this metal, in particular in the dental circles. Unfortunately, this concept has been difficult to evaluate. Originally "osseointegration" defined the <u>clinical state</u> of commercially pure titanium implants, however with the rise of a biological interest in osseointegration its definition has developed to include the observed clinical and biological reactions elicited by various implant materials. It is widely believed that "osseointegration" is not the result of an advantageous tissue response to a particular material but rather the lack of a negative tissue reaction (Stanford and Keller, 1991). In other words, the surface of titanium may not be inductive to bone formation but well tolerated by the bone-forming cells (Masuda et al., 1998). It appears that this is consistent with the importance of non-reactivity in biocompatibility of implant materials.

1.2.2. Surface of titanium: the key to its biocompatibility

Biocompatibilty of titanium is determined by its physical and chemical properties. The relative inertness of titanium makes it available as a replacement for

bone and cartilage in surgery. The ionic stability of titanium is due to the stable oxide film present on its surface. Paradoxically, it is the reactivity of the bulk metal that makes the formation of a resistant oxide layer possible. The passive titanium dioxide layer forms spontaneously with exposure to air and makes the bulk metal virtually noncorrodible (Williams, 1977) in physiological solutions.

The chemical or physical state of the surface may affect the adsorption of ions and proteins that support cell adhesion (Ellingsten, 1991). Factors such as manufacturing process, cleaning and sterilization may influence the physicochemical properties of the surface. A high surface energy is often necessary for the formation of short and long range chemical bondings. Critical surface energy of 20-30 dynes/cm exhibit minimal biological adhesiveness whereas materials with a critical surface energy above 30 dynes/cm support bio-adhesion (Brunette, 1988). The zone between 30 to 50 dynes/cm is the surface energy range empirically observed to correlate with the best biological adhesion (Baier, 1988).

As previously mentioned, the passivated state of the surface of titanium and the formation of an oxide layer are crucial to its biocompatibility. Surface purity and cleanliness are achieved by cleaning methods that minimize the contamination to the oxide layer. The procedures for cleaning of implant surfaces often include passivation of the surface by strong acid solutions, removal of oils and hydrophobic contaminants by solvents, ultrasonic cleaning and autoclavation. The thickness of the oxide layer, its crystallinity and composition are also important factors to consider when cleaning surface of titanium (Kasemo and Lausmaa, 1991). These properties are mainly

controlled by purity of the bulk metal, passivation procedures, and the temperature used in the cleaning steps.

When biomaterials are fabricated as components of implants it is likely that topography will be imposed on the surface of the material, either deliberately or by accident. This may occur without the knowledge of the fabricator. At a molecular level, it is improbable that a molecularly smooth surface will be provided except in the rare case of certain mica surfaces (Curtis and Wilkinson, 1997). Surface roughness is another aspect of the surface of titanium that has been extensively studied using cell culture methods. It is believed that surface irregularities can be used to modulate cellular activities such as migration, growth and attachment. In particular, investigators are interested in the influence of groove-ridge topographies on cell migration (Chehroudi and Brunette, 1991). The suggested sizes of the irregularities for optimal cell attachment vary from 100 μm – 400 μm (Botha, 1997). These dimensions are normally within the size-range of most cells. For example, the length of skin fibroblasts varies between 50 μm – 200 μm (our own observations). It is often observed that cells align to the substrate topography in order to minimize distortion of their cytoskeleton (Oakley and Brunette, 1993). In fibroblasts, the alignment of the cytoskeleton may determine cellular orientation and thus indicate the direction of migration. In fact, micromachining of titanium has been proposed as a method to divert downward migration of epithelial cells in the sulcular area around intraoral implants (Brunette et al., 1983).

Cell attachment and spreading occurs on biocompatible surfaces irrespective of its roughness (Brånemark et al., 1977, Keller et al., 1989; Moriatorty et al., 1990). For example, surface irregularities of 3 μm – 5 μm offer an excellent surface for bone

formation (Zweymuller et al., 1988). The concept of using smooth surfaces for implants emphasizes the role of surface chemistry as opposed to surface topography in cell adhesion and growth. In fact, it is unclear whether cells react to the topography per se or if the methods of fabrication of topography actually produce chemical patterns to which cells respond to (Curtis and Wilkinson, 1997). This problem was approached by Pritchard et al. (1995) who used patterning systems to fill adjacent spaces with different proteins or silanes so that the surface was free of irregularities deeper than a molecule in height. Cells still adhered to the patches of adhesive material. It may be argued that the disordered molecules present at the junctions may guide the cells. Nevertheless, it is generally agreed that moving or extending cells appear to be localized more frequently at the region of discontinuities of the surface rather than randomly attached to patches of adsorbed proteins. One must also consider the dimensions of surface irregularities. Britland and co-workers (1992) cultured cells on surfaces with varying groove-depths and laminin was patterned perpendicular to these surface-irregularities. When the groove-depths were less than 500 nm, cells followed the orientation of laminin. However, on deeper grooves (> 5 μm) cells followed the path of topographical cues. Clark et al (1990; 1991) showed that on groove/ridge topography the extent of reaction is related to groove width as well as to depth and probably also to the number of adjacent grooves. Cells react to a single cliff and increasingly so with increasing cliff height in the range 1-20 μm (Clark et al., 1987). When the grooves or ridges are appreciably wider than the cells, effects on orientation are not very marked, although cells may align to one edge (Clark et al., 1987). Clark (1992) showed that BHK cells react to groove/ridge topography with a pitch (repeat) of 260 nm. These grooves were 600 nm deep. Curtis and

Wilkinson (1997) found that fibroblasts moving on 12.5 or 25.0 μm wide groove/ridges showed more contact inhibition than on planar surfaces. This effect increased as the grooves became narrower. The minimum width of topography to which a cell can react to is still unknown. There is general evidence that the extent of orientation increases with groove depth up to about 25 μm from topographies of about 1 μm relief (Curtis and Wilkinson, 1997). Even biological surface patterning such as the edges of neighboring cells or intercellular material may act as grooves to provide cell guidance (Vesely et al., 1992). The evidence in support of a dominant role for surface topography in orientation and migration of cells is overwhelming.

It is proposed that cells may respond to topography of a substrate by modulation of their cytoskeletal elements (Oakely and Brunette, 1993; Curtis and Wilkinson, 1997). As cells form adhesion complexes on a substrate the cytoskeletal components of the adhesion sites may respond to the substrate topography. For example, the degree of intracellular tension exerted by the actomyosin complexes may vary at different regions of a cell relative to the topographical profile of the substrate. Tension is exerted at convex regions, whereas in concave areas the cytoplasm is compressed. The evidence of Oakley and Brunette (1993) shows that microtubules first appear in the bottom of grooves whereas microfilaments are initially present on the groove-ridges. This is consistent with the biological roles attributed to these cytoskeletal elements by principles of tensegrity (Ingber, 1993). According to tensegrity model proposed by Ingber, actin microfilament lattice behaves as tensile structures and microtubules act as compression-resistant struts.

1.2.3. Tissue culture polystyrene is an excellent surface for cell attachment

The polystyrene molecule is a long carbon chain with benzene rings on every other carbon (Gibbs, 1995). For this reason, it is a very hydrophobic compound that, in a native form, is unsuitable for cell culture. The exact mechanism of treating the surface of polystyrene for cell culture is kept confidential by the manufacturing companies. However, it is common knowledge that treatment of polystyrene with radiation or other techniques can alter the chemistry of its surface by breaking the benzene rings. This process incorporates carboxylic acid in the exposed carbons of the broken rings thus making the surface highly negatively charged. The resulting surface is primarily hydrophobic with intermittent carboxyl groups capable of ionic interactions with positively charged groups on biomolecules and ions. Passive adsorption can occur in the hydrophobic regions of the surface but it is the hydrophilic interactions that actively adsorb a biolayer of serum proteins that is required for attachment and growth of cells in culture.

A substantial part of our understanding of cellular behavior is shaped by the observations made of cells in culture, in particular on tissue culture polystyrene. Its excellent adhesive properties have made this material the substrate of choice in many biological research laboratories. As a result, many cellular events observed on tissue culture polystyrene are directly correlated to in vivo activities. For example, formation of focal adhesions and the associated stress fibers is commonly believed to be a hallmark of optimal cell-substrate contact, however these particular adhesion sites are considered to be primarily an *in vitro* phenomenon (Burridge et al., 1990). From a biomaterial

perspective this is important since what may appear to be optimal adhesion on polystyrene is not necessarily an indication for optimal biocompatibility.

1.2.4. Cell adhesion

The importance of cell adhesion to so many life processes has prompted considerable research activity in many areas of science including implantation of artificial devices. The abundance of information present in the literature makes it nearly impossible for any one review to cover every aspect. Here, we will briefly discuss those aspects of cell adhesion that pertain to this work.

One of the most important parameters used in assessment of biocompatibility is cellular adhesion. *In vivo*, cells are either attached to other cells, so-called cell-cell adhesion or they are attached to the extracellular matrix. *In vitro,* a third type of cell adhesion also occurs between cells and an artificial substrate. It appears that evolution did not prepare cells to attach to non-organic substrates, but according to Hench (1989) adhesion of biopolymers to non-organic matter was the primary event that led to the formation of precytic structures. If this hypothesis were true, it would clearly suggest that cell-substrate adhesion preceded other forms of cell adhesion. This would also imply a major role for biomaterial interactions in the creation of life! Although the origin of life is far from being unraveled, scientists have discovered many facts about the mechanisms by which cells adhere to various substrates.

Cell adhesion to the extracellular matrix is mediated through membrane receptors. These transmembrane molecules are glycoproteins that mediate binding interactions at the extracellular surface and determine the specificity of cell–cell and cell–ECM

recogni.tion. They include members of the integrin, cadherin, immunoglobulin, selectin, and pro•teoglycan (for example, syndecans) superfamilies.

Strikingly, there are common properties among many cell adhesion molecules that link these to the same primordial recognition domain (Ruoslahti and Obrink, 1996). The adhesive domains in fibronectin, immunoglobulin (Ig) type cell-cell adhesion proteins, and cadherins are all structurally related. Homophilic binding or self-association of imunoglobulins and cadherins is the primary mode for cell-cell adhesion. On the other hand, heterophilic associations of integrins and selectins with extracellular ligands such as fibro•nectin attach cells to the matrix. However, at times integrin-integrin binding may mediate cell-cell adhesion or binding between Ig family members and cadherins with integrins may mediate cell-matrix adhesions (Ruoslahti and Obrink, 1996). It is proposed that the recognition by integrins of their ligands may have its origins in homophilic binding. There is some evidence to suggest that the RGD (arginine - glycine - aspartic acid) sequence in the integrin ligands bind to a site in integrins with a somewhat similar composition. Other common features among most adhesion molecules include the low affinity of binding to their ligands and dependency on divalent cations for receptor-ligand interaction. It is believed that the low affinity bindings act coordinately to create a Velcro®-like effect and by causing depletion of cations, chelating agents such as EDTA or EGTA disrupt these adhesive interactions.

An important function of adhesion molecules is to mediate signals from the outside (ECM) to the inside of cells and vice versa (Clark and Brugge, 1995). This process is called outside-in and inside-out signaling. For example, the integrin mediated adhesive interactions are responsible for blood clotting. The activation of $\alpha_{IIb}\beta_3$ integrin,

which initiates platelet aggregation, is an excellent example of inside-out signaling. On the other hand, integrins such as the fibronectin receptor $\alpha_5\beta_1$ can recognize clues from the ECM and modulate cell behavior by transmitting the signal to the cell through its cytoskeleton. For example it is known that at low densities of RGD cells attach but do not spread (Burridge and Chrzanowska-Wodnicka, 1996). At medium densities, cells spread but do not form focal adhesions (FA's), however, at high densities (spacing > 140 nm) of RGD's FA's form. On the intracellular side of the plasma membrane, cell adhesion receptors associate with cytoplasmic plaque or peripheral membrane proteins. Cytoplasmic plaque proteins such as vinculin, talin and α-actinin serve to link the adhesion systems to the cytoskeleton, to regulate the functions of the adhesion molecules, and to mediate signals initiated at the cell surface by the adhesion receptors. Focal adhesions are specialized cellular structures developed by many cells in culture where aggregates of integrins span the membrane interacting with the ECM on the outside and cytoskeletal components such as actin on the inside of cells. The bundles of actin filaments present at these sites are known as stress fibers and it is believed that they generate isometric tension in cells. The tension produced by stress fibers creates the traction required for cell locomotion.

1.2.5. Regulation of the adhesive interactions

Affinity modulation is thought to be the major mechanism for regulating the activity of integrins. Factors that activate integrin binding include growth factors, peptides and attachment (Burridge and Chrzanowska-Wodnicka, 1996). Affinity modulation of integrin has been most extensively studied in platelets (Ginsberg et al.,

1992; Schwartz et al., 1995). The major platelet integrin $\alpha_{IIb}\beta_3$ has been shown to undergo conformational changes during activation. This results in a change in the binding affinity of the integrin. A high affinity binding state of integrin $\alpha_{IIb}\beta_3$ binds platelets to soluble fibrinogen whereas low affinity interactions mediate the adhesion of inactivated platelets to immobilized fibrinogen. It is believed that this facilitates recruitment of platelets to a preexisting hemostatic platelet plug.

Divalent cations are required for ligand binding in integrins, cadherins, and selectins. Biochemical, mutagenesis, and structural data support a model in which the critical aspartic acid residues in the ligand and receptors binding sites enable the ligand and receptor to jointly coordinate a divalent cation (Edwards et al., 1988). In the platelet integrin $\alpha_{IIb}\beta_3$, ligand binding and cation binding both map to the same segment of the α subunit (D'Souza et al., 1994). It has been shown that ligand binding to this segment causes the cation to be extruded from the site thus rendering the cation-receptor complex a transient state. This suggests that changes in divalent cation concentration may also be a factor in regulation of the binding affinity or adhesive states of many integrins.

The molecular mechanisms underlying affinity modulation are poorly understood but it is known that conformational changes can occur at long range over the length of the molecule. The activating sites are localized to the tail region near the membrane anchor, while the ligand-binding region of integrins is found in the extracellular domain of the proteins. An important role of the cytoplasmic domain of the β subunit is to target the integrin molecule to the focal adhesions, deletion of this cytoplasmic region blocks localization of the heterodimer to these sites (Burridge and Chrzanowska-Wodnicka, 1996). The formation of intimate and firm contacts between cells or between cells and

matrix is the result of linking of adhesive molecules to the actin cytoskeleton. It is believed that this linkage generates the force required for spreading and migration of cells.

The focal adhesion is a common type of adhesive contact that cells make with the ECM. Focal adhesions are comprised of integrins as the major adhesion receptors which are associated with the cytoplasmic plaque proteins, including talin, vinculin, α-actinin, tensin, paxillin, and a number of protein kinases (Gumbiner, 1993; Turner and Burridge, 1991). Both talin and α-actinin were shown to bind to integrins in vitro with relatively low affinity (Burridge and Chrzanowska-Wodnicka, 1996). α-actinin binds to and cross links the actin filament and talin binds to integrins and vinculin. Vinculin binds not only to talin but also to actin microfilaments, α-actinin, paxillin and tensin. Thus at focal contacts binding between individual plaque proteins and/or a combination of these interactions may link integrins to the actin microfilaments.

The formation of focal adhesion contacts is associated with the process of cell spreading. Thus, focal adhesions are thought to serve as sites for coordination between cell adhesion and cell motility. Actually, highly motile cells often lack easily distinguishable focal adhesions, probably because they are more transient, smaller, or less distinctively distributed. Nevertheless, the focal adhesions that are more prominent in adherent stationary cells probably represent a highly assembled state of the molecular complexes in vitro. The assembly of focal adhesions is regulated both by extracellular ligand binding events and by intracellular signaling events. Binding of ligands such as collagen, fibronectin, laminin, fibrinogen and vitronectin localizes β1- and β3-containing integrins into focal adhesions (Sastry and Horwitz, 1993). The cytoplasmic domains of

the β-subunits have intrinsic signals for focal adhesion localization, but incorporation of the integrins into focal adhesions is prevented by the α-subunits of the heterodimers. Upon binding of the ligand this inhibition is relieved thus allowing the β-subunit cytoplasmic tail signals to recruit the integrin dimer into the focal adhesion. For effective focal adhesion assembly, both receptor clustering and occupancy by ligand are required (Miyamoto et al., 1995). A combination of receptor occupancy and clustering triggers a synergistic response that includes the reorganization of the cytoskeleton and associated cytoplasmic plaque proteins and the activation of local signaling pathways. Focal adhesion assembly and disassembly are also regulated by locally generated intracellular signals.

Phosphorylation of tyrosine and serine-threonine residues in some proteins is known to be a common response to integrin engagement in many cell types including fibroblasts. Protein kinases mediate the enzymatic reactions required for phosphorylations of proteins. Particularly central to integrin activation is the localization of focal adhesion kinase (FAK) to the focal adhesions (Burridge et al., 1992). Because FAK activity and tyrosine phosphorylation of focal adhesion proteins are also triggered by integrin occupancy and clustering, these signaling events seem to link the assembly of the complete focal adhesion complex to the initial ligand binding event. The identification of the cytoskeletal proteins paxillin and tensin as substrates for tyrosine kinases suggests a possible mechanism for the assembly and regulation of integrin-mediated signaling complexes and pathways.

It is believed that clustering of integrins into focal adhesions depends on the density of the extracellular ligands. Thus at a higher ligand density more integrin

molecules are intimately aligned with each other in focal adhesion contacts. Both ligand occupancy and clustering of integrins are required for the formation of focal adhesion (Massia and Hubble, 1991). At the focal adhesions, an abundance of signaling proteins and cytoskeletal proteins provide the necessary elements to link the extracellular matrix to the cytoskeleton via the integrins. FAK is activated through autophosphorylation. The activation of FAK starts a chain of events that ultimately leads to the formation of focal adhesions. Since FAK is shown to bind directly to integrins (Schaller et al., 1995), it is believed that its autophosphorylation may be a consequence of integrin clustering (Kornberg et al., 1991; Defillipi et al., 1994). It is known that integrin clustering and not ligand binding alone is required for this activation. Based on this evidence Burridge has proposed a model according to which stress fiber formation (Hall, 1994) generates the tension required to cluster the integrins. As a result of this tension the integrins and their associated FAK molecules are pulled into close contact thus providing the means for dimerization and autophosphorylation of FAK.

It appears that the origin of stress fibers and FAs reflect the response of cells in culture to an apparent wound environment. Many of the factors present in serum stimulate Rho-mediated contraction. The Rho subfamily of the ras superfamily of GTPases hydrolyze GTP into GTP and is essential for serum-induced formation of focal adhesion and stress fibres (Hotchin and Hall, 1995). Inhibition of Rho causes the collapse of the actin cytoskeleton and disruption of FAs (Huttenlocker et al., 1995). The activation of Rho in response to integrin-mediated adhesion may follow activation of protein kinase C and the release of arachidonic acid which signal inflammatory events (Chun and Jacobson, 1992). It is shown that blocking the metabolism of arachidonic acid to

leukotrienes prevents cell spreading. Synthesis of leukotrienes and stimulation of Rho may in turn activate Rac which is known to be required for the formation of membrane ruffling (Ridley and Hall, 1992). In fact, the response of cells adhering to and spreading on ECM resembles cells responding sequentially to cdc42, Rac and Rho. Cdc 42 is upstream of Rac and its activation leads to the formation of filopodial extensions. Lamellopodia are formed as a result of Rac activation and finally after spreading of cells, the stress fibers and focal adhesions are a consequent of Rho activation (Burridge and Chrzanowska-Wodnicka, 1996). One way that Rho may stimulate stress fiber formation is by activation of myosin light chain kinase (MLCK) thus linking the myosin molecules to the actin cytoskeleton (Garcia, 1999; Burridge, 1999). Contraction of fibronectin matrix may in turn expose cryptic self-assembly sites within fibronectin molecules and thus enhance adhesion (Zhong et al., 1998). A rigidly held extracellular matrix provides more resistance to the isomeric tension exerted by the cells in culture (Burridge and Chrzanowska-Wodnicka, 1996). It is conceivable that attachment of cells to highly adhesive surfaces, such as tissue culture plastic, leads to an increased tension and an extensive development of focal adhesions and stress fibers. A strong attachment of cells to the substrate may be considered as a marker of viability *in vitro* but optimal cell growth and migration occurs at an intermediate level of adhesion strength (Huttenlocker et al., 1995). The formation of extensive stress fibers and focal adhesions may not be an absolute marker of optimal cell-substrate attachment.

1.2.6. Measurement of the strength of cell adhesion

A commonly used method of adhesion-assay measures the plating efficiency of a particular type of cell in culture. Although this method may be informative, little knowledge is gained about the physical property of cell-substrate interface.

As a cell crawls forward, its ability to move depends on the strength of the bonds that attach it to the substrate (Jay et al., 1995). The strength of cell adhesion is important not only in cell migration. Modulation of adhesive strength has been shown to be a determining factor in cell growth and differentiation (Ben-Ze'ev et al., 1988). For this reason, at times it is more relevant to assay cell adhesion on the basis of the force that is necessary to detach cells. One of the most efficient methods in estimating the forces of detachment of cells is using a centrifugation assay (Hubbe, 1981). In this method adherent cells in a fluid media are placed in a centrifuge and then the cells are accelerated at various rates in a direction perpendicular to the substrate's surface. The number of detached cells or the cells remaining on the substrate or both are counted. The centrifugational force is known and the average mass of the cells is calculated by measuring its density and volume. In this way, the force that is required to detach a single cell is estimated (see section 2.2.6). The main advantage of this method is the even distribution of applied force over the entire cell (Hubbe, 1981). In addition, since the direction of the centrifugal force is perpendicular to the surface, the contributions of tangential components, which may separate cell-cell instead of cell-substrate adhesions, are minimized. Due to the extremely high accelerations required to release cells by centrifugal force that is directed perpendicular to the surface (Hubbe, 1981; Lotz et al.,

1989) attempts to detach normal (non-transformed) cells by this method have so far failed to measure the values for strength of adhesion. High centrifugal forces cause deformation of the large experimental chambers, however, smaller chambers may tolerate increased accelerations.

A theoretical analysis by Ward and Hammer (Ward and Hammer, 1993) predicts that cross linking of the cytoskeletal elements present at focal contacts increases the strength of cell adhesion by >100 fold. According to this model, in the absence of cross-linking of the cytoskeletal components, the cells may detach by peeling. Comparison of their theoretical data with experimental results of Lotz and co-workers (1989) show that glioma cells detach from fibronectin substrates by peeling whereas detachment of normal fibroblasts may require cells to fracture-off the substrate. The authors conclude that rigidity of cell-substratum attachment sites caused by cytoskeletal linkage may markedly enhance attachment strengths to values that require experimentally impracticable forces. Lotz and coworkers (1989) found that strength of adhesion of glioma cells to fibronectin at 37° C was 3.6×10^{-4} dynes/cell. Jones (1966) measured the force necessary to detach fibroblasts to be 6.0×10^{-6} dynes/cell, however little is known about the nature of the substrate used in these experiments. Adhesion of fibroblasts was also quantified on different biomaterials by using a fluid mechanic approach that measures shearing stress (Bundy, 1994). In this study, the authors did not measure the force exerted on a single cell, however this value may be derived using the force per unit area. Assuming that the total contact area of a cell is 6×10^{-6} cm^2 (Lotz et al., 1989), the shear adhesive strength of fibroblasts on Titanium-6Aluminum-4Vanadium is calculated to be 3.6×10^{-3} dynes/cell. This value was slightly lower for cells attached to non-tissue culture-treated

polystyrene (2.7×10^{-3} dynes/cell). As explained by Hubbe (1981), one must be cautious in comparing the magnitudes of forces of detachment reported in various studies since the procedures and cell lines may vary greatly among these studies.

1.2.7. Cell migration

A biphasic dependence of cell migration speed and the strength of cell adhesion have been established (Dimilla et al., 1993). Weak or moderate strength of attachment favors migration, whereas strong attachment tends to inhibit cell movement. Cell migration is a complex process that can be considered as a repeated cycle of lamellipod extension and attachment, cytoskeletal contraction, and tail detachment (Palecek et al., 1996). Cell locomotion is initiated by protrusion of the leading edge via polymerisation of actin, to form the lamellopodium that subsequently attaches to the substratum. Attachment to the substrate is mediated by integrin adhesion to the extracellular matrix. The adhesive interactions are used to produce the traction required to release the attachments at the rear of the cell. Retraction and release is a crucial part of cell movement (Lauffenburger and Horwitz, 1996). Tracking studies of the cell membrane receptors of fibronectin ($\alpha_5\beta_1$ integrins) on migrating fibroblasts have provided insights about the release mechanism as well as the fate of receptors following release of adhesions (Regen and Horwitz, 1992). It is reported that as much as half of the integrins present in adhesion complexes are ripped from the cells and left on the substratum as the cell releases and moves forward (Regen and Horwitz, 1992). This membrane "ripping" may be a physiological phenomenon (Palecek et al., 1996). Observation of migrating corneal fibroblast *in vivo* has shown that pieces of cell membrane are left attached to the

substrate (Hay, 1985). Neutrophils are also known to release major portions of their cortical cytoplasm. In culture, these cell fragments can retain mobility for a day or more (Malawista and De Boisfleury Chevance, 1982). It appears that both receptor dissociation from the substrate and ripping out of the integrin-containing membrane regions occur during detachment of the cell posterior (Regen and Horwitz, 1992). The strength of adhesion in the cell anterior must be sufficient to generate force whereas at the cell rear weaker interactions allow the release and forward-rebound of the cell body. The asymmetry of the strength of cell adhesion in the cell anterior versus the cell posterior is mainly regulated by two mechanisms (Huttenlocher et.al, 1995). On one hand, the affinity of integrins to their ECM ligands may be modulated and on the other hand alterations in the levels of cytoskeletal-associated proteins may modulate the rigidity of integrin-cytoskeletal linkages. Where release of the cell rear from the substrate requires high contractile forces, recruitment of myosin II at the posterior region of the cell facilitates this process. Myosin II is the major type of myosin present in nonmuscle cells and it is also known as nonmuscle myosin.

Myosin II is not involved in protrusion however due to its abundance in the body of motile cells, this molecule has been postulated to be involved in generation of traction force (Tilney, 1975). Indeed, genetic ablation of myosin II in Dictyostelium did not completely block cell locomotion (Fukui, 1990) but the net rate of locomotion (reflecting traction) was significantly reduced or completely blocked in myosin II nulls (Doolittle et al., 1995). From a biomaterials perspective, it is important to note that the reduction in locomotion of myosin II nulls was most severe when cells were grown on more adhesive

substrates (Jay et al., 1995). In other words, increased contractility may be necessary to move the cells on highly adhesive substrates.

A contraction model presently explains the generation of traction force by myosin II (Cramer and Mitchison, 1995). According to this model, contraction of actin filaments by myosin II generates equal tension in all directions in the cell body. Polarization of cell motility is proposed to be a result of higher adhesion at the front relative to the back of the cell. A related contractile model is based on polarized cortical contraction/relaxation (Bray and White, 1988). Myosin II driven contraction is thought to be responsible for generating cortical tension, an important factor in shaping cells. Myosin II is also responsible for local contractions, e.g., cytokinesis (Oegema and Mitchinson, 1997).

1.2.8. Substrate-attached material

Substrate-attached material (SAM) is a term used by Culp and co-workers (1978; 1979) to describe partially purified adhesive cell surface sites that is prepared by treating a variety of cell types with a chelating agent (EGTA). EGTA is a calcium-specific chelator that causes the adherent cells to round up and retract away from their substrate. In this way it facilitates the mechanical removal of cell bodies by shearing forces. As the result, the most tenacious adhesive sites of cells remain bound on the substrates together with their associated molecules. It is believed that by depleting calcium, EGTA may weaken the adhesive interactions that require this divalent cation for binding to their ligands (Britch and Allen, 1980).

Analysis of SAM has revealed that it contains 1-2% of the cell's protein content (Culp et al., 1979) and is composed of phospholipids (Cathcart and Culp, 1979), focal

adhesion contacts, close contacts, fibronectin (Lark and Culp, 1983), proteoglycans and fibronectin-associated glycosaminoglycans (GAG:s) (Rollins and Culp, 1979). It was demonstrated that the glycosaminoglycans of SAM, in the newly formed adhesion sites (<2 hours in culture) are enriched in heparan sulfate and depleted in hyaluronic acid and chondroitins whereas in mature SAM (>72 hours in culture), a high proportion of the later GAG:s were found (Revel et al., 1974; Revel and Wolken, 1973). According to these investigations, little or no nucleic acid was detected in SAM suggesting that this material is not simply composed of attached cells.

A tightly adsorbed layer of serum proteins is also found to be present on the substrate that mediate the adhesive contacts in SAM (Culp et al., 1979). In a two dimensional electrophoresis system, it was shown that SAM contains serum albumin and in addition several cytoskeletal proteins which were identified as actin, myosin, α-actinin and intermediate filaments (probably vimentin). Fibronectin was also present in SAM however the fibronectin spot showed a considerable heterogeneity in its isoelectric focusing which was suggested to be due to the variable degree of sialic acid residues on this molecule (Vessey and Culp, 1978). Interestingly, Culp found that as the fibroblasts density increased in culture the intensity of fibronectin-specific fluorescence decreased in the SAM isolated from fibroblasts grown on glass coverslips. However, no change was observed in the amoumt of fibronectin in the SAM found on plastic coverslips (Culp et al., 1979). Apparently the differences in the interfacial substances present on the two substrates were due to the surface properties of each material. These studies by Culp and coworkers significantly increased our level of understanding about the biochemical and morphological composition of the adhesion structures at the cell-substratum interface.

Nyfakh and Svitkina (1983) used a similar approach to study the cell-substratum adhesion sites. They gently lysed the fibroblasts with saponin, a substance extracted from soap plant, thus leaving the cells' undersides on the substratum. Analysis of the saponin-isolated focal contacts by SDS-PAGE showed a single band of an unknown protein at 51 kDa. The authors concluded that saponin removes the cytoskeletal elements associated with focal adhesion sites. Nyfakht's method for the isolation of focal adhesions by saponin was later used by Niederreiter and co-workers (Neideritter et al., 1994) to prepare samples for analysis by two-dimensional electrophoresis. More than 50 protein spots were detected by this method. This is in sharp contrast to the results of Nyfakh and Svitkina (1983) who detected only a single protein band in SDS-PAGE gels of a similar preparation. Aside from the fact that two-dimensional electrophoresis is a more powerful method of separating proteins, perhaps a difference in the way by which proteins were extracted also played a role in the obtained results.

The range of proteins found in the substrate-attached material include components of serum, extracellular matrix, cell membrane, adhesion molecules and cytoskeletal proteins associated with adhesion sites. This suggests that SAM may closely represent the true-interface at the cell-substrate junction. For this reason, we believe that by studying this particular fraction of cells in culture we may gain a better understanding of the interfacial phenomenon between cells and biomaterials.

1.2.9. Cell-titanium interface

Despite the known importance of tissue-biomaterial interface in long-term stability of tissue-integrated implants, the lack of understanding of even the most elementary biochemical and cellular processes at this vital junction is the major barrier to the development and establishment of clinical procedures that would enhance the biocompatibility of host with implant materials.

Various studies have suggested the presence of a 20 nm proteoglycan (PG) layer against the side of *in vivo* implant (Carsson et al., 1988; Albrektsson et al., 1982). Further studies, in culture, have also confirmed the presence of a ruthenium red-staining layer and a unique interfacial layer, observed in transmission electron microscope preparations, between the proposed PG layer and the oxide surface of cpTi (Davies et al, 1990; De Bruijan et al., 1993; Garvey and Bizios, 1994). Davies and coworkers (1990) described the morphology of this interface as two sublayers between the cell bodies and the metal surface. The layer closest to titanium contained fewer collagen fibres and was lightly stained with ruthenium red, however the sublayer adjacent to the cells was composed of denser collagen matrix and was strongly stained. At the ultra-structural level the titanium-osteoblast interface (Davies et al., 1991) has been shown to contain an as yet unknown material containing sulphur, calcium and phosphorous. The seeding of small calcium phosphate crystallites rapidly calcifies the sulphate species. Using antibodies specific to chondroitin sulphate the presence of this moiety at the interface of titanium and osteoblast has been established. Metabolic labelling of cells with radioactive elements has also shown that, on average, 3.5 fold more proteoglycans is incorporated

into the extracellular fraction of cells grown on metal implants than on the tissue culture plastic controls (Klinger et al., 1998).

In an elegant ultrastructural investigation by Nanci and co-workers (1994), it was demonstrated that a layer rich in glycoconjugates is present at the interface between titanium and osteoblasts *in vivo*. This layer was intensely immunolabeled for osteopontin and α_2HS-glycoprotein. Based on the structural and compositional similarities between this interface and cement lines that form during osteogenesis, it was concluded that the host response to titanium may be similar to natural bone interfaces.

An important factor to consider when analysing the results of many ultrastructural studies of the interface between cells and materials is the presence of adsorbed proteins from the serum on the experimental surfaces. The detection method(s) must distinguish serum proteins from cellular proteins, both of which may be present at the interface. Labelling with ruthedium red or immunohistochemistry does not necessarily indicate the source of the biochemical components found at the interface.

Serum contains many glycoconjugated proteins, which are heavily negatively charged. It is suggested that the positively charged calcium ions may form a bridge between the negatively charged surface of titanium oxide and the negative surface-groups of serum proteins thereby overcoming the forces of electrostatic repulsion (Parsegian, 1983). Klinger and co-workers (1998) believe that this model may be too simplistic since EDTA is not effective in eluting ^{35}S-labeled proteoglycans adsorbed to $CaCl_2$ treated titanium powder. The observation that guanidine HCL but not EDTA can release the proteoglycans suggests that the protein cores may be involved in adsorption of proteoglycans to metals.

Whatever the mechanism of protein adsorption to metals may be, it is well know that serum proteins are readily adsorbed to metal substrates. Attempts have been made to identify the serum proteins that adsorb to titanium but these have either concentrated on a single or a few particular proteins or they have not separated and identified all of the adsorbed proteins (Liu et al., 1998; Walivaara et al., 1996; Nygren et al., 1997; Ellingsen, 1991). Among the serum proteins known to adsorb to titanium dioxide are albumin and fibrinogen (Liu et al., 1998), factor XII and kininogen (Walivaara et al., 1996), prothrombin and thrombin (Nygren et al., 1997), α-HS-glycoprotein and IgG (Ellingsen, 1991). These have been identified by various radiolabeling or immunodetection methods. In a study by Ellingsen (1991), adsorbed serum proteins to titanium dioxide and hydroxyapatite where dissolved in EDTA. Analysis by SDS-PAGE and immunodetection techniques revealed that both surfaces appeared to take up the same proteins selectively from human serum. A criticism of this study is the lack of complete separation between protein–bands in the one-dimensional SDS-PAGE gels. A two-dimensional SDS-PAGE system could conceivably resolve many more proteins in the samples of adsorbed serum proteins. This is important since several abundant serum proteins have similar molecular weights. For example, α1-antichymotrypsin, fibrinogen γ chain, fibrinogen β chain, IgG γ chain and IgD δ chain run in the same vicinity of the gel as serum albumin (Thode et al., 1998). All of these proteins were shown to adsorb to iron-oxide particles using two-dimensional SDS-PAGE electrophoresis. The relative abundance of serum albumin may easily mask the presence of less abundant proteins in a one-dimensional gel. Clearly, the adsorption of serum proteins on titanium dioxide needs to be further studied using more sensitive detection techniques.

1.2.10. Proteomics

"Proteomics is an emerging area of research of the post-genomic era that deals with the global analysis of gene expression using a combination of techniques to resolve (high resolution two-dimensional polyacrylamide gel electrophoresis, 2D PAGE), identify (peptide sequencing by Edman degradation, mass spectrometery, Western immunoblotting, etc.), quantitate (scanners, phosphorimager, etc.) and characterize proteins, as well as to store (comprehensive 2D PAGE databases), communicate and interlink protein and forthcoming DNA sequence and mapping information from genome projects (http://biobase.dk/cgi-bin/celis)" (Celis et al., 1998).

The advent of 2D PAGE enabled scientists to separate and analyze complex mixtures of proteins represented by cells, tissues and even whole organisms. Using the standard format (20 cm x 20 cm) 2-D gels, it is possible to resolve more than 2000 proteins from whole cell and tissue extracts. These results can be significantly improved by using larger gel formats that can potentially detect up to 10,000 protein spots (Dunn , 1997). This high degree of resolution is made possible by combining isoelectric focusing in the first- and SDS-PAGE in the second-dimension. In the first dimension gel, solubilized proteins are separated according to their isoelectric point (pI). This gel is then applied to the top of a SDS-slab gel and electrophoresis is carried out to separate the proteins on the basis of their molecular weight (MW). To take full advantage of the power of resolution provided by 2D SDS-PAGE a sensitive protein detection technique, such as silver staining, is required for analysis of the gels. Protocols may vary but the basic protocol for 2D SDS-PAGE uses ampholytes in the first dimension urea-gels to create a pH gradient (O'Farrell, 1975). In order to obtain reproducible results one must,

among other factors, pay particular attention to the cooling of the systems under high current, the detergents used in the IEF gels and the effect of denaturing agents on the proteins. By using shorter and thinner IEF gels, significantly lower currents are required to run the gels thus essentially eliminating the need for a cooling apparatus and expensive high voltage power supply sources. This is made possible at the cost of decreasing the resolution of the protein spots in the gels although a shorter running times provide a definite advantage over the conventional methods. An example of such a system is the BIO-RAD's Mini-PROTEAN II for 2D SDS-PAGE.

Until recently, the protein identity of the spots could only be confirmed by western immunoblotting and/or Edman degradation techniques (Dunn, 1997). With the advent of more refined techniques of mass spectrometry, it is now possible to use the extracts from in gel digests of each silver stained protein spot to create a peptide mass map [110] (Schevchenko et al., 1996). This information may then be used to rapidly identify each protein by searching in an interactive web-based interface of sequences of known proteins.

Matrix-assisted laser desorption/ionization (MALDI) ionizes molecules with molecular masses of 100 – 100,000 daltons (Da) for analysis by mass spectrometry (MS). In MALDI-MS gas-phase ions are generated by the laser vaporization of a solid matrix/analyte mixture. The matrix contains photoexcited acidic or basic sites for ionization of sample molecules in ion/molecule collisions. The matrix adsorbs the radiation from the laser thus resulting in the simultaneous vaporization and ionization of the sample molecules. Ions are directed into the mass analyzer and the mass/charge (m/z) ratio is usually plotted against ion abundance (Fenselau, 1997). Time-of-flight (TOF)

analyzers are most commonly used with MALDI due to their high degree of sensitivity. MALDI TOF instruments are capable of detection in the attomole to femtomole range, their mass accuracy is generally within 0.1- 0.01% and their resolving power can exceed 1 part in 20,000 (Fenselau, 1997). The peptide mass map, which results from the MALDI analysis, is used to interrogate a protein database.

The Expert Protein Analysis System (ExPASy) was created in 1993 and was the first world wide web server dedicated to molecular biology (Hoogland et al., 1999). The server provides access to several proteomic databases containing protein sequence sequence information and twenty-three 2D SDS-PAGE reference maps which contain 592 protein entries (June 30, 1999). The ExPASy server is linked to the SWISS-PROT database of proteins, which includes 83367 entries (January 15, 2000). Among the multitude of software available for proteomic research are PepIdent and TagIdent. The former tool can identify proteins by using peptide mass fingerprinting data, pI and MW. Experimentally measured, user-specified peptide masses are compared with the theoretical peptides calculated for all proteins in SWISS-PROT. TagIdent tool generates a list of proteins close to a given pI and MW. Both types of software are extremely helpful in rapid identification of proteins in 2D SDS-PAGE systems (see http://www.expasy.ch/tools/#proteome). The Danish Centre for Human Genome Research's 2-D PAGE Databases (http://biobase.dk/cgi-bin/celis) is another excellent web-site for comparative evaluation of 2D PAGE data, in particular for skin cells. The MRC-5 2D database includes information on 262 proteins identified by this database and the human skin fibroblast database identifies 41 major proteins synthesized by these cells.

With the available 2D PAGE technology and the efficient methods for identification of proteins in SDS-PAGE gels, it is possible to map cellular responses to various biomaterials. In the near future, a database of biocompatibility is a realistic goal. This database could provide global information regarding the different biological reactions to various biomaterials and these may be able to identify the common factors of biocompatibility among these materials.

1.3. Specific aims

1.3.1. To find substrate-specific changes in protein expression by fibroblasts

To predictably modify cellular behavior on various materials, it is necessary to know the material-specific response of cells. Any behavioral change in cells is primarily brought about by a change in the synthesis and/or structure of cellular proteins. For this reason, it was our objective to determine whether substrate-specific changes occur in the expression of proteins of fibroblasts grown on titanium compared with tissue culture polystyrene. Both substrates are known to be suitable for culture of cells, whereas cpTi is an excellent biocompatible material *in vivo* (Gould et al., 1990; Gibbs, 1995; Adell et al., 1990).

1.3.2. To quantify the strength of cell adhesion to titanium and tissue culture polystyrene

Cellular adhesion is an important parameter in assessment of biocompatibility. Traditionally, stronger cell adhesion has been correlated with superior compatibility of the substrate. This idea is however challenged by recent observations that show an

intermediate strength of cell adhesion to be more suitable for cellular proliferation and migration (Dimilla et al., 1993). This suggests that material biocompatibility may require an optimal strength of cell adhesion to facilitate cell movement and interaction with their environment. We therefore aimed to quantify the strength of cell adhesion of fibroblasts to cpTi and tissue culture polystyrene.

1.3.3. To determine the composition of serum-adsorbed biofilms on titanium and tissue culture polystyrene

Components of extracellular matrix (ECM) such as fibronectin mediate adhesion of cells to various substrates (Wojciak-Stothard et al., 1996). The biological-interface between titanium and adherent cells is the junction between the adsorbed serum proteins, extracellular matrix, cell membrane components and the membrane-associated cytoskeleton. The initial interaction of all known substrates, including titanium (Ellingsen, 1991) with living tissues involves the adsorption of the components of the surrounding fluids, mainly from plasma, to the material surface (Sevastianov, 1991; Scarborough et al., 1969). The deposited proteins form a biofilm, the composition of which is determined by the surface properties of the material. The interaction of cells with this conditioning layer is a determinant of the cellular response that is manifested in the synthesis of proteins and the molecular organisation of cells. We aimed to identify the composition of the adsorbed biofilm on titanium and tissue culture polystyrene.

1.3.4. To gain insight into the composition, morphology and material property of the interface

The ECM is connected to the cytoskeleton by specific transmembrane receptor molecules. The tenacity with which cells adhere to a given substrate (strength of cell adhesion) therefore depends on the type and concentration of ECM ligands, the number of membrane-receptors, the receptor-ligand affinity and the strength of the cytoskeletal linkage to the membrane receptors. Surface chemistry and topography of biomaterials may alter ECM production and its assembly (Altankov et al., 1996; Chauo et al., 1995). Changes in the concentration and/or distribution of components of ECM at the cell-substratum interface may alter the strength of cell adhesion. By studying the underside of cells that remain behind after detaching the cells from titanium and tissue culture polystyrene, we hoped to gain more insight into the composition, morphology and the material property of the interface of fibroblasts attached to each surface.

1.3.5. To improve fibroblast adhesion to titanium

When fibroblasts are detached from glass or plastic with chelating agents, a significant amount of cellular material is left behind (Culp et al., 1979). This "substrate-attached material" (SAM) represents, in part, the remnants of focal adhesions, as well as some "close contact" material (Rollins and Culp, 1979). Culp (1974) reported that transformed cells become less mobile and resisted movement away from the colony edges when cultured on SAM. This property of SAM could not be mimicked by adsorbed serum alone.

At times it may be clinically useful to obtain a strong seal between titanium and its surrounding tissues. One of our objectives was to study the effects of SAM on adhesion of fibroblasts to titanium. We were also interested in finding the possible changes that may occur in the expression of cellular proteins when SAM-covered titanium was used as a substrate for skin fibroblasts.

1.3.6. To initiate establishment of a 2D database of proteins expressed by fibroblasts on titanium and tissue culture polystyrene

The basis for clinical success of any implant material is its ability to elicit a proper response at the tissue, cellular and molecular levels. Ultimately, the difference between a biocompatible material and a surface that can merely support cell attachment and growth is determined at the molecular level. Yet, there is a lack of consensus on what constitutes molecular biocompatibility. In order to study the changes in protein make-up of cells in contact with the surface-adsorbed biofilm, it is necessary to employ a method that is capable of resolving even subtle changes in protein composition. We aimed to take the first steps in initiating a 2D database of proteins expressed in human skin fibroblast cultured on titanium. Our ambition in doing so was to map the substrate-specific proteins responsible for biocompatibility of titanium and other materials.

CHAPTER 2: MATERIALS & METHODS

2.1. MATERIALS

2.1.1. Cell culture

Dulbecco's Minimal Essential Medium containing 10% (v/v) fetal bovine serum and antibiotic-antimycotic were all purchased from Gibco BRL, USA. Ninety-six -well "strip plates" with a well diameter of 6.4 mm and a growth area of 0.32 cm^2, made of tissue culture-treated, sterile and non-pyrogenic medical grade polystyrene, were obtained from Costar Inc. (Pleasanton, CA., USA). The wells from these plates could be separated and centrifuged individually. 100 mm culture dishes were purchased from Costar Inc. (Pleasanton, CA., USA). Commercially pure titanium discs were custom-manufactured (Nobel Biocare, AB Göteborg, Sweden) to be 2.00 mm thick and 6.35 mm in diameter and to fit tightly at the bottom of the wells in the 96-well strip plates. Titanium foils were 99.7% pure, 0.127 mm thick and purchased from Aldrich Chemical Company, USA. Chemicals for cleaning the titanium surfaces were purchased from Baker Chemicals (N.J., U.S.A).

2.1.2. Colorimetric hexosaminidase assay for analysis of cellular growth rate

The substrate for hexosaminidase, P-nitrophenyl-N-acetyl-beta-D-glucosaminide, Citric acid, Triton X-100, glycine and EDTA were purchased from Sigma (St. Louise, MO, U.S.A). Microplate reader was a product of Thermomax^{TM}, Molecular Devices Corp., CA., USA). The statistical software program GraphPad Prism 2.0 was made by GraphPad Software Inc., CA, USA.

2.1.3. Centrifugation detachment assay

Ninety-six-well "strip plates" were purchased from Costar (Pleasanton, CA., U.S.A). Titanium discs were custom manufactured by Nobel Biocare (Göteborg, Sweden). 1 ml cryotubes were purchased from Nunc, Roskilde, Denmark. A swinging bucket ultracentrifuge rotor (SW50.1) was made by Beckman Inc., U.S.A. The Coulter Counter was a model ZM produced by Coulter Counter Electronics Ltd, Luton, England and the ultra centrifuge was a model LM-8 (Beckman). Trypsin, EDTA and trypan blue were bought from Sigma.

2.1.4. Preparation of substrate-attached material

HEPES and ethylene bis (oxyethylenenitrilo) tetraacetic acid (EGTA) were purchased from Sigma.

2.1.5. Total protein assay

Sodium dodecyl sulfate (SDS) was purchased from Bio-Rad, USA. We used Centricon microconcenterators with a molecular weight cut-off of 10,000 Da. (Amicon, MA, USA). Spin-X UF centrifuge filters had a molecular weight cut-off of 10,000 Da (Coring Costar, MA, USA). Speedvac concentrator was made by Savant corporation (NY, USA). The Ninhydrin solution and glacial acetic acid were from Sigma and the microplate reader was Thermomax™ purchased from Molecular Devices Corp (CA., USA).

2.1.6. Fluorescence immunostaining

The non-fat dry milk was from Bio-Rad. Mouse monoclonal antibody against human cellular fibronectin was purchased from Sigma and the Goat polyclonal antibody (catalog number AB1950) against human integrin $\alpha 5/\beta 1$ or $\beta 5$ was from Chemicon (CA, USA). Fluorescein-conjugated goat (catalog number 401394, Calbiochem) and rabbit (product number, F-7367, Sigma) IgG were purchased from Sigma and Calbiochem-Novabiochem Corp., (CA, USA), respectively. Aquaperm mounting medium was from Lipshaw Immunon (PA, USA) and Kodak TMAX-400 films (Eastman Kodak, NY, USA) were used to photograph images provided by confocal microscopy.

2.1.7. Protein extraction for two dimensional gel electrophoresis

Dithiothreitol (DTT) and Biolyte ampholytes (3.0-10.0) were from Bio-Rad. CHAPS(3-[(3-Cholamidopropyl)dimethylammonio]-1-propane-sulfonate), phenyl-methylsulfonyl fluoride (PMSF) and butylated hydroxytoluene (BHT) were purchased from Sigma. Urea was from Fisher Scientific (TX, USA) and the microconcentrators with a molecular weight cut-off of 10,000 Da. were from Amicon.

2.1.8. First and second dimension electrophoresis

N,N-methylene-bisacrylamide (Bis), acrylamide and Biolyte ampholyte (3.0- 5.0) and (5.0 – 8.0), tétraethylenemethylenediamine (TEMED), ammonium persulfate, sodium dodecyl sulfate (SDS) ,N,N-methylene-bisacrylamide (Bis) and acrylamide were purchased from Bio-Rad. [3-(3-Cholamidopropyl)-dimethylamino-1-propanesulphonate]

CHAPS and Noniodet (NP 40) were from Sigma. Determination of isoelectric points and molecular weights were done by comparison with 2D SDS-PAGE of protein standards obtained from Bio-Rad.For staining of the gels with silver, sodium thiosulphate, silver nitrate, formaldehyde and acetic acid were obtained from Fisher Scientific.

2.1.9. Immunoblotting

Immobilon membranes were from Pharmacia, USA and non-fat milk was from Bio-Rad. Glycine, Tween 20 and methanol were from Fisher Scientific. Mouse monoclonal antibodies against vinculin (clone h VIN-1), cellular fibronectin (clone FN-3E2) were purchased from Sigma. Mouse ant-actin monoclonal antibody (catalog number MAB1501) was purchased from Chemicon. Perioxidase conjugated secondary antibody and diaminobenzidine, hydrogen peroxidase and cobalt chloride were purchased from Sigma.

2.1.10. Matrix-assisted laser desorption ionization mass spectrometry

For digestion of silver stained protein-spots excised from the gels, acetonitrile, ammonium carbonate (NH_4HCO_3), dithiothreitol (DTT), iodoacetamide, trypsin and trifluoroactic acid were purchased from Fisher Scientific. Samples for MALDI/MS were prepared using alpha-cyano-4-hydroxy-*trans*-cinnamic acid (Aldrich), methanol and acetone were from Fisher Scientific.

2.1.11. Deglycolysation by N-Glycosidase-F digestion

The enzyme N-Glycosidase F (NGF) was purchased from Boehringer Mannheim, GmbH. Microconcentrators (Ultrafree 15, Millipore, USA) had a molecular weight cut-off of 15000 Da., SDS and DTT were purchased from Bio-Rad.

2.1.12. Radiolabeling fibroblasts with [^{35}S] methionine and fluorography

Culture-medium without methionine was from GibCo BRL. Methionine labelled with [^{35}S] had a specific activity of 10 μCi / μL (Amersham Pharmacia Biotech, USA). Methanol and acetic acid were from Fisher scientific. Dimethyl sulfoxide (DMSO) and diphenyloxazole (PPO) were purchased from Sigma. X-ray films (X-OMAT AR, Kodack, USA) were used to produce the fluorographic images.

2.2. METHODS

2.2.1. Cell culture

Fibroblast cultures were established from the dermis of three normal individuals as described (Nakano and Scott, 1986). Human skin fibroblasts were grown in Dulbecco's Minimal Essential Medium containing 10% (v/v) fetal bovine serum and 1% (v/v) antibiotic-antimycotic at 37° C in an atmosphere of 5% (v/v) CO_2 in air. Cells between passages 2 and 9 were used. The cells were first grown in 75 cm^2 culture flasks in order to harvest a large number of cells required for the experiments. Depending on the experiment, ninety-six-well "strip plates", 100 mm culture dishes, titanium discs or titanium foils were used as substrates.

2.2.2. Titanium substrates

The discs were cleaned in 30% (v/v) nitric acid for 30 minutes and then, according to the standard Brånemark protocol (Hobo et al., 1989), i.e. sonication in butanol for 10 minutes, rinsing twice in 99% (v/v) ethanol and sonication for 10 minutes in 99% (v/v) ethanol. The discs were then rinsed and sonicated for 10 minutes in sterile deionized water in sterile glass containers. Subsequent procedures were carried out in a laminar flow hood and the discs were handled using autoclaved plastic instruments. A plastic suction tip was used to transfer each disc into a well and to tap it down into the bottom.

To obtain sufficient protein from SAM fractions, fibroblasts were cultured in 100 mm tissue culture dishes, with or without titanium foils. Titanium foils were cut to fit firmly at the bottom of each dish. Surface treatment of titanium foils was the same as for titanium discs.

2.2.3. Surface Characterisation

The surface roughness parameters of each substrate were evaluated by TopScan 3D, profilometric analysis using confocal design optics (Wennenberg et al., 1993). The laser beam (He-Ne) was about 1 μm in diameter. The measuring area was 245 x 245 μm for all measurements and each measurement consisted of 246 scans in each x and y direction. The resolution in the z direction (height) was about 20 nm. For the TPS surfaces (wells or culture dishes) two measurements were taken on 5 samples (total of 10 measurements). Ten titanium discs and ten titanium foils were measured, each at 2 sites (20 measurements in total for each titanium surface). All parameters were analyzed by

one-way ANOVA using GraphPad Prism™ version 2.00 (GraphPad Software Incorporation, USA) as the statistical program.

2.2.4. Growth rate analysis

To assess fibroblast growth rates, wells with or without titanium discs were seeded with 78 cells/mm^2 (2,500 cells/well) in 200 µL of medium. The number of cells attached to the substrates after 3 hours in culture was measured in six wells using the colorimetric assay for hexosaminidase (see section 3.5). At this particular seeding density, essentially all the fibroblasts attached to both substrates. The same assay was repeated in six more wells each day for 10 days to obtain growth curves.

Student's t-test (unpaired) was used to compare the mean number of fibroblasts for each day of the experiment and for each substrate. P-values <0.05 were considered significant.

2.2.5. Determination of cell numbers

The method of Landegren (1984) which uses p-nitrophenol-N-acetyl-β-D-glucosaminide as a synthetic substrate for the ubiquitous cytoplasmic enzyme hexosaminidase, was employed, with the modification that the substrate concentration was doubled to 15 mM. A standard curve was prepared relating hexosaminidase activity as measured by the colorimetric assay to number of cells (Fig. 2.1.). For this purpose human skin fibroblasts were grown in 75 cm^2 flasks until confluent. They were subsequently washed in PBS and harvested with 0.25% (w/v) trypsin. The cells were washed in PBS three times, resuspended in PBS and the number of cells was determined
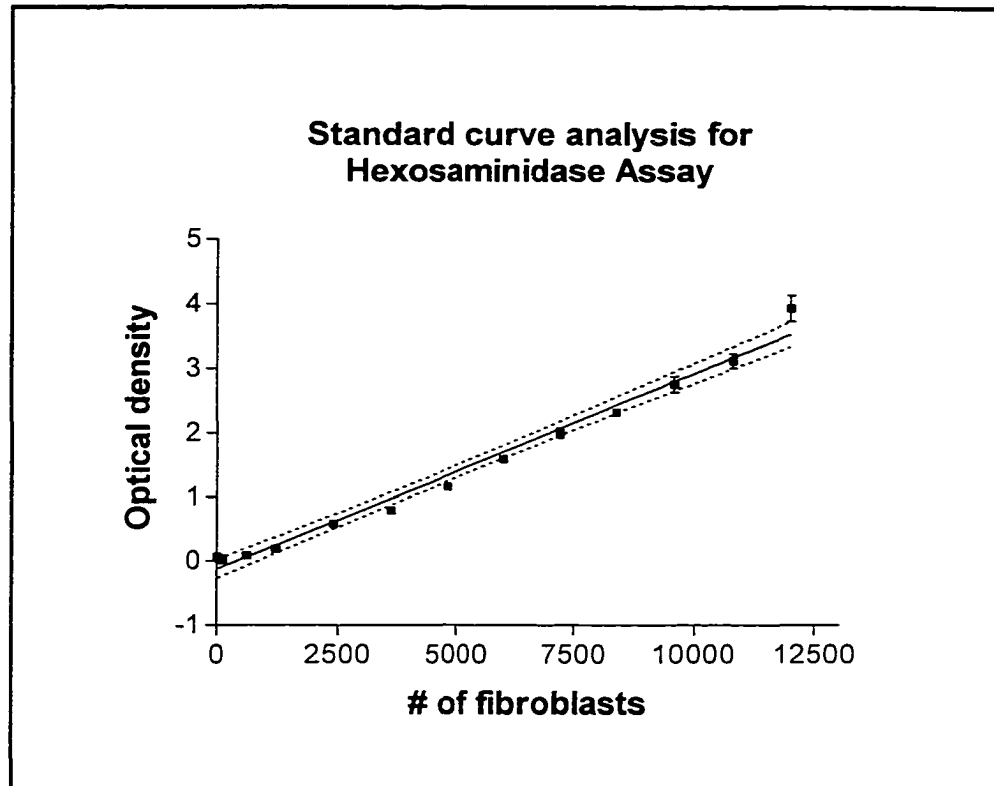
Fig. 2.1. Standard curve for hexosaminidase assay. Optical density was plotted against number of cells, giving a regression coefficient (r^2) of 0.98.

by staining an aliquot of the cell suspension with 0.05% (w/v) trypan blue and counting on a haemocytometer. Aliquots containing 60-12000 cells/75 μL were distributed into 96 well plates (n=6). To each well 75 μL of the substrate was added and the plate was incubated at 37° C for 1 hour. In order to read the absorbency of the solution without interference from the titanium discs, the contents were transferred to an empty well. One hundred μL of PBS and 100 μL of the developing reagent (150 mM glycine/5 mM EDTA, pH 10.4) was added to each well and the absorbance was immediately read at 405 nm on a microplate reader. The data were entered into the statistical program (GraphPad Prism™) and analysed by linear regression. Optical density was plotted against number of cells, giving a regression coefficient (r^2) of 0.98. The software allowed for derivation of a table relating optical density to cell number and this standard curve was used in centrifugational detachment assays to determine the number of cells remaining in each well. Percentage detachment was calculated from the ratio of the number of cells remaining attached on the substrate surface to the mean number of cells present in non-centrifuged wells. Cells detached from titanium foils were counted on a haemocytometer.

2.2.6. Centrifugation detachment assay

The following method is a modification of that described by Lotz et. al. (1989). Ninety-six well plates with or without titanium discs were seeded with 219 cells/mm² (7,000 cells/well), nine wells per group. Measurements were made on days 1, 3 and 5. Each well was gently filled to the top with PBS prewarmed to 37° C and inverted into a 1 ml cryotube previously filled with prewarmed PBS and the cap was closed. Each cryotube was then placed into a swinging bucket ultracentrifuge rotor (Fig. 2.2.). The
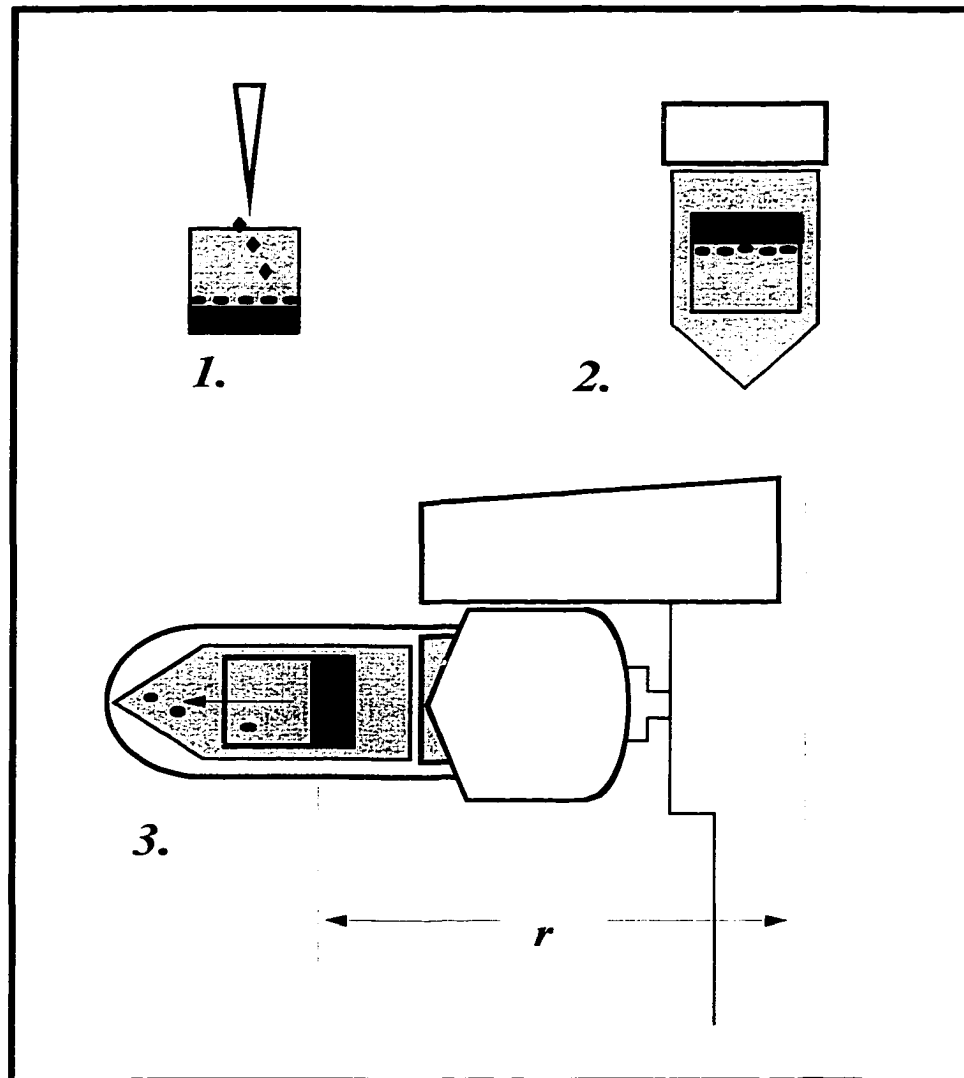
Fig. 2.2. Centrifugation detachment assay is carried out in three steps: 1) cells are cultured in 96 strip wells, 2) each well is placed in an inverted position inside a tightly fitting tube filled with PBS, 3) the wells are centrifuged at various speeds and the number of detached cells are determined and compared to the total number of cells.

radius of the rotor to the cell surface was measured and used in calculations of relative centrifugal force (RCF) where RCF is defined as the ratio of the weight of a particle in the centrifugal field to the weight of the same particle when acted on by gravity alone (Wilson and Goulding, 1992).

The maximum allowed force under these experimental conditions was 40,000 x g beyond which point the tubes deformed. The centrifuge was run for 10 minutes at 1,600, 16,900, 22,500 or 40,000x g (g= 981 dynes/gram). The force applied to the cells was calculated using the formula (Hubbe, 1981):

Formula 1. *F = (density of the cell - density of the medium) x volume of the cell x*

RCF x 981

The density of the cells was measured by Ficoll density gradient centrifugation (Sharpe, 1988) and found to be 1.02 g/cm^3. The density of PBS was taken to be 1.00 g/cm^3. Determinations of cell volume were made using a calibrated Coulter Counter. The average cell volume was found to be 1.0×10^{-8} cm^3.

At the maximum RCF the difference in the centrifugational radius caused by the 2mm thickness of the titanium disc is a negligible 0.10×10^{-8} dynes/cell.

2.2.7. Preparation of substrate-attached material

Normal skin fibroblasts were cultured on titanium discs (n=6). After 1, 3 or 5 days, the cells were washed gently three times with PBS and detached by incubating in HEPES buffer containing 1.0 mM ethylene bis (oxyethylenenitrilo) tetraacetic acid

(EGTA) for 1 hour at 37°C. The cultures were washed again three times in PBS to ensure complete removal of all cells. These surfaces were re-seeded with fibroblasts, as described below, without further treatment (Fig. 2.3.).

To obtain sufficient amounts of SAM protein for chemical analysis (see section 3.10), fibroblasts were cultured in 100 mm tissue culture dishes, with or without titanium foils, cut to fit firmly at the bottom of each dish.

2.2.8. Growth rate analysis on SAM-coated substrates

Both cpTi discs and TPS wells were coated with SAM from the third day in culture and then seeded with 7,000 cells per well. Cells were counted at 3 hours and each day thereafter for the same 5 day period as in the detachment assay described below.

2.2.9. Detachment assay on substrate-attached material coated cpTi

Fibroblasts (7,000 cells/well) from the same passage, for which growth curves had been obtained, were seeded onto the SAM-coated discs. A group of uncoated cpTi discs was included for each day (n=6). After 1 and 5 days incubation, groups of six wells were centrifuged at 40,000 x g. The detachment assay was performed as described in section 3.6.

2.2.10. Assay for total protein

Five 100 mm TPS dishes and five TPS dishes fitted with titanium foils were seeded at the same density as the microwell plates (219 cells/mm^2). After 5 days in
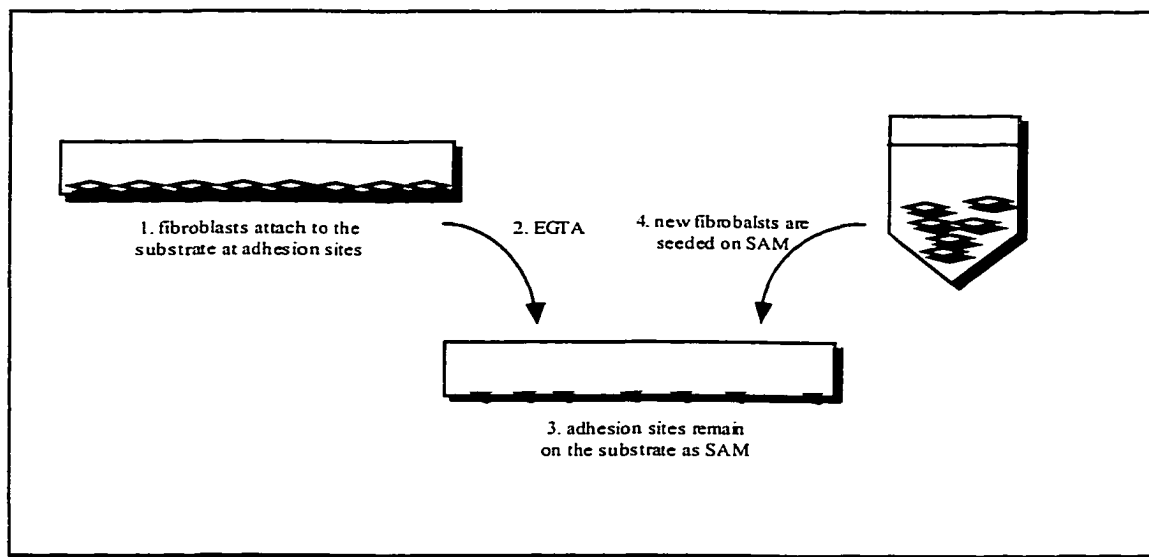
Fig. 2.3. Preparation of SAM coated cpTi, 1) fibroblasts are seeded on cpTi, 2) after incubation for various time intervals, the cells are rinsed and EGTA is added for 1 hour at 37° C, 3) extracellular matrix and cell adhesion sites remain attached to cpTi as SAM, 4) new fibroblasts are seeded on SAM-coated cpTi.

culture, cells from each group of five dishes were released with EGTA and pooled. An aliquot was used for counting by haemocytometer. The fibroblasts were centrifuged and the cell pellet was dissolved in 5 ml of 0.5% (w/v) sodium dodecyl sulfate (SDS). Five millilitres of 0.5% (w/v) SDS was also used to extract the substrate-attached material on both substrates. The cell and SAM fractions were each concentrated approximately 10-fold in Centricon microconcentrators with a molecular weight cut-off of 30,000 Daltons. The samples were transferred to Spin-X UF concentrators with the same molecular weight cut-off to be further concentrated to 85-120 uL. One to five microliter of each sample was lyophilised in a Speedvac concentrator for 2 hours. Twenty-five µL of 13.5 M NaOH was added to the samples and these were autoclaved at 121° C for 5 minutes. Forty microliter of glacial acetic acid and 80 µL of ninhydrin solution were added to each tube, which was then vortexed and incubated in a boiling water bath for 20 minutes. After the samples had cooled to room temperature, 400 µL of propan-2-ol (50% v/v) was added to each tube. Two hundred µL of each sample was transferred to a 96 well plate and the absorbance was read at 570 nm on the microplate reader. These values were compared to a standard curve prepared with bovine serum albumin. This experiment was repeated twice and the results compared using Student's t-test.

2.2.11. Fluorescence immunostaining

Intact cells and substrate-attached material from the fifth day were immunostained in triplicate. The samples were initially incubated for 1 hour with 2% (w/v) non-fat dry milk in PBS to block any non-specific interactions. Primary mouse antibody against human cellular fibronectin and a goat antibody against human integrin $\alpha5/\beta1$ or $\beta5$ were

used. The primary antibodies were diluted 1:500 in PBS and an aliquot was added to each well and incubated overnight at 4°C. After the samples were brought to room temperature they were rinsed 3 times with PBS. Fluorescein isothiocyanate (FITC)-conjugated goat or rabbit secondary antibody was added to each well which was incubated for 1 hour at 37° C and then rinsed three times with PBS. Specificity controls were carried out by omission of the primary antibodies. A thin layer of mounting medium was evenly spread on each substrate and allowed to dry. In order to observe the specimens, the cpTi discs were carefully punched out of each well and fixed on glass cover slips. The samples were observed directly under an inverted microscope equipped with UV illumination, and photographed at 10-20 X magnification using Kodak TMAX-400 film. Laser confocal microscopy was used at excitation wavelength of 488-568 nm, 565 beam splitter; 530 DF 30 filter for FITC detection; photomultiplier gain 700 V; laser attenuation 40 mV and pinhole 50 μm. Images were collected using the Image Space 3.20 software of the confocal microscope. Photographs were taken from the collected images under identical conditions using the camera directly connected to the computer screen.

2.2.12. Preparation of adsorbed proteins from serum

In the experiments involving analysis of adsorbed serum proteins, the 96-well strip with or without titanium discs were filled with 150 μL of the culture medium with 10% fetal bovine or human serum and incubated for 5 days.

2.2.13. Protein extraction

Samples of fibroblasts in culture or adsorbed serum proteins were extracted using the sample buffer according to methods of Hochstrasser (Hochstrasser et al., 1988) with some modifications. After 1 or 5 days in culture, cells were rinsed three times in PBS and extracted using a buffer containing dithiothreitol (DTT, 0.65 M), CHAPS (3-[(3-Cholamidopropyl) dimethylammonio]-1-propane-sulfonate)(0.65M), urea (8.9M), 2% (v/v) Bio-Lyte ampholyte (3.0-10.0), PMSF (1 mM) and butylated hydroxytoluene (BHT)(0.23 mM) in distilled water. One hundred μL of the extraction buffer was added to the first of 8 wells in each experimental group and after 5 minutes this was transferred to the next well until all wells in each group were extracted. The extract was centrifuged at 90,000X g in order to remove large cellular fragments, such as the nuclei which may cause smearing of the first dimension gels. The samples were concentrated 5X using microconcentrators with a molecular weight cut-off of 10,000 Daltons and kept at -80 ° C. Samples extracted from cpTi and TPS were kept at the same volume through out the extraction procedures.

Solubilization of total serum proteins from fetal bovine or human serum were carried out by preparing a 1:500 dilution of 10% fetal bovine or human serum in the extraction buffer.

2.2.14. First dimension isoelectric focusing

Separation of the proteins was carried out essentially as described by Hochstrasser and co-workers (1988), with some modifications. Isoelectric focussing gels, using N,N-methylene-bisacrylamide (Bis) as the crosslinking agent, contained 9.25 M urea, 16.7%

acrylamide/BIS (respectively 30% (w/v) and 0.8% (w/v) dissolved in deionised water as stock), 1% (v/v) Bio-Lyte™ (5.0-8.0) and 4.4% (v/v) Bio-Lyte™ (3.0-10.0) and 5.5 % CHAPS/Nonidet (NP40) solution (30% w/v CHAPS) and 10% (v/v) Nonidet (NP40) in distilled water. The detergent solution was added after degassing the mixture containing the acrylamide/BIS. Seven µL of TEMED and 15 µL of ammonium persulfate (10%) (w/v) were added to this mixture to initiate polymerisation.

A Mini-Protean II ™ system (Bio-Rad, USA) was used for isoelectric focusing. The upper chamber was filled with degassed NaOH solution (20 mM) (catholyte) and the lower chamber was filled with degassed H_3PO_4 solution (6 mM) (anolyte). With the upper chamber filled with anolyte gentle suction was used to remove the air bubbles from the top of the gel tubes and sample reservoirs. The cell was connected to the power supply and the gel tubes were pre-electrophoresed at 200 V for 10 minutes, 300 V for 15 minutes and 400 V for 15 minutes. Twenty µL of overlay solution (500 µL of extraction buffer: 500 µL of distilled water : 40 µL of 0.05% w/v bromophenol blue) was added to the top of the gels. The samples (10-30 µL) were gently underlaid below the overlay solution and the tubes were electrophoresed at 500 V for 10 minutes and at 750 V for 3.5 hours.

After the first dimension was complete, the tubes were removed from the tube adapters and disconnected from the sample reservoirs. A 1.0 mL syringe filled with equilibration buffer (6% (v/v) of 0.05% (w/v) bromophenol blue solution, 19% (v/v) of 10% (w/v) SDS solution, 14% (v/v) of 0.5 mol/litre Tris-HCl buffer, pH 6.8 and 49% (v/v) of deionised distilled water) was connected to one end of the gel tube ejector. A tube gel was inserted in the other end of the gel ejector and the gel was slowly extruded

into a 1.5 ml Eppendorf tube along with approximately 150 µL of the equilibration buffer and immediately placed at -80° C.

2.2.15. Second dimension SDS-PAGE

Gels for SDS-PAGE were prepared according to Laemmli (Laemmli, 1970). Gels, 7.5% or 10%, were cast in Mini-Protean II dual slab cells. The IEF capillary gels were thawed and placed on a clean glass slide, excess equilibration buffer was removed by gentle suction and the tube gel was transferred to and pushed down between the glass plates. The running buffer was prepared and cooled. The gel apparatus was placed in an ice-bath and the gels were run at 50 V for 15 minutes and then at 160 V for 50 minutes at constant voltage.

2.2.16. Silver staining

After electrophoresis, the gels were fixed in 50% (v/v) methanol and then in 5% (v/v) acetic acid in water for 20 minutes. They were then washed for 10 minutes with 50% (v/v) methanol in water and additionally for 10 minutes with water to remove the remaining acetic acid. The gels were sensitised by a 1-minute incubation in 0.02% (w/v) sodium thiosulphate, and then rinsed with two changes of water for 1 minute each. After rinsing, the gels were submerged in 0.1% (w/v) silver nitrate and incubated at 4° C for 20 minutes. After incubation, the silver nitrate was discarded and the gels were rinsed twice with water for 1 minute and then developed in 0.04% (v/v) formalin in 2% (w/v) sodium carbonate with intensive shaking. As soon as this solution turned yellow it was replaced

by fresh liquid until the proteins were clearly visualised in the gels. Development was stopped by soaking the gels in 5% (v/v) acetic acid. The gels were stored in distilled water at 4° C until analysed.

2.2.17. Measurement of isoelectric point (pI) and molecular weight (MW)

2D SDS-PAGE standards were electrophoresed in the first and second dimension concomitantly with the experimental samples. By measuring the position of the standard proteins in the gel, standard curves were derived using a statistical program. The standard curves were used to generate the apparent pI and MW of the spots in question. The theoretical values for pI and MW of the proteins were calculated from their amino acid sequences using the available online tools (Compute pI / MW) for each Swiss Protein entry.

2.2.18. Identification of actin and vinculin by immunodetection

In order to identify vinculin, actin and fibronectin in the 2-D SDS-PAGE gels, western blotting was performed. Immediately after the second dimension electrophoresis was completed, the gel was placed on a piece of Immobilon-P membrane that was presoaked in 100% methanol for 15 seconds to activate the membrane. Electroblotting was performed for 1 hour at 60 V in a mini transfer apparatus. The transfer buffer consisted of 25 mM Tris base, 192 mM glycine and 10% (v/v) methanol. The membrane was then air dried at room temperature. After wetting the membrane with 100% methanol, they were incubated with 2% (w/v) non-fat milk dissolved in PBS for 1 hour in order to

block non-specific binding. Mouse monoclonal antibodies against vinculin, cellular fibronectin and actin (1:500 dilution in 0.8% (v/v) Tween-PBS) were added to the membranes and incubated for 2 hours at room temperature. After washing the membranes 4 X 5 minutes in PBS, peroxidase-conjugated secondary antibody (1:1000 dilution in 0.1% (v/v) Tween-PBS) was added to the p.apers and incubated for 1.5 hours at room temperature. A solution of diaminobenzidine (DAB) in PBS (0.5 mg/mL) was prepared. Three microliter of 1% (w/v) Cobalt chloride . and 3 μL of hydrogen peroxidase (30% v/v) was added to 10 mL of the DAB solution. The membranes were then washed 4 X 5 minutes in PBS and transferred to this solution and left until sufficient colour developed. As a control, immunoblotting was performmed without the primary antibody. The membranes were washed and dried and scanned. The pI and the MW of the spots in the gels were estimated by comparing to 2D SDS-PAGE standards that were run simultaneously with each experimental group. In addition, cellular fibronectin was run simultaneously as a standard.

2.2.19. In gel digestion

Protein spots were excised from the gel. The gel pieces were put into 0.6-mL vials and rinsed with 100 mM ammonium carbonate (NH$_4$HCO$_3$) to ensure the pH was about 8.5. This NH$_4$HCO$_3$ solution was removed by a pipette and replaced with 10 μL of the same buffer solution and 2 μL of 90mM dithiotreitol (DTT). The gels were smashed using the tip of a thin 0.25-mL plastic vial. After incubation for 30 min at 50° C, the suspension was cooled to ambient temperature. Two microliter of 200 mM iodoacetamide was then added. The gel samples were incubated at room temperature for 30 min. 1 μL

of 0.2 μg/μL trypsin was added for digestion at 37° C for 2 to 5 hours. Peptides were extracted three times into 20 μL of 75%(v/v) acetonitrile in 0.25% (v/v) trifluoroacetic acid (HPLC grade) / water with vortexing for 20 second and sonication for 20 minutes, followed by addition of 10 μL of acetonitrile. The pooled extracts were evaporated to dryness under vacuum.

2.2.20. Sample preparation for MALDI analysis

A two-layer method was used for coating probes for MALDI mass spectrometry (Dai et.al, 1997). The first-layer solution was prepared with 10 mg of matrix (α-cyano-4-hydroxy-*trans*-cinnamic acid) in 1 mL methanol/acetone (reagent grade)(1:4 v/v). The second-layer solution was a saturated solution of matrix in 40% (v/v) methanol in water. Five μL of the second-layer solution was added to each vial containing dried sample. The vial was vortexed to dissolve the sample. Two μL of the first-layer solution was deposited onto a probe tip to form a thin layer. Onto this layer, 0.5 - 1 μL of the sample/matrix mixture was deposited and allowed to dry. The sample layer was washed three times with water.

2.2.21. MALDI mass spectrometry

Mass spectral data on protein digests were collected on a home-built time-lag focusing MALDI TOF mass spectrometer, described in detail elsewhere (Whitall and Li, 1995). In general 60 laser shots (3-5 FJ pulse energy) were averaged to produce a mass spectrum. Spectra were acquired and processed with Hewlett-Packard supporting software and reprocessed with the Igor Pro software package (WaveMetrics, Inc., Lake

Oswego, OR). The pulse delay was set to 0.25μs and the pulse voltage was optimized at 2.8kV for the best resolution in peptide mass range. The individual spectra were internally calibrated with trypsin autolysis peptide peaks and matrix peaks.

2.2.22. Peptide mass mapping and identification

The mass search program PeptIdent (http://expasy.hcuge.ch/cgi-bin/peptident.) was used. The protein mass range and isoelectric point estimated by the position of the protein spot in the gel were entered initially with an assumed accuracy of +/- 10%. If this initial search did not produce a result the estimated accuracy was relaxed to +/- 20%. For "well-behaving" globular proteins the mass can be determined with accuracy of 5-10%, however a much lower degree of precision can be expected on smaller gels. In addition protein modifications such as glycosylation must be considered (Jungblut, 1997). The cleavage reagent was known to be trypsin. Since the time of "ingel" digestion was fairly short (30 min.) we only allowed for 1 missed cleavage (Jimenez CR et.al., 1998). Cysteine was designated to be carboxamidomethylated by iodoacetamide and methionine was not permitted to be oxidized. The mass tolerance for peptides was set at +/- 500 ppm (Schevchenko et.al., 1996). Peptides found in a blank piece of gel were subtracted from each sample and the remaining peaks were used in the database search. After identification of the highest scoring proteins, the theoretical monoisotopic and average tryptic peptide masses for each protein were calculated (http://www.expasy.ch/cgi-bin/peptide-mass) and manually compared with the masses measured by MALDI/MS. In order to test the reliability of the peptide mapping procedures, spots containing easily identifiable proteins such as actin and bovine serum albumin were analyzed in the same

and bovine serum albumin were analyzed in the same manner. Some easily distinguishable spots were identified by comparison with the Human Skin Fibroblasts-IEF database (http://biosun.biobase.dk/~pdi/2Dgallery/P473mirror_map.html) or by comparison to the human plasma database (http://www.expasy.ch/cgi-bin/ch2d-compute-map?PLASMA_HUMAN,P2161). Presently, there is no bovine plasma 2D gel database available on the Internet therefore serum proteins were compared to the Swiss 2D PAGE's human 2D gel database.

2.2.23. Deglycosylation of proteins by N-Glycosidase F

The presence of a glycoprotein in one protein spot was established by testing the effect of digestion with the enzyme N-glycosidase F (Boehringer-Mannheim online-catalog, http://biochem.roche.com/pack-insert/1365169A.pdf). Samples of whole cell lysates (2mL, in extraction buffer) from confluent cells were washed in 10 ml of 0.1 M sodium phosphate buffer (pH 6-8.5) by filtering through a microconcentrator (Ultrafree 15, Millipore, USA). To 20 μl of this sample, 10 μl of incubation buffer containing 0.055 units of N-glycosidase-F (Boehringer-Mannheim, GmbH) was added The incubation buffer consisted of 25 mM EDTA, 0.1% (w/v) NP-40, 0.2% (w/v) SDS and 1.0% (w/v) DTT in 120 μl of solution. This solution was incubated at 37° C overnight and the samples were resuspended in the extraction buffer by washing and reconcentrating with 450 μl of fresh extraction buffer. As control, 20 μl of the same sample was treated with the same procedure but without enzyme.

2.2.24. Radiolabeling with [^{35}S] methionine

SAM-coated cpTi discs were prepared as described in section 3.7. Fibroblasts (7 x 10 ^{3} cells) were seeded on each of three SAM-coated cpTi and three uncoated cpTi discs. The culture medium (150 μL/well) contained methionine-free DMEM (Gibco BRL) with 10% (v/v) methionine-free FBS (Gibco BRL) to which 10 μCi [^{35}S] methionine was added. Twenty-four hours later, the medium was removed and the wells were rinsed twice with PBS and the cells were extracted with 50 μL/well of extraction buffer (see section 3.13).

A similar procedure was used to obtain [^{35}S] methionine-labelled proteins from fibroblasts grown on SAM-coated and uncoated cpTi discs after 72 and 120 hours in culture except that the fibroblasts were initially seeded in normal DMEM containing 10% (v/v) FBS. Twenty-four hours before extraction, the cells were rinsed twice with methionine-free medium (Gibco BRL) and each well was filled with 150 μL of culture medium without methionine containing 10% (v/v) methionine-free FBS (Gibco BRL). To radioactively label the proteins, 10 μCi of [^{35}S] methionine was added to each well and the wells were incubated for 24 hours. Two-dimensional SDS-PAGE analyses were performed as described in sections (3.14 and 3.15).

2.2.25. Fluorography

Fluorography was performed according to a protocol by Celis (1997). The gels were fixed for 60 min in methanol:acetic acid:H$_2$O (450ml:75ml:475ml) at room temperature and then placed in 120 mL of DMSO and shaken for 20 min for two times. They were transfered into 120 ml DMSO containing 0.4% (w/v) 2,5-diphenyloxazole for

After this solution was removed, the gels were washed twice in water for 15 min, marked

and dried in a gel drier apparatus for 3 hours at 60 ° C. The dried gels were placed on X-

ray films in the dark and placed in -80° C for 24 hrs before development.

CHAPTER 3: RESULTS

3.1. Surface roughness of the substrates

Table 3.1., shows the results of the profilometric analysis of the substrates used in our experiments. All four parameters of surface roughness showed a significant difference when analyzed by one-way ANOVA ($p<0.0001$) (Table 3.1). The larger distances between irregularities (in x direction) found on the TPS culture dishes resulted in a smoother surface as compared to TPS wells (Table 3.1. and Fig. 3.1a, 3.1c.). The frequency of the irregularities on the two types of TPS surfaces (wells and culture dishes) was considerably lower than on the two different cpTi surfaces (discs and foils). From Table 3.1., it is evident that the height of the irregularities on both types of TPS surfaces were smaller than the corresponding values measured on cpTi surfaces. Overall, the surfaces of cpTi substrates were rougher than the TPS surfaces (Fig 3.1a.-3.1d.).

We found that the two different titanium surfaces had different profiles. The foils had a porous surface-texture whereas the surfaces of the discs were mostly grooved. The irregularities on the cpTi foils were significantly deeper than those on cpTi discs (Table 3.1. and Fig. 3.1a. and 3.1b.). This resulted in an overall increase of 7.4% in the surface area of cpTi foils as compared to the cpTi discs.

3.2. Growth of fibroblasts on tissue culture polystyrene and titanium surfaces

Typical growth curves are depicted in Figure 3.2. Three hours after seeding 2,500 cells/well, nearly all fibroblasts attached to both substrates. The doubling times were calculated by performing linear regression analysis of the data points during the log phase of growth and found to be 43 hours for cells on cpTi discs and 56 hours for cells on TPS wells. In three separate experiments the fibroblasts were always found to

Table 3.1. Profilometric measurements of the various substrates used in our studies. All values were shown to be significantly different by one-way ANOVA and Bonferroni post test (p<0.0001).

substrate	Height of irregularities (μm)		Distance between peaks in x direction (μm)		Distance between peaks in y direction (μm)		% increase in surface area	
	mean	S.D.	mean	S.D.	mean	S.D.	mean	S.D.
cpTi discs	0.25	0.05	9.99	1.39	5.02	0.40	10.49	3.64
cpTi foils	0.36	0.04	11.05	1.10	4.54	0.07	17.89	2.94
tps wells	0.12	0.07	11.97	2.94	4.38	0.74	2.23	2.56
tps dishes	0.10	0.03	21.82	5.30	3.84	0.12	1.67	1.11
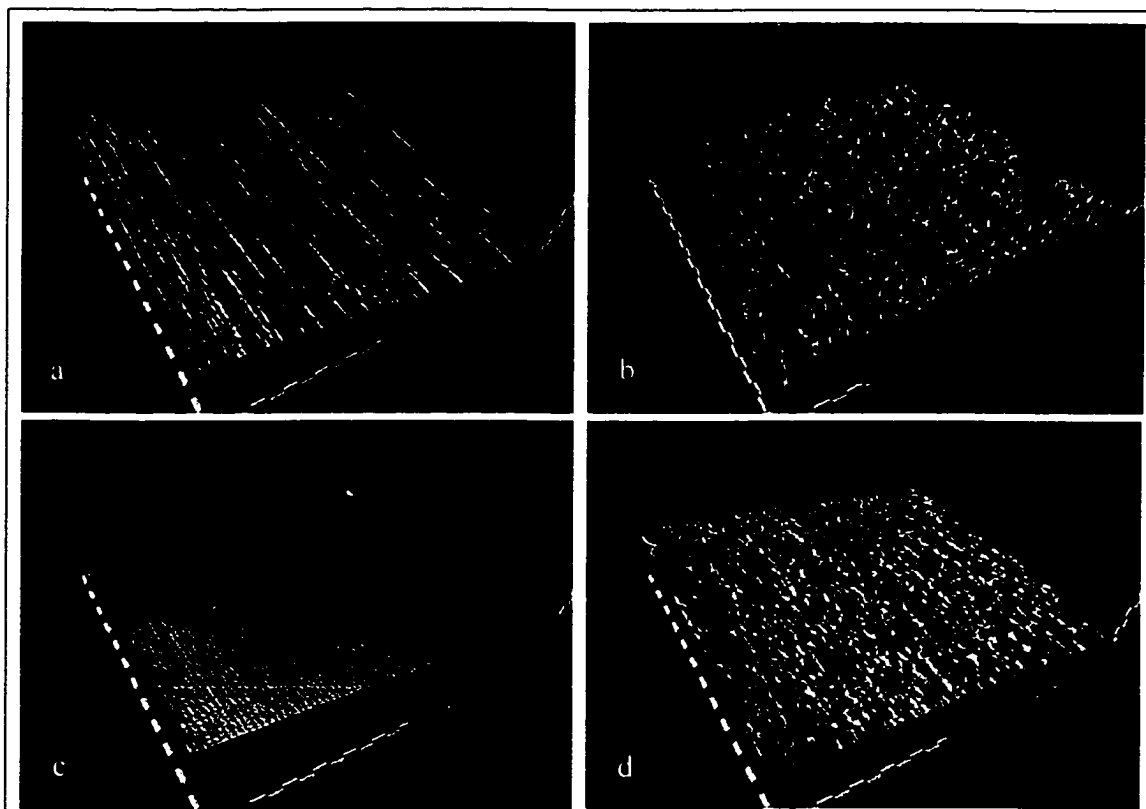
Fig. 3.1. Profilometric analysis of the experimental surfaces, a) TPS dishes, b) cpTi foils, C) TPS wells, d) cpTi disks.
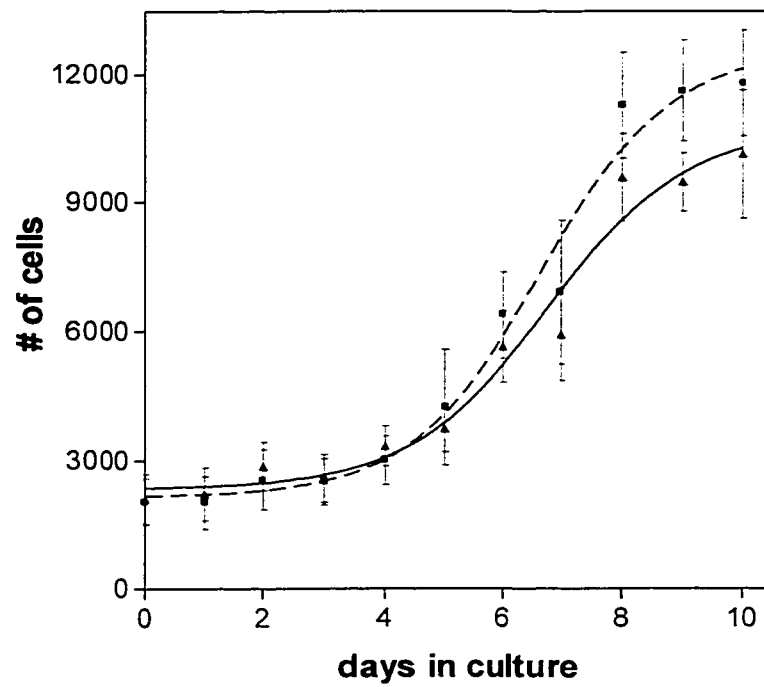
Fig. 3.2. Growth of fibroblasts on cpTi ▬ and TPS ▲ surfaces.

Results are shown as the mean number of cells in six wells +/- 1 S.D.

grow faster on titanium than on plastic but the differences were not statistically significant when analyzed by non-linear correlation analysis of all data points on the growth curves.

3.3. Fibroblasts adhere less strongly to titanium than to tissue culture polystyrene

Figure 3.3. illustrates the results of centrifugational detachment assays on cells cultured for various times on cpTi discs or TPS wells. At no point during the 5 day incubation period did the fibroblasts cultured on TPS show a detachment rate higher than 10%, even at 40,000 x g, whereas the detachment rate for fibroblasts cultured on cpTi was dependent on time in culture. On day 1 only about 15% of the fibroblasts were detached from cpTi after 10 minutes at 40,000 x g but at 3 days this had risen to 75% and at 5 days to about 90%. The difference in percentage of cells detached from cpTi by 40,000 x g on day 5 compared to day 1 was highly significant by Student's t-test ($p<0.001$), as was the difference between cells detached from cpTi and plastic by 40,000 x g at day 5 ($p<0.0001$). Using Formula 1(section 2.2.6) the force exerted at the point where 50% of the fibroblasts had detached was calculated to be 7.40×10^{-3} and 6.26×10^{-3} dynes/cell, at 3 days and 5 days respectively. These experiments have been repeated with dermal fibroblasts from two other donors with essentially the same results (data not shown).

3.4. Substrate-attached material enhances attachment of fibroblasts to titanium

Three hours after seeding, significantly more cells had attached to non-coated than to SAM-coated surfaces (Fig. 3.4.). During the subsequent 5 days (the duration of
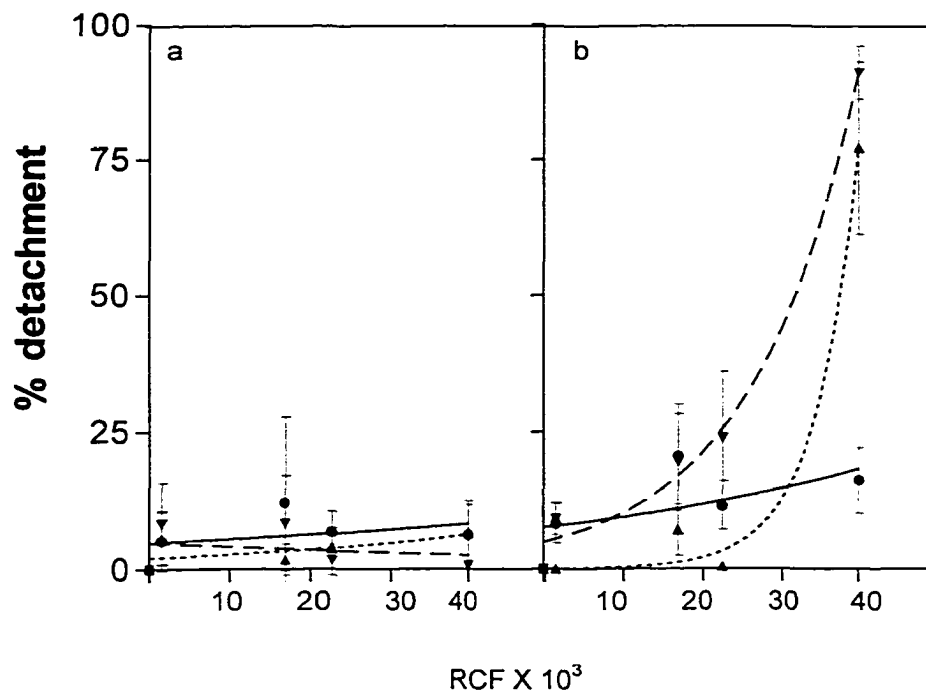
Fig. 3.3. Detachment of fibroblasts at various relative centrifugational force (RCF) from: a) TPS, b) cpTi. Fibroblasts were grown on these surfaces for 1 day —●— , 3 days --Δ- and 5 days —∇— . Results are shown as mean +/- 1 S.D. for 3 separate experiments with 5 wells used for each point.
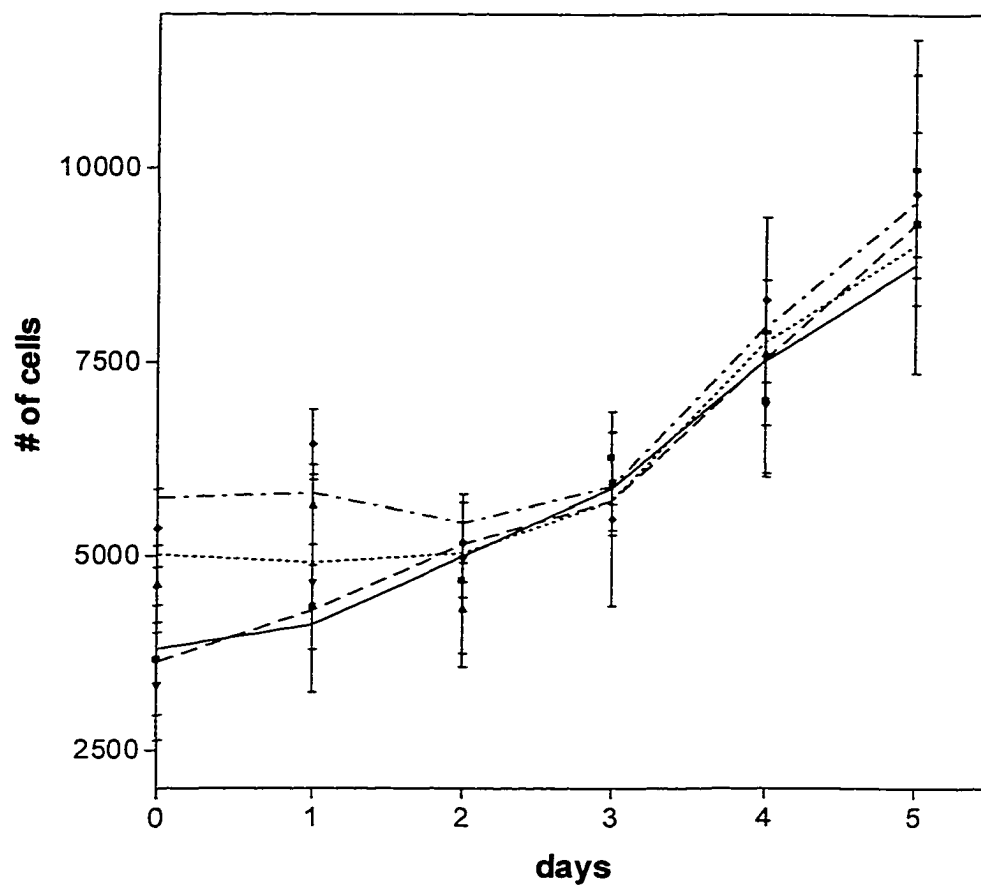
Fig. 3.4. Growth of fibroblasts on uncoated cpTi —■—, uncoated TPS—∇— ,

SAM-coated cpTi --Δ-- and SAM-coated TPS—◆— . Results shown are the

means +/- 1 S.D. for 6 wells.

the experiment), there did not appear to be any significant difference in the rate of proliferation of fibroblasts on these two surfaces.

Figure 3.5. shows the percentage detachment of fibroblasts cultured on cpTi coated with SAM. As expected, after 1 day of culture on uncoated cpTi or cpTi coated with 1, 3 or 5 day SAM, fewer than 15% of the cells were detached at 40,000 x g. There was no statistically significant difference between the groups, one day after seeding (one-way ANOVA). However, after 5 days in culture, fibroblasts grown on SAM prepared from 3 or 5 day cultures showed a significantly lower detachment (~6 fold) than those on non-coated surfaces or those coated with SAM from 1 day cultures (p < 0.001 in all cases). These results show that despite an initial lower efficiency of attachment, the adherence of fibroblasts is significantly enhanced when cpTi is coated with SAM prepared from the later cultures.

3.5. More protein remains on tissue culture polystyrene than on titanium

Table 3.2. shows the results of the assays for total protein. There was no significant difference in the total amount of protein (cells and SAM) on the two surfaces (1.08-2.02 x 10^{-4} mg/mm^2). However, the amount of protein left in the SAM fraction on TPS surfaces was approximately twice that on cpTi surfaces. The corresponding quantities from the cell fractions also reflect the fact that more cellular material remained in SAM extracted from TPS surfaces.
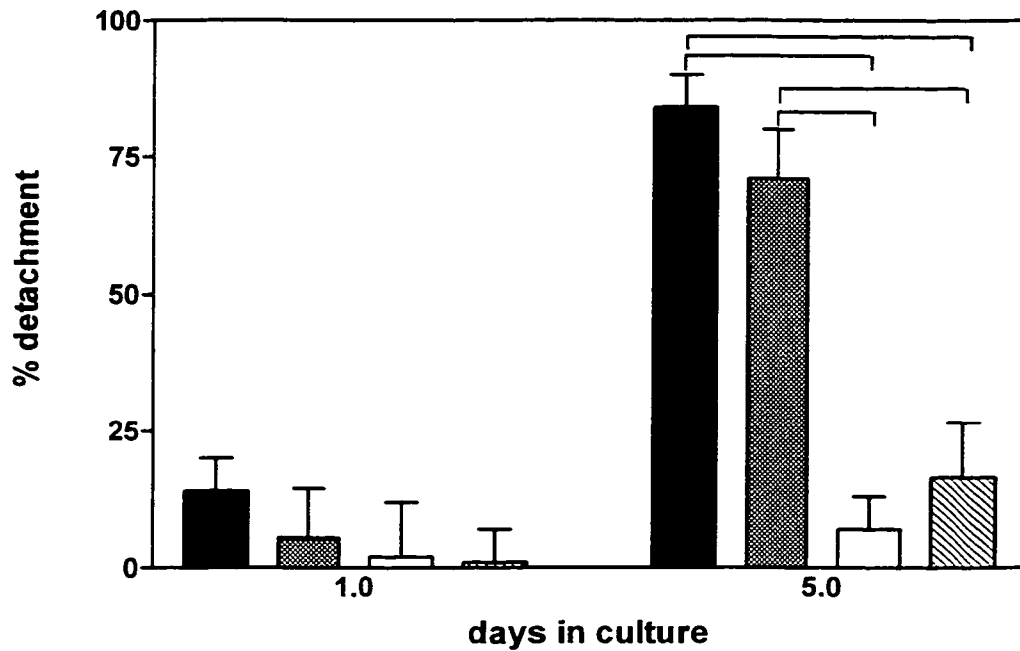
Fig. 3.5. Detachment of fibroblasts, 1 day vs. 5 days after seeding, from SAM-coated and uncoated cpTi. Uncoated cpTi ■, cpTi coated with 1 day SAM ▩, cpTi coated with 3 day SAM ▭ , cpTi coated with 5 day SAM ▩. Results shown are the average of 5 wells + 1 S.D. Brackets connect bars which were significantly different ($p < 0.001$) by one-way ANOVA and Bonferroni post test.

Table 3.2.   Quantification of protein on cpTi and TPS from five 100 mm

tissue culture dishes.

	cpTi protein (mg)	TPS protein (mg) ± S.D.
Cell fraction	5.21±0.50	4.38±0.06
SAM fraction*	0.39±0.02	0.65±0.04
Protein/mm^2 ‡	$2.02\mathrm{x}10^{-4}$	$1.80\mathrm{x}10^{-4}$
Protein/cell ‡	$5.70\mathrm{x}10^{-7}\pm1.70\mathrm{x}10^{-8}$	$6.03\mathrm{x}10^{-7}\pm1.00\mathrm{x}10^{-8}$
%SAM*	7.15±0.77	12.90±0.57

*t-test shows a significant difference (p<0.05, n=2)

‡ Total protein (cell + SAM)

### 3.6.	Organisation of fibronectin and its receptors differ on titanium and tissue culture plastic

Figure 3.6. shows the results of the immunofluorescence staining of cellular fibronectin and its receptor at 5 days in culture. The data shown are representative of two separate experiments with 5 samples in each group. The matrix of intact cellular fibronectin on TPS (Fig. 3.6a.) is made up of dense and compact patches of fibrillar structure and in some areas it is devoid of fibres. On titanium (Fig 3.6d.) the fibres are evenly spaced and organised into a uniform network that follow the direction of the grooves. Substrate-attached material on TPS appears to be made up of larger fragments, resembling fibrillar aggregates, whereas SAM labelled on titanium discs is made up of smaller fragments of individual fibres (Fig. 3.6b., 3.6e.). Interestingly, these fragments follow the direction of the grooves present on the cpTi as a result of the polishing.

Fluorescently-labelled fibronectin receptors ($\alpha5/\beta1$ or $\beta5$) in SAM from fibroblasts grown on cpTi show a random and diffuse distribution (Fig. 3.6f.). The receptors were more numerous in the SAM that had been prepared on TPS and they closely followed the outlines of the cells (Fig. 3.6c).

### 3.7.	More serum proteins adsorb onto titanium than on tissue culture polystyrene

In order to distinguish cellular proteins from proteins adsorbed from serum, we incubated the two cpTi and TPS surfaces with culture medium containing 10% (v/v) fetal bovine serum for 5 days and analyzed the results by 2D-PAGE. Figure 3.7. shows silver-stained gels of the adsorbed biofilms collected from cpTi (Fig. 3.7a) and TPS (Fig 3.7b) and Table 3.3. lists the serum proteins that were identified. Several of these proteins
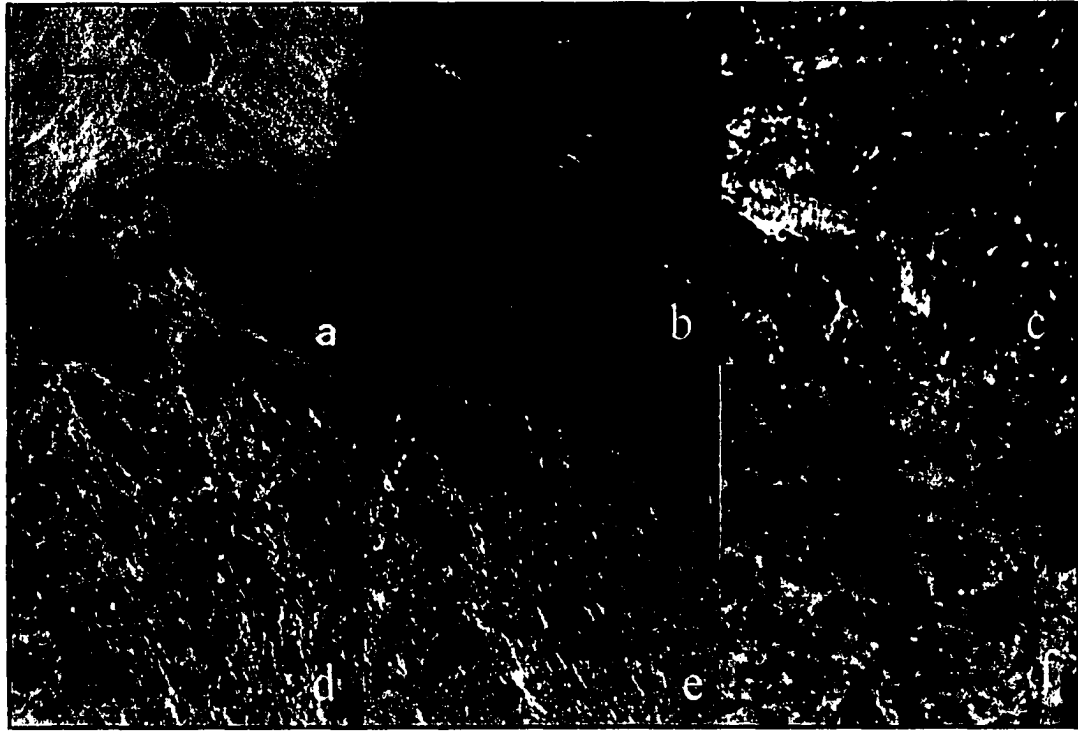
Fig. 3.6. Immunofluorescence staining for fibronectin and its receptor (α5/β1 or β5) in intact cells or SAM, after 5 days in culture. Cellular fibronectin beneath intact fibroblasts on TPS (a) and cpTi (d) Cellular fibronectin in SAM on TPS (b) and cpTi (e) (Magnification, 250 X, bar = 10μm) Images from confocal microscopy of fibronectin receptors on TPS (c) and cpTi (f) (magnification 500 X, bar = 20μm) The bar in 5a applies to all parts of the figure
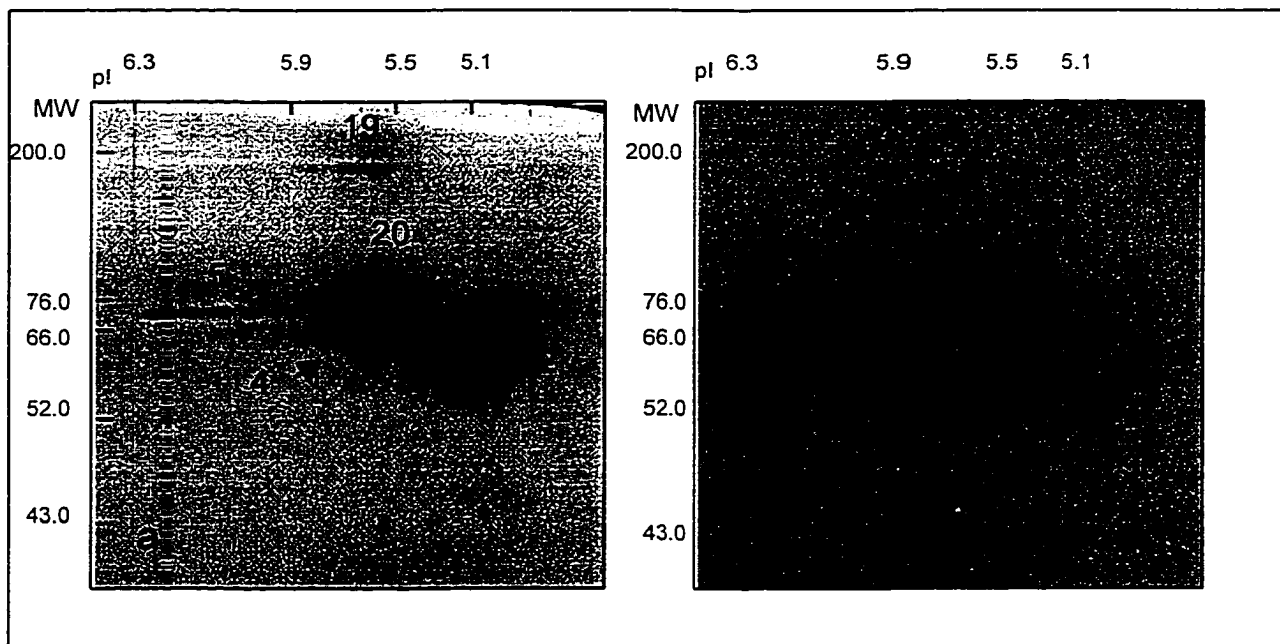
Fig. 3.7. Silver stained 2D- SDS PAGE of bovine serum adsorbed proteins extracted from a) cpTi and b) tps surfaces. cpTi surface shows significantly higher adsorption of serum proteins (spots 1-5, 19-21). All the spots were identified except spot 19 (see table 3.1.).

Table 3.3. Adsorbed proteins from bovine and human serum

Spot No.[1]	Protein name (species)[2]	Accession Code[3]	identification Method[4]	Apparent[5]		Theoretical[6]	
				pI	MW	pI	MW
1	Fetuin[7] (b), α2 HS glycoprotein (h)	P12763	Swiss 2D, MALDI(9/27)	4.00	60.0	5.10	36.4
2	Thrombospondin 1 (b,h)	Q28178	Swiss 2D, MALDI(5/29)	4.50	57.0	4.22	52.1
3	α-fetoprotein (b, h)	P02772[8]	Swiss 2D, MALDI(5/28)	5.10	58.0	5.54	65.3[8]
4	Serum albumin (b, h)	P02769	Swiss 2D, MALDI(15/42)	5.50	65.0	5.60	66.4
5	Plasminogen (b, h)	P06868	Swiss 2D, MALDI(11/21)	6.10	72.0	6.40	63.1
19	Unknown (b)			5.40	>100.0		
20	Serum albumin (b)	P02769	Swiss 2D, MALDI(12/21)	5.50	72.0	5.60	66.4
21	Serotransferrin (b)	Q29443	Swiss 2D, MALDI(5/13)	5.80	66.0	6.50	75.9
22	Haptoglobin 1 β-chain (h)	P00737	Swiss 2D	5.50	43.0	6.30	27.3
23	Serum albumin (h)	P02768	Swiss 2D, MALDI(9/25)	5.65	65.0	5.67	66.5
24	Serum albumin (h)	P02768	Swiss 2D, MALDI(12/39)	5.75	65.0	5.67	66.5
25	IgG heavy chain γ (h)	P99006	Swiss 2D	6.40	51.0		
26	IgG light chain (h)	P99007	Swiss 2D	6.40	25.0		
27	Complement 3 (C3DG)(h)	P01024	Swiss 2D, MALDI(4/16)	5.00	39.0	5.00	38.9
28	Apo A-1 (h)	P02647	Swiss 2D	5.20	23.0	5.27	28.1
29	Haptoglobin 1 α-chain (h)	P00737	Swiss 2D	5.40	17.0	5.23	9.20
30	VTDB (h)	P02774	Swiss 2D	5.00	58.0	5.20	51.2
48	Serum amyloid P (h)	P02743	Swiss 2D	5.30	26.0	6.12	23.3

Footnotes to Table 3.3.

1. Spot numbers refer to the numbers given in 2D SDSPAGE gels in Figures 3.7. – 3.9. and 3.10. - 3.11.

2. Proteins identified by MALDI/MS were Spot 1-2, 4-7, Spot 16, Spot 19-21. Proteins identified by comparison to human 2D database are Spot 8-14 and Spot 17-18. Spot 19 could not be identified by either method.

3. Swiss Protein codes start with a letter, accession codes of the proteins found in Human 2D database start with a number. These codes facilitate retrieval of information about each protein from the appropriate database.

4. Swiss 2D refers to the human plasma 2D, Human 2D refers to the human skin or the MRC5 – IEF database, MALDI refers to matrix assisted laser desorption mass spectrometry and the numbers in the parenthesis are the numbers of peptides matched/number of peptides found. IB refers to immunoblotting, 2D-std refers to comparison to standard 2D proteins.

5. Apparent values of pI and MW were measured from the 2D SDS PAGE gels.

6. If the given sequence of the database belongs to the precursor molecule, the signal fragment is not used in calculating the pI and MW. No values were assigned if the sequence of the protein could not be found in the database.

7. Treatment with N-acetyl glycosidase-F identified the protein as a glycoprotein.

8. Amino acid sequence of bovine α-fetoprotein is not available for peptide mass mapping, therefore this spot was analyzed by peptide mass mapping of its mouse homolog.

(spots 1 – 5) were also seen in the extracts collected from whole cells (Figs. 3.8. and 3.9.). The adsorption of serum proteins is noticeably much higher on cpTi than on TPS. Spots 1-5 were clearly much more abundant in both the adsorbed biofilm and in whole cell-extracts collected from cpTi (Fig 3.7a, 3.8a and 3.9a). It is important to note that the extraction and loading volumes were the same for samples from cpTi and TPS.

To test whether this surface adsorption was selective, proteins in total (non-adsorbed) bovine serum were also investigated by 2D-PAGE. Since the same spots appeared in the biofilms adsorbed from bovine serum as in the total serum (Fig.3.10.), we concluded that the adsorption was non-selective.

Adsorption of human serum proteins was also analyzed by 2D-PAGE (Fig.3.11.). As with the fetal bovine serum, human serum-proteins appear to adsorb non-selectively to both surfaces (but see below).

Protein spots 1-5 were common to both the fetal bovine and human sera, however spots 1, 2 and 3 were present at higher levels in the bovine serum. Overall, more proteins were detected in the human serum (Table 3.3.). Human serum proteins 22, 24, 25, 26 and 29 were not detectable in the TPS biofilm, despite their relatively high concentrations in the serum (Fig. 3.11a and 3.11c).

Mass spectrometric analysis of the tryptic digests of the separated bovine serum proteins identified spot 1 as fetuin (Fig. 3.12.), also known as α-2-HS-glycoprotein (A2HS). This identification was confirmed by repeating the analysis twice in two separate experiments. Furthermore, this spot was also identified in the Swiss 2D-PAGE human plasma database. The protein appears as a series of 4 spots, the largest of which is also the most basic (Fig 3.13.). This sort of pattern is commonly seen for proteins with
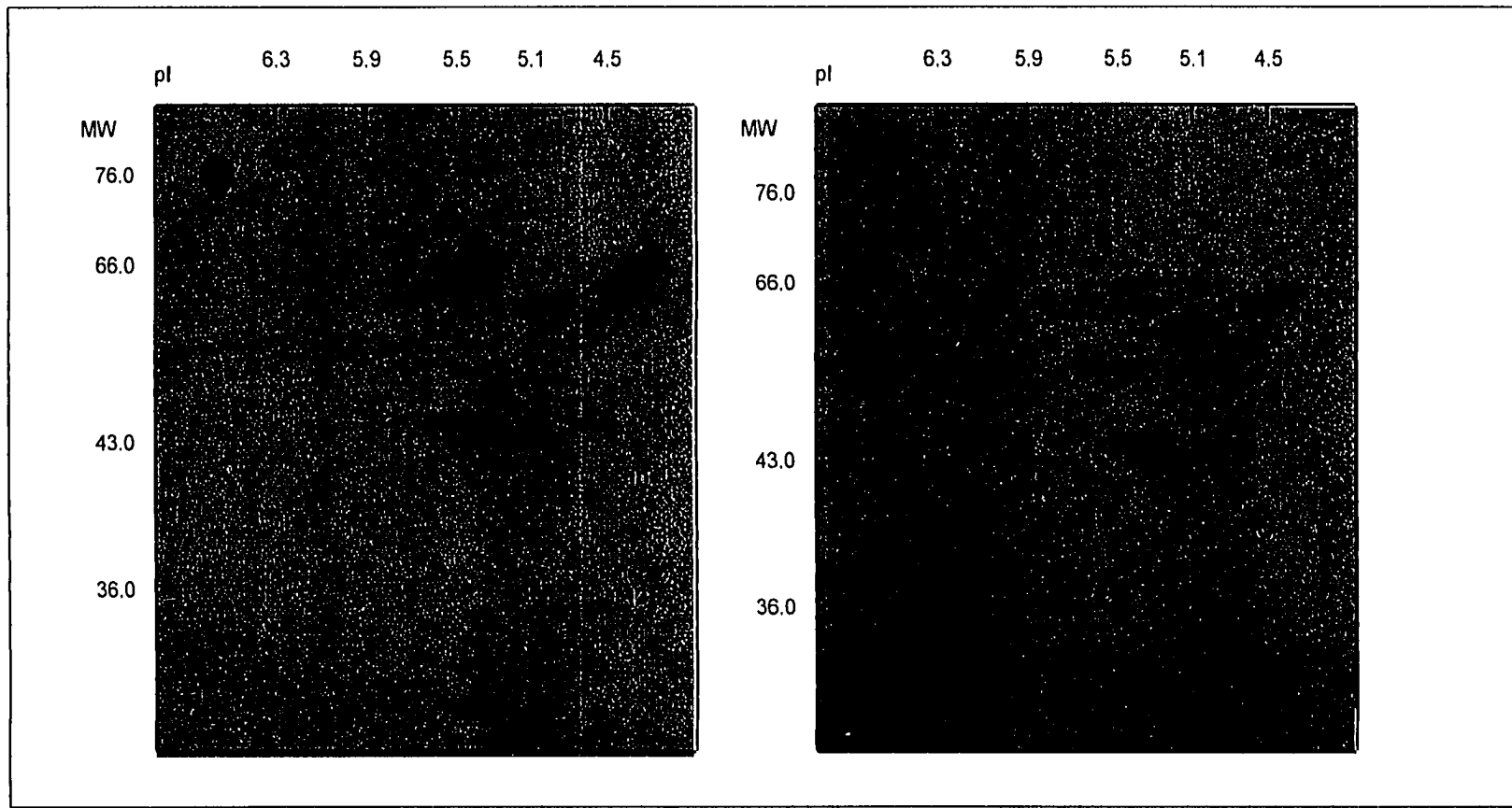
Fig.3.8. Silver stained 2D- SDS PAGE of total cell extracts from day 1 on a) cpTi and b) tps surfaces. Protein spots 1-5 show increased concentration on cpTi. The increased staining of protein spot 8 on tps is particular to this gel only and was not a consistent finding in other similar samples.
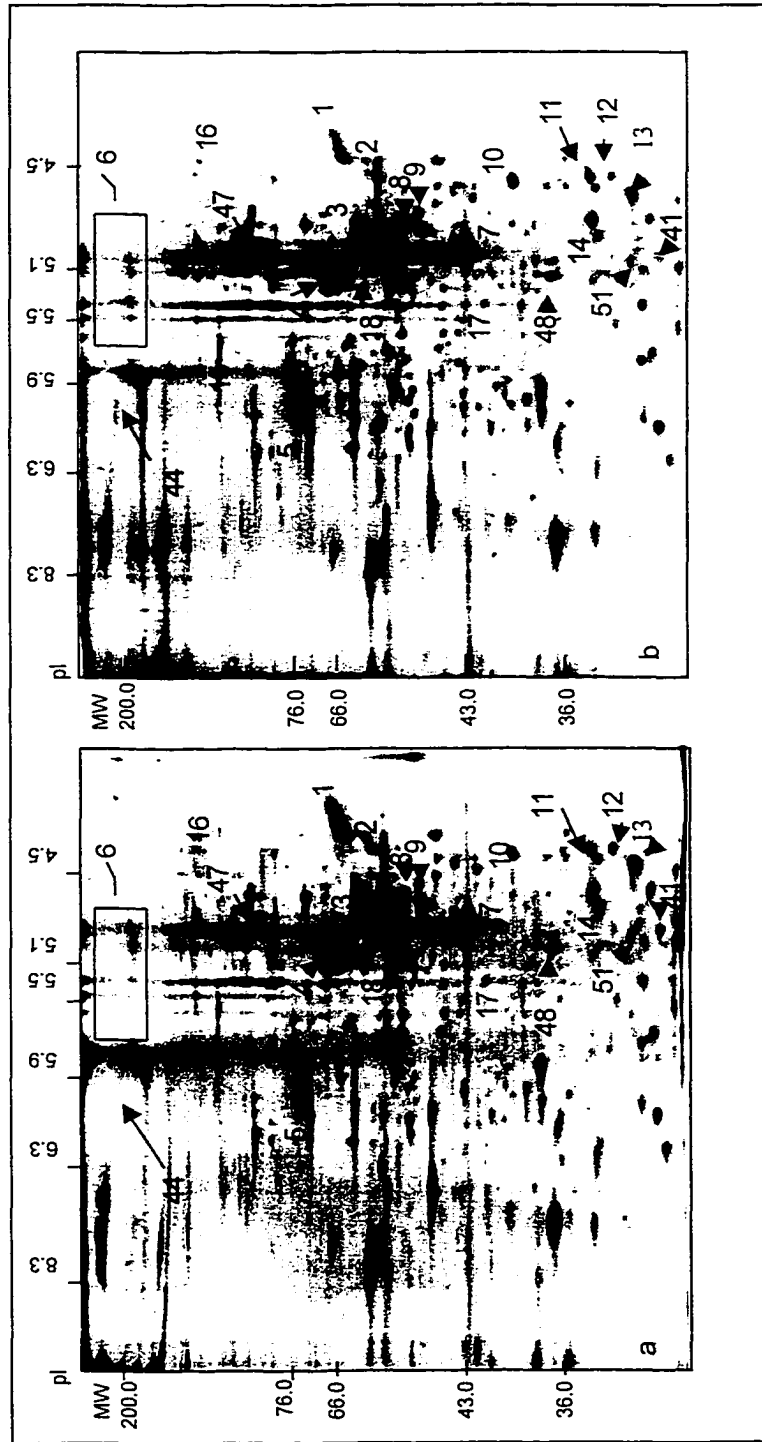
Fig.3.9. Silver stained 2D- SDS PAGE of whole cell extracts from day 5 on a) cpTi and
b) tps. Protein spots 6 and 44 show increased expression on tps.
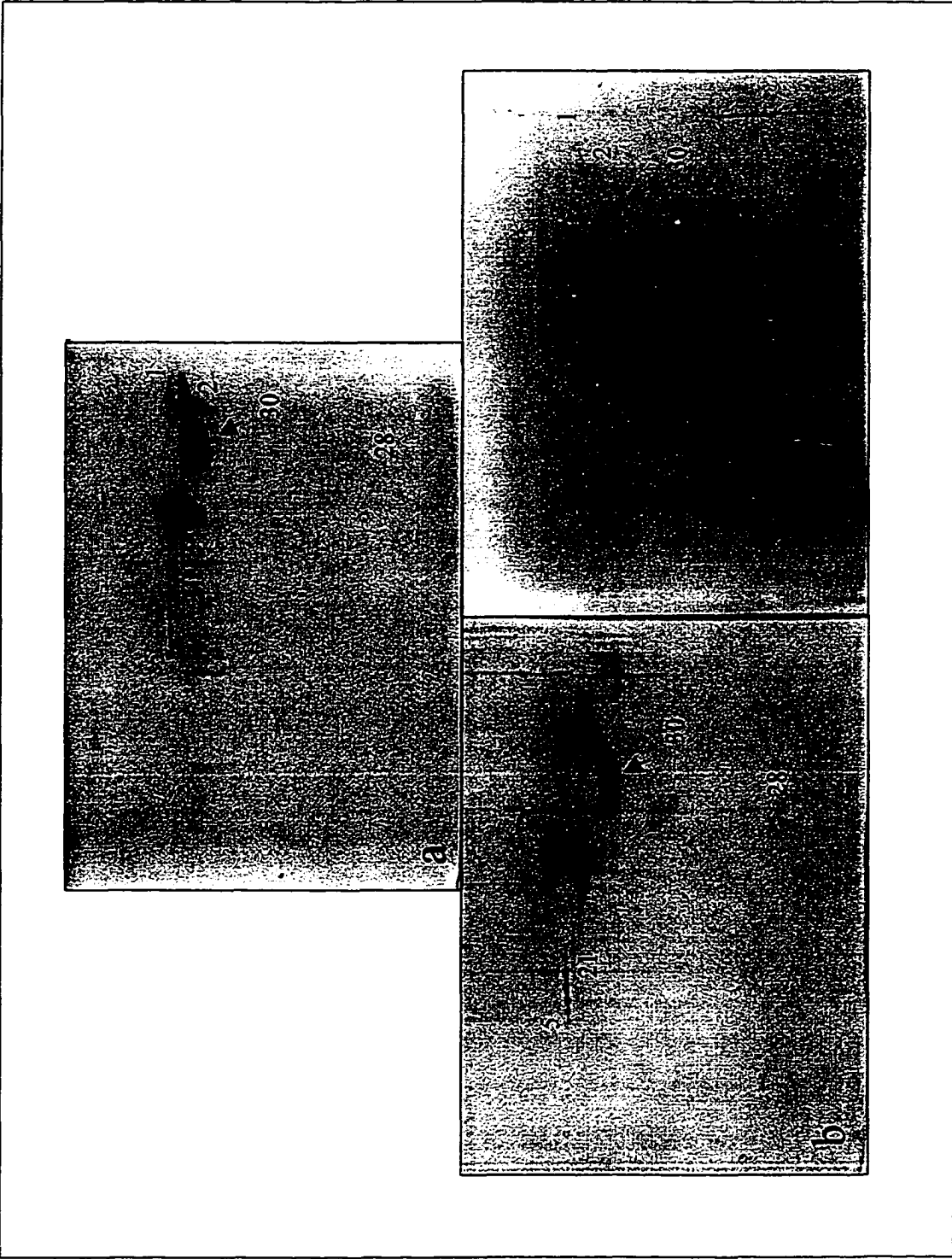
Fig. 3.10. Silver stained 2D-SDS PAGE of proteins in fetal bovine serum a) whole serum, b) adsorbed proteins to cpTi, c) adsorbed proteins to TPS.
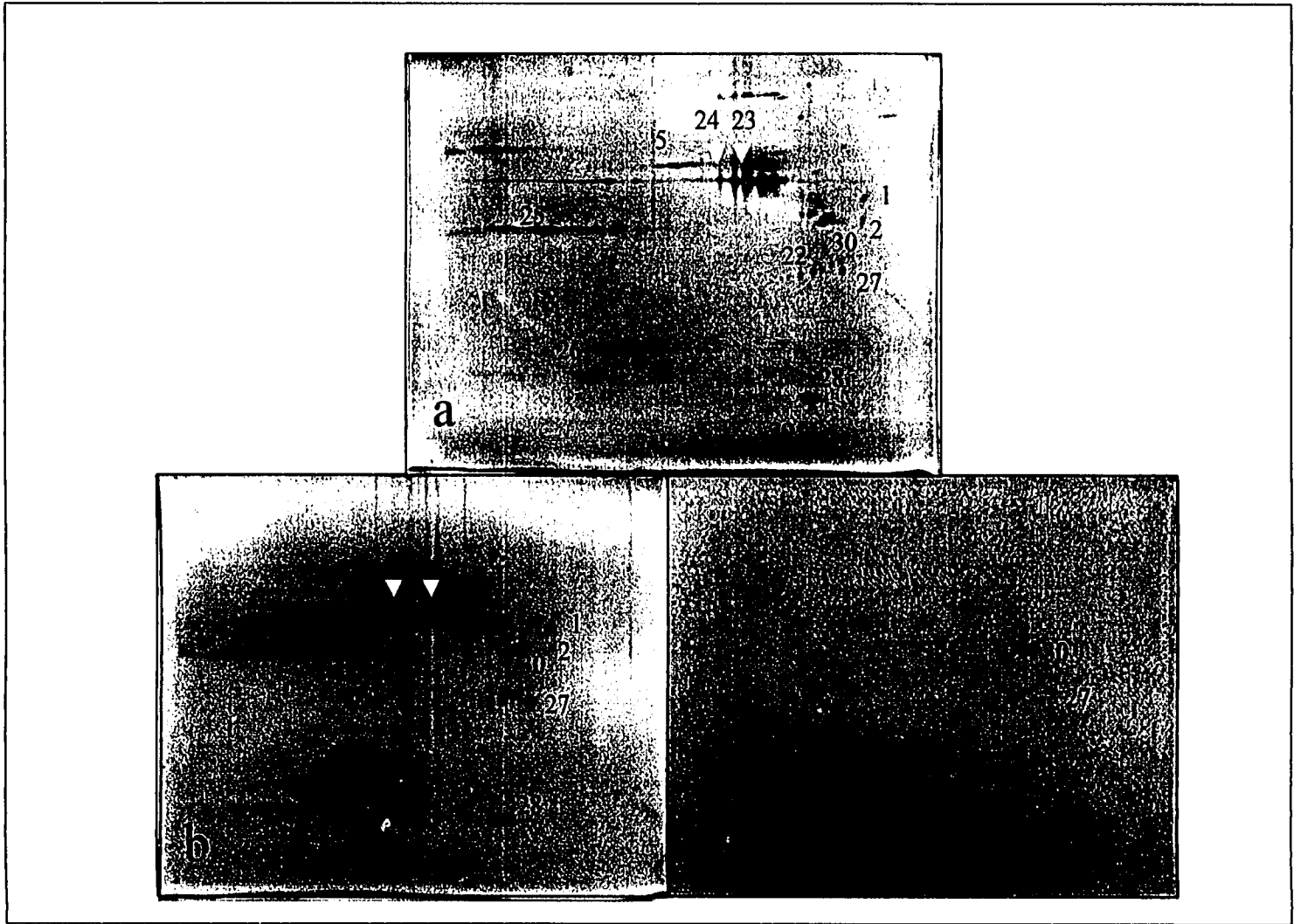
Fig.3.11. Silver stained 2D-SDS PAGE of a) proteins in human serum, b) adsorbed proteins of human

serum to cpTi and c) adsorbed proteins of human serum to tps. The adsorption appears to be non-selective

to both surfaces.

Fetuin (P12763)
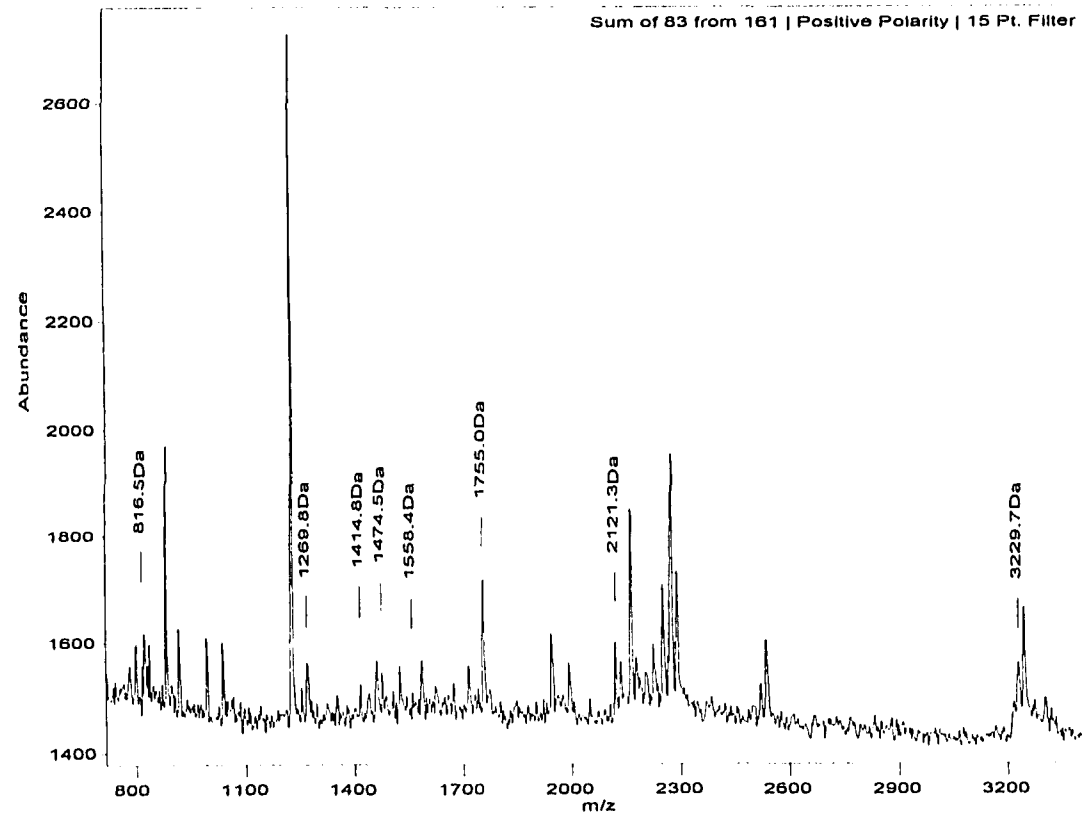
Fig. 3.12. Mass spectrum of the tryptic peptides of spot 1 from 2D SDS PAGE of whole cell extracts identified as fetuin.
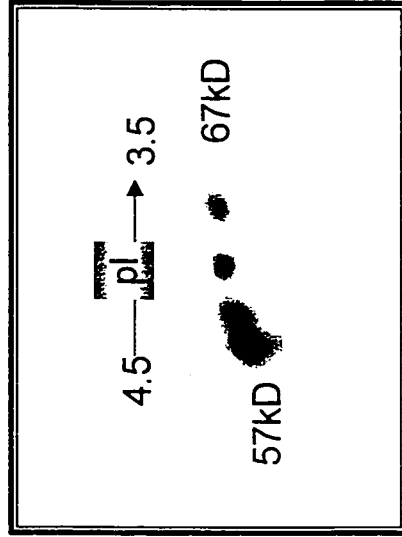
Fig.3.13. The four isoforms of fetuin molecule are shown as present in the silver-stained 2D SDS PAGE.

several glycosylation sites where addition of oligosaccharides contributes to the formation of larger and more acidic isoforms. The effects of deglycosylation with N-glycosidase F (Fig. 3.14.) confirmed that spot 1 is a glycoprotein.

Spot 2 was tentatively identified as thrombospondin 1 (TSP1), however only 5/29 peptide masses matched and we could not confirm this spot in the human plasma 2D database. The search in the bovine database for the peptide masses obtained for spot 3 did not show any matches, however a search in the mammalian database showed 4 peptide mass matches for the mouse vitamin D binding protein (VTDB). Since VTDB is a homolog of α-fetoprotein (FETA), which is the second most abundant protein in the fetal bovine serum after serum albumin, we suspected that spot 3 might contain FETA. Indeed, manual peptide mass matching yielded 5 matches with mouse FETA and in addition the theoretical pI (5.54) and MW (65 kDa) of FETA are close to our measured values. The Swiss Protein database does not include a sequence for bovine FETA, which explains why our first search did not identify this protein. Spot 4 was identified as serum albumin and this was confirmed by comparison to the human plasma 2D gel database. Spot 5 was found to contain bovine plasminogen (PLMN). This was confirmed in two independent experiments. Plasminogen runs as a series of spots run at an apparent pI of 6.30 - 5.90.

The less extensively adsorbed bovine serum protein spots 19, 20, 21 and 30 (Fig. 3.7.) were analyzed by MALDI/MS. We identified spot 20 as bovine albumin and spot 21 was found to contain serotransferrin. We were not able to extract sufficient material from spot 30 for peptide mass mapping but comparison to the Swiss 2D-PAGE human
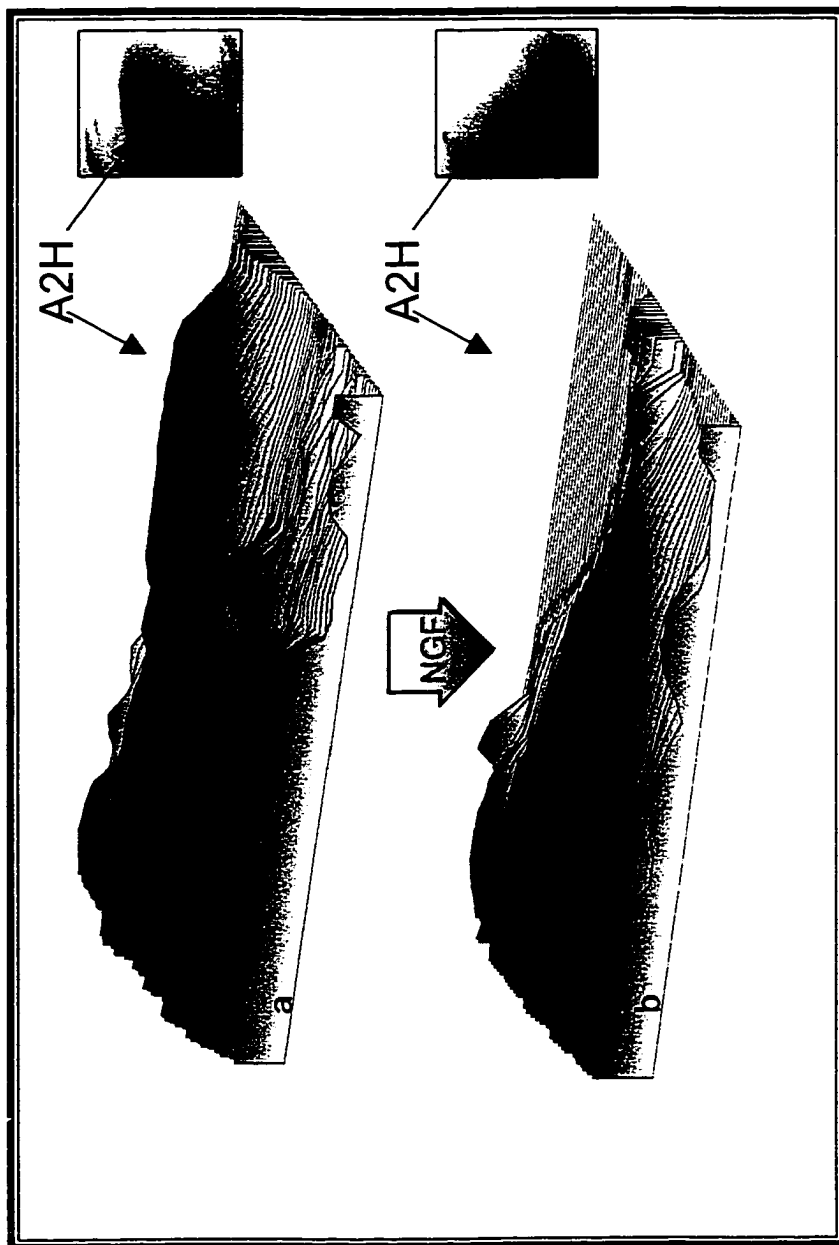
Fig. 3.14. Densitometric results of the fetuin (A2H) spot a) before and b) after treatment with N Glycosidase F.

plasma database suggests that spot 30 contains the vitamin D binding protein (VTDB) and corresponds to spot 30 from human serum (Fig. 3.11.).

Spots 22 and 29 in Figure 3.11. were identified as haptoglobin 1 by comparison to the Swiss Protein 2D gel database. As expected, MALDI/MS analysis of spots 4, 23 and 24 confirmed them to contain isoforms of human serum albumin. Two prominent components of immunoglobulin: IgG light chain (spot 25) and IgG heavy chain (spot 26), were readily identifiable by comparison to the Swiss 2D human plasma database. Analysis by MALDI/MS showed spot 27 to contain complement 3. This was further confirmed by comparison to the database. Apolipoprotein A-1 (Apo A-1) (spot 28) and serum amyloid P (spot 48) were also identified in the database.

3.8. Proteins in substrate-attached material

Many of the proteins collected from the SAM on both surfaces were serum-adsorbed proteins (Fig. 3.15.). On cpTi the SAM contains significantly more serum proteins. These serum proteins could also be found in the extracts collected from the whole cell lysates (Fig. 3.8. and 3.9.) and in the adsorbed serum proteins (Fig 3.7.). This suggests that these adsorbed proteins remain as a substantial part of the interface, even after 5 days in culture.

Among the cellular proteins present in SAM, (Table 3.4.) fibronectin (spot 44) is more abundant in the SAM collected from TPS (Fig. 3.15, spot 44, compared to "housekeeping proteins", spots 7, 9a-9c, 17, 47). Morphological study of fibrillar fibronectin in SAM by immunofluorescent labelling (section 3.6.) corresponds well with these results. A noticeable increase in the relative concentration of spots 48, 49 and 51,
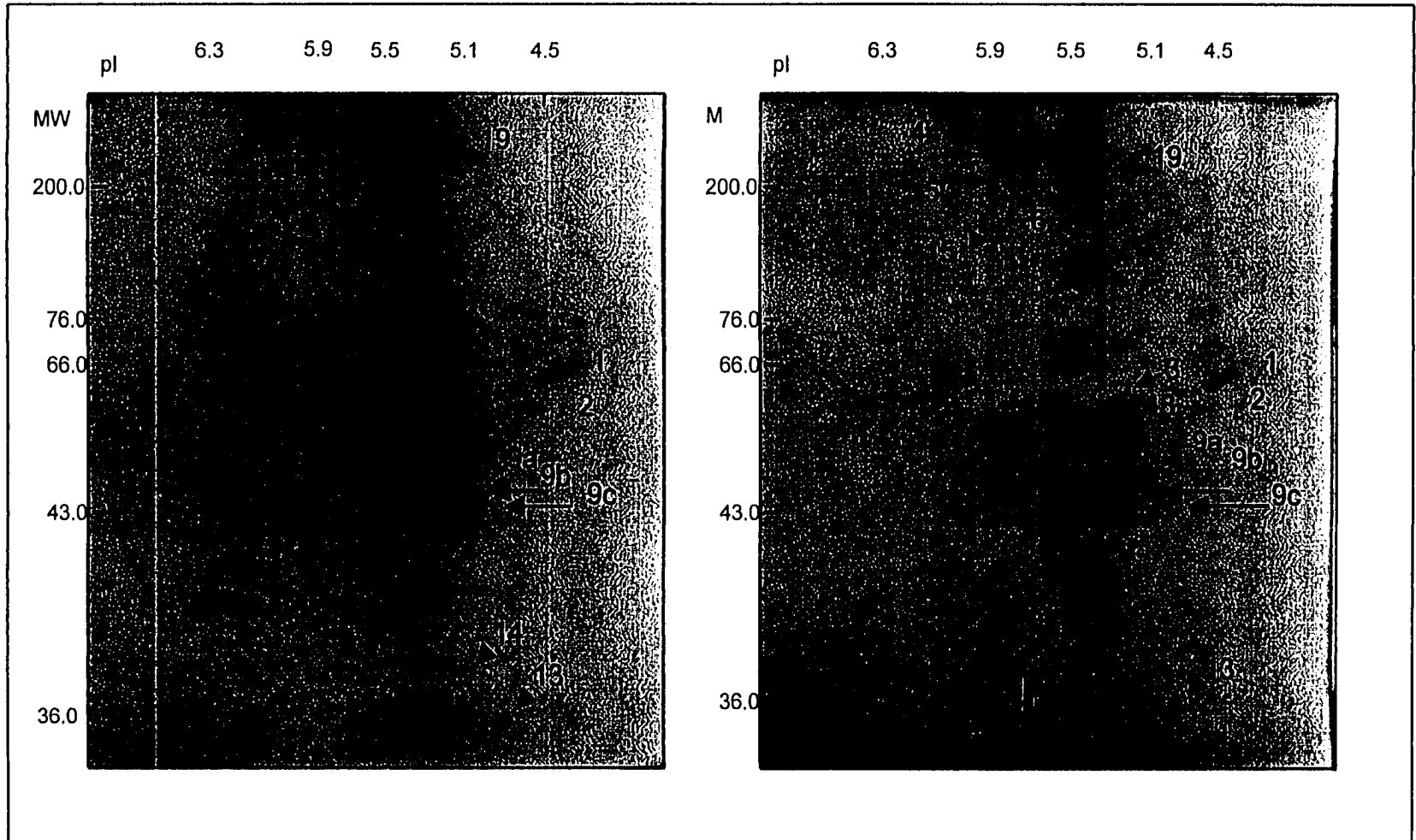
Fig.3.15. Two dimensional gels of proteins in SAM collected from fibroblast after 5 days in culture: a) on cpTi and, b) on TPS. The TPS gel has a slightly higher loading.

Table 3.4. Protein spots detected in SAM

Spot No.[1]	Protein Name (species)[2]	Accession Code[3]	Identification Method[4]	Apparent[5]		Theoretical[6]	
				pI	MW	pI	MW
1	Fetuin[7] (b), α2 HS glycoprotein (h)	P12763	Swiss 2D, MALDI(9/27)	4.00	60.0	5.10	36.4
2	Thrombospondin 1 (b,h)	Q28178	Swiss 2D, MALDI(5/29)	4.50	57.0	4.22	52.1
3	α-fetoprotein (b, h)	P02772[8]	Swiss 2D, MALDI(5/28)	5.10	58.0	5.54	67.3[8]
4	Serum albumin (b, h)	P02769	Swiss 2D, MALDI(15/42)	5.50	65.0	5.60	66.4
5	Plasminogen (b, h)	P06868	Swiss 2D, MALDI(11/21)	6.10	72.0	6.40	63.1
6	Non muscle myosin heavy chain type A	P35579	Human-2D, MALDI(15/27)	5.50	200.0	5.50	226.0
7	Actin-γ	P02571	Human-2D, MALDI(18/57), IB	5.30	43.0	5.29	41.6
9	Vimentin variant	8422	Human-2D	5.00	50.0		
9a	Vimentin degradation product	1301	Human-2D	5.00	48.0		
9b	Vimentin degradation product	0304	Human-2D	4.85	46.0		
9c	Vimentin degradation product	9307	Human-2D	4.80	44.0		
13	Tropomyosin 5	9118	Human-2D	4.80	31.8	4.48	28.3
14	Annexin V	8216	Human-2D	5.00	32.4	4.83	35.7
15	Vinculin	P18206	Human-2D, MALDI(10/48), IB	5.80	110.0	5.83	116.5
17	PAI-2	6307	Human-2D	5.50	40.0	5.46	46.6
18	α -tubulin	7513	Human-2D	5.10	61.2	5.02	50.2
19	Unknown (b)			5.40	>100.0		
41	Neuron cytoplasmic protein (PGP 9.5)	6104	Human-2D	5.40	27.0	5.33	24.8
44	Fibronectin (h)	P02751	STD, IB	5.80	250.0	5.45	263.0
47	α-actinin (h)	7717	Human-2D	5.30	98.0	5.30	98.1
48	Unknown (h)			5.50	37.0		
49	Unknown (h)			5.50	35.0		
50	Non muscle myosin heavy chain-B (h)		MALDI(5/24)	5.50	220.0	5.44	229.0
51	Unknown (h)			5.30	32.0		

Footnotes to Table 3.4.

1. Spot numbers refer to the numbers given in figures of 2D SDSPAGE gels.

2. Proteins identified by MALDI/MS were Spot 1-2, 4-7, Spot 16, Spot 19-21. Proteins identified by comparison to human 2D database are Spot 8-14 and Spot 17-18. Spot 19 could not be identified by either method.

3. Swiss Protein codes start with a letter, accession codes of the proteins found in Human 2D database start with a number. These codes facilitate retrieval of information about each protein from the appropriate database.

4. Swiss 2D refers to the human plasma 2D, Human 2D refers to the human skin or the MRC5 – IEF database, MALDI refers to matrix assisted laser desorption mass spectrometry, IB refers to immunoblotting, 2D-std refers to comparison to standard 2D proteins.

5. Apparent values of pI and MW were measured from the 2D SDS PAGE gels.

6. If the given sequence of the database belongs to the precursor molecule, the signal fragment is not used in calculating the pI and MW. No values were assigned if the sequence of the protein could not be found in the database.

7. Treatment with N-acetyl glycosidase-F identified the protein as a glycoprotein.

8. Amino acid sequence of bovine α-fetoprotein is not available for peptide mass mapping, therefore this spot was analyzed by peptide mass mapping of its mouse homolog.

compared to housekeeping proteins, is seen in SAM which is not detected in the whole cell extracts (Fig. 3.9.).

3.9. Fibronectin and myosin heavy chain A are upregulated on tissue culture polystyrene

On day 5 of incubation, a higher expression of spots 6 and 44 is detected in extracts from TPS (Fig. 3.9b). This is consistent with the results from section 3.8. The presence of cellular fibronectin (spot 44), vinculin (spot 15) and actin (spot 7) were confirmed by immunoblotting (Fig. 3.16.). The position of cellular fibronectin in the standard 2D PAGE (Fig. 3.17.) also matched the spot detected in the immunoblot (spot 44).

Analysis of spot 6 by MALDI/MS (Fig. 3.18.) showed it to be the non-muscle isoform of myosin heavy chain type A. This was confirmed twice in two separate experiments. In addition, the protein was also identified in the human MRC5 fibroblast database. This protein and fibronectin were the only cellular proteins that we found that were differentially expressed by fibroblasts cultured on the two surfaces.

3.10. Identification of other proteins spots

Table 3.5. lists the silver stained protein spots from human skin fibroblasts identified by various procedures. The spot-numbers in (Fig. 3.8. and 3.9.) correspond to the protein spots depicted in the master map (Fig. 3.19.). In total, twenty-eight cellular proteins were identified, most of which could be confirmed by comparison to various 2D PAGE databases. Six proteins were identified by MALDI/MS. Results of MALDI/MS

Fig. 3.16. Immunoblot of two-dimensional gel showing the spots for detected proteins
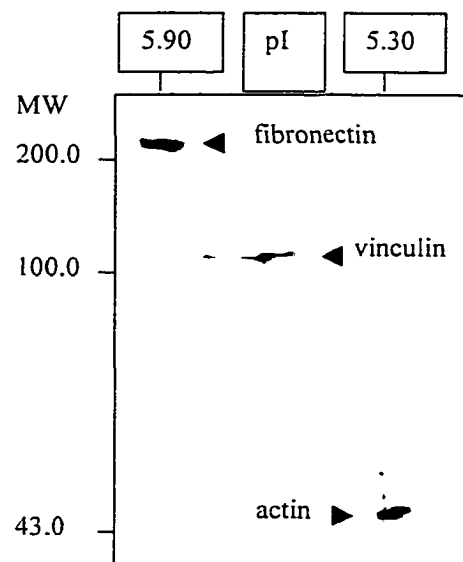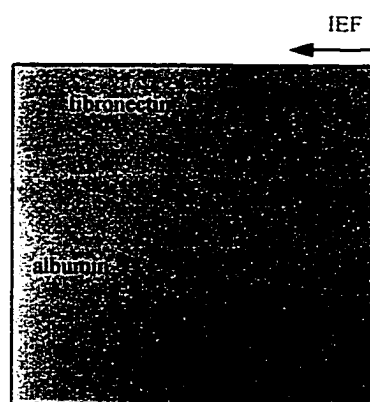
Fig.3.17. Silver stained two-dimensional gel of standard for cellular fibronectin and albumin.

Non muscle myosin type A (P35579)
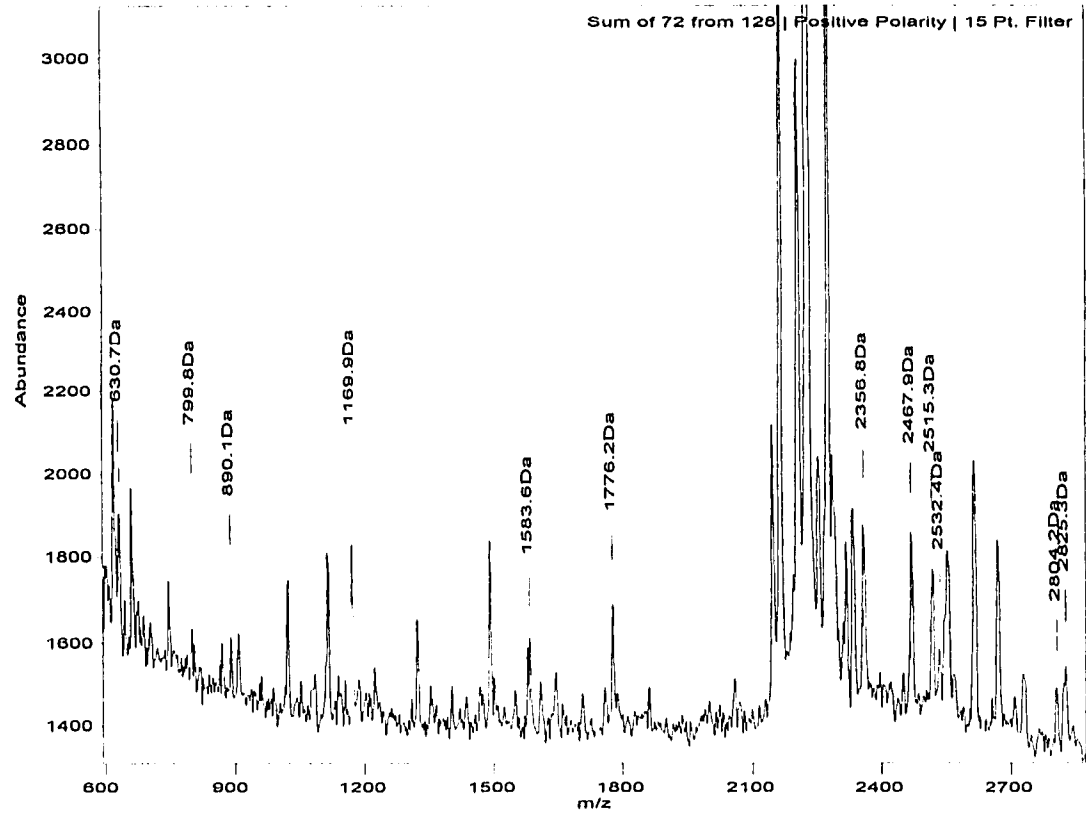
Fig.3.18. Mass spectrum of the tryptic peptides of spot 1 from 2D SDSPAGE of whole

cell extracts identified as fetuin.

Table 3.5. Proteins from human skin fibroblasts

Spot No.[1]	Protein Name[2]	Accession Code[3]	Identification Method[4]	Apparent[6]		Theoretical[6]	
				pI	MW	pI	MW
6	Non muscle myosin heavy chain type A	P35579	Human-2D, MALDI(15/27)	5.50	200.0	5.50	226.0
7	Actin-γ	P02571	Human-2D, MALDI(18/57), IB	5.30	43.0	5.31	41.7
7a	Actin-β	P02570	Human-2D, MALDI(17/57), IB	5.30	43.0	5.29	41.6
8	Vimentin	8520	Human-2D	5.00	52.0	5.06	53.5
9	Vimentin variant	8422	Human-2D	5.00	50.0		
9a	Vimentin degradation product	1301	Human-2D	5.00	48.0		
9b	Vimentin degradation product	304	Human-2D	4.85	46.0		
9c	Vimentin degradation product	9307	Human-2D	4.80	44.0		
10	Tropomyosin	9227	Human-2D	4.80	38.5	4.69	32.7
11	Tropomyosin 2	9119	Human-2D	4.80	37.5	4.63	32.9
12	Tropomyosin 4	9119	Human-2D	4.80	33.3	4.68	32.8
13	Tropomyosin 5	9118	Human-2D	4.80	31.8	4.48	28.3
14	Annexin V	8216	Human-2D	5.00	32.4	4.83	35.7
15	Vinculin	P18206	Human-2D, MALDI(10/48), IB	5.80	110.0	5.83	116.5
16	Thrompospondin 4	P49746	MALDI(5/15)	4.40	110.0	4.43	104.2
17	PAI-2	6307	Human-2D	5.50	40.0	5.46	46.6
18	α -tubulin	7513	Human-2D	5.10	61.2	5.02	50.2

33	Hsp 90	1608	Human-2D	5.00	87.0	4.94	85.0
34	BiP (grp 78)	8619	Human-2D	5.00	75.0	5.03	72.1
35	Hsp 70	6602	Human-2D	5.30	65.0	5.37	71.0
36	T-plastin (fimbrin)	6513	Human-2D	5.40	63.0	5.52	70.4
37	Hsp 60	7517	Human-2D	5.30	55.0	5.70	61.0
38	β-tubulin	8511	Human-2D	4.80	55.0	4.75	49.8
39	Rho GDI	8123	Human-2D	4.80	25.0	5.03	23.2
40	Translationally controlled tumor protein	8113	Human-2D	4.80	23.0	4.84	19.6
41	Neuron cytoplasmic protein (PGP 9.5)	6104	Human-2D	5.40	27.0	5.33	24.8
42	Annexin I	5209	Human-2D	6.10	35.0	6.64	38.6
43	α-enolase	2418	Human-2D	7.20	47.0	6.99	47.0
44	Fibronectin	P02751	STD, IB	5.80	250.0	5.45	263.0
45	Myosin light chain	8002	Human-2D	4.50	17.0	4.56	16.8
46	Inititiation factor 4D	7006	Human-2D	5.00	17.0	5.08	16.7
47	α-actinin (h)	7717	Human-2D	5.30	98.0	5.30	98.1
48	Unknown (h)			5.50	37.0		
49	Unknown (h)			5.50	35.0		
50	Non muscle myosin heavy chain-B (h)		MALDI(5/24)	5.50	220.0	5.44	229.0
51	Unknown (h)			5.30	32.0		

For footnotes see Tables 3.3. and 3.4.
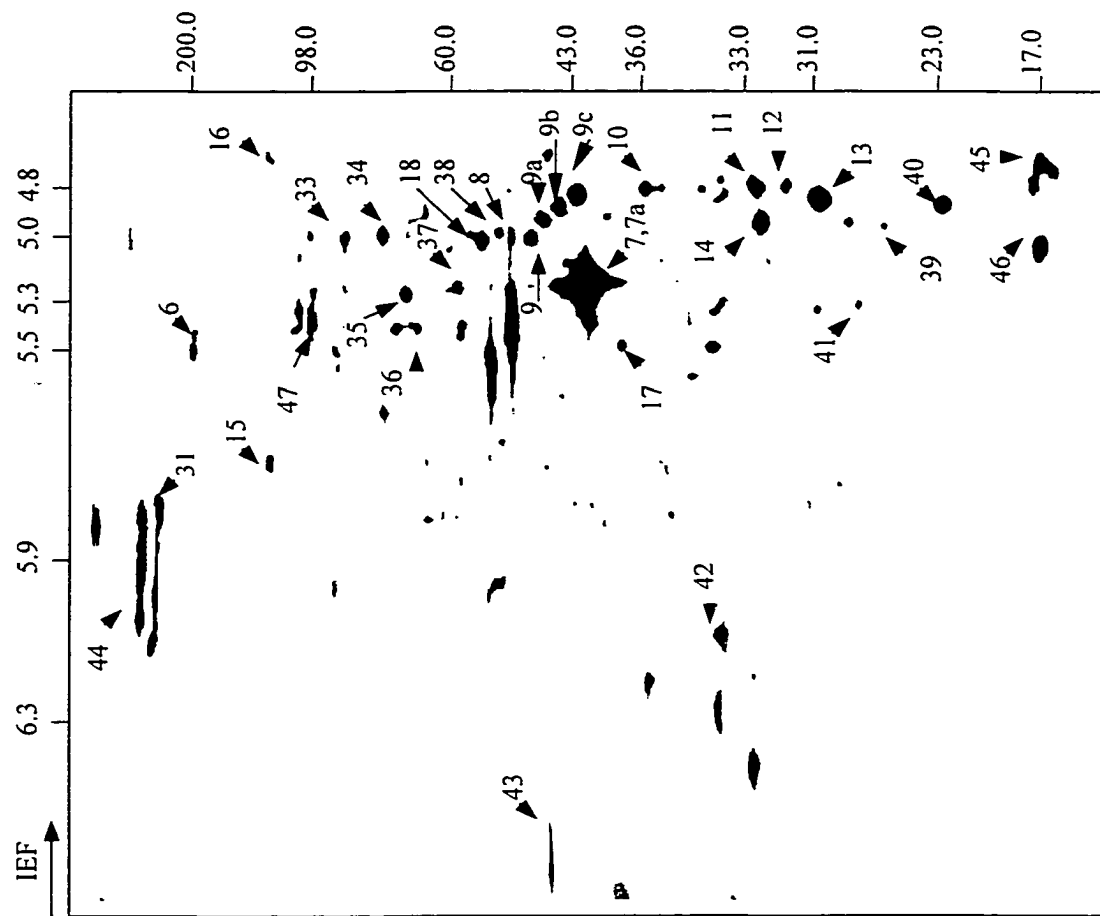
Fig.3.19. A schematic map of cellular proteins found in two-dimensional gels of whole cell lysate of skin fibroblasts.

showed that spot 7 contain the two actin isoforms (spot 7 and spot 7a) of non-muscle type. The occurrence and position of these spots in 2D PAGE gels of many cell lines are common. Vimentin and its degradation products (spots 8, 9a, 9b, 9c), tropomyosins (spot 10, 11,12, 13), annexins (spot 14, 42), plasminogen activator inhibitor-1 (spot 17) and β and α-tubulin (spot 18, 38) were identified by comparison to the Human Skin 2D database on the basis of their isoelectric points, molecular weights and their proximity to other protein spots. Thrompospondin 4 (spot 16) could only be identified by MALDI/MS analysis.

3.11. Expression of cellular proteins by fibroblasts grown on titanium coated with substrate-attached material

Figures 3.20. – 3.22. show 2D SDS-PAGE gels of [^{35}S] methionine labelled proteins. The samples were from extracts of fibroblasts grown on cpTi coated with SAM and non-coated cpTi, 1 day (Fig. 3.20.), 3 days (Fig. 3.21.) and 5 days (Fig. 3.22.) after seeding. The most striking difference is seen in the spot corresponding to NMMHC-A (spot 6), 1 day after seeding (Fig. 3.20.). This protein appears to be highly expressed on SAM coated cpTi but it is lacking in extracts collected from non-coated discs. This difference becomes less noticeable at later periods in culture. It should be emphasised that on day 1 (Fig. 3.20.) the loading of the sample from the SAM coated discs is less than the loading of the samples from the non-coated discs.

Relative to NMMHC-A (spot 6), the expression of NMMHC-B (spot 50) appears to be down regulated on SAM-coated discs on the first day of incubation (Fig. 3.20.) but
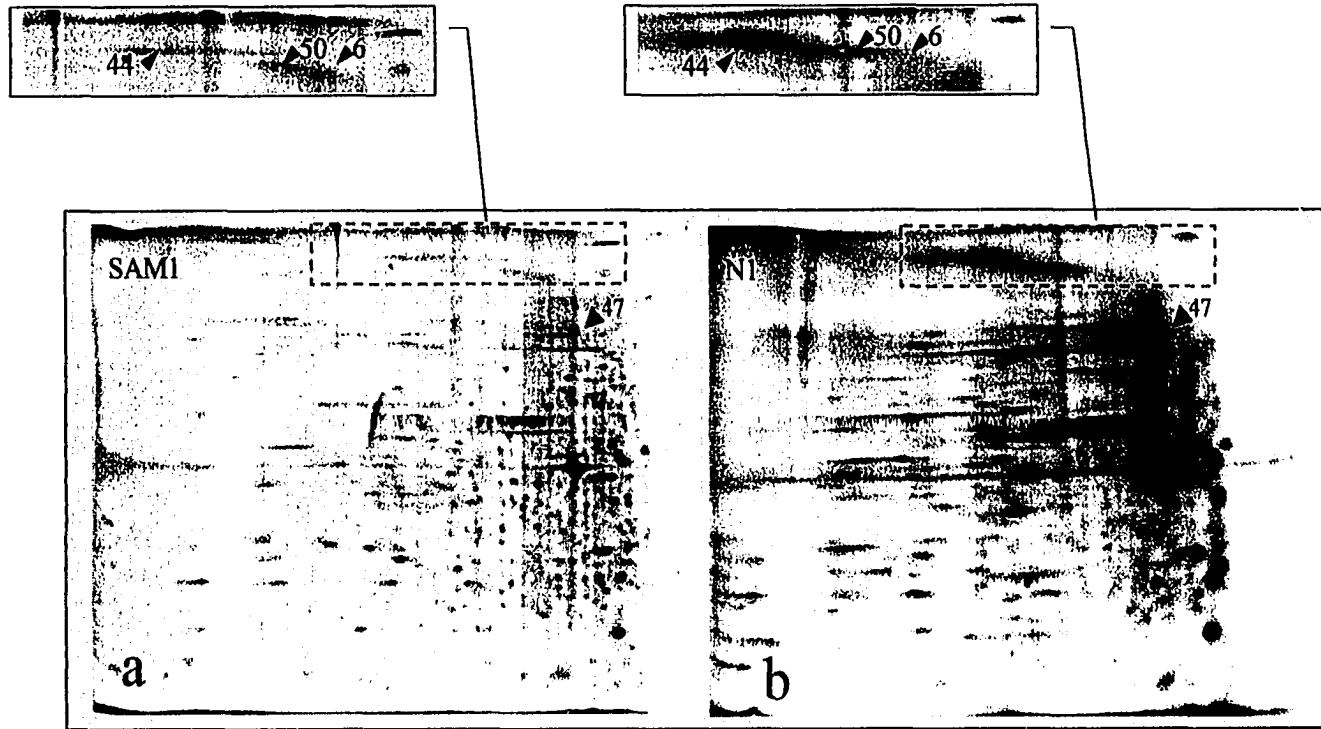
Fig.3.20. Two-dimensional gels of radiolabeled proteins in extracts collected from skin fibroblasts grown for 1 day on a) cpTi coated with SAM, b) cpTi. Despite a lower loading of gel (a), a higher concentration of non muscle myosin type A (spot 6) is evident on SAM-coated cpTi.
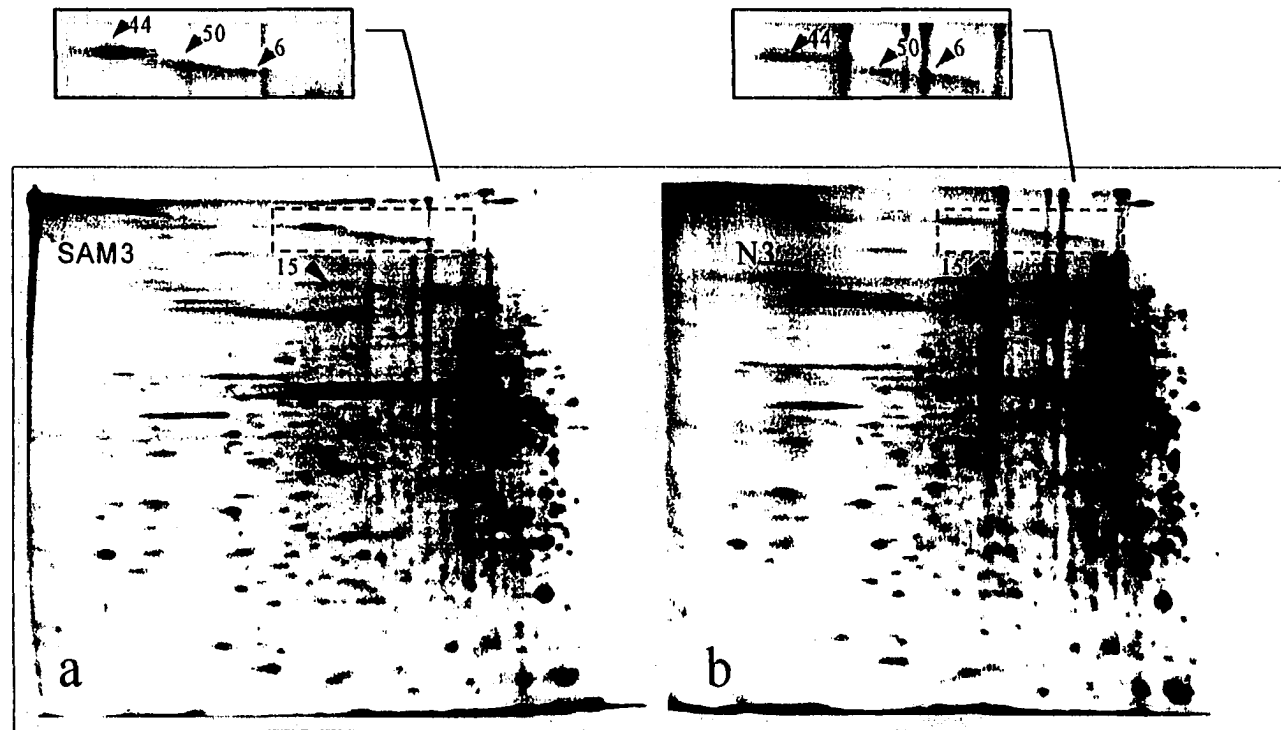
Fig.3.21. Two-dimensional gels of   radiolabeled proteins in extracts collected from skin

fibroblasts grown for 3 days on a) cpTi coated with SAM, b) cpTi. Despite a lower loading of

gel (b), a higher concentration of   Non-muscle myosin type B (spot 50) is evident on SAM

coated cpTi.
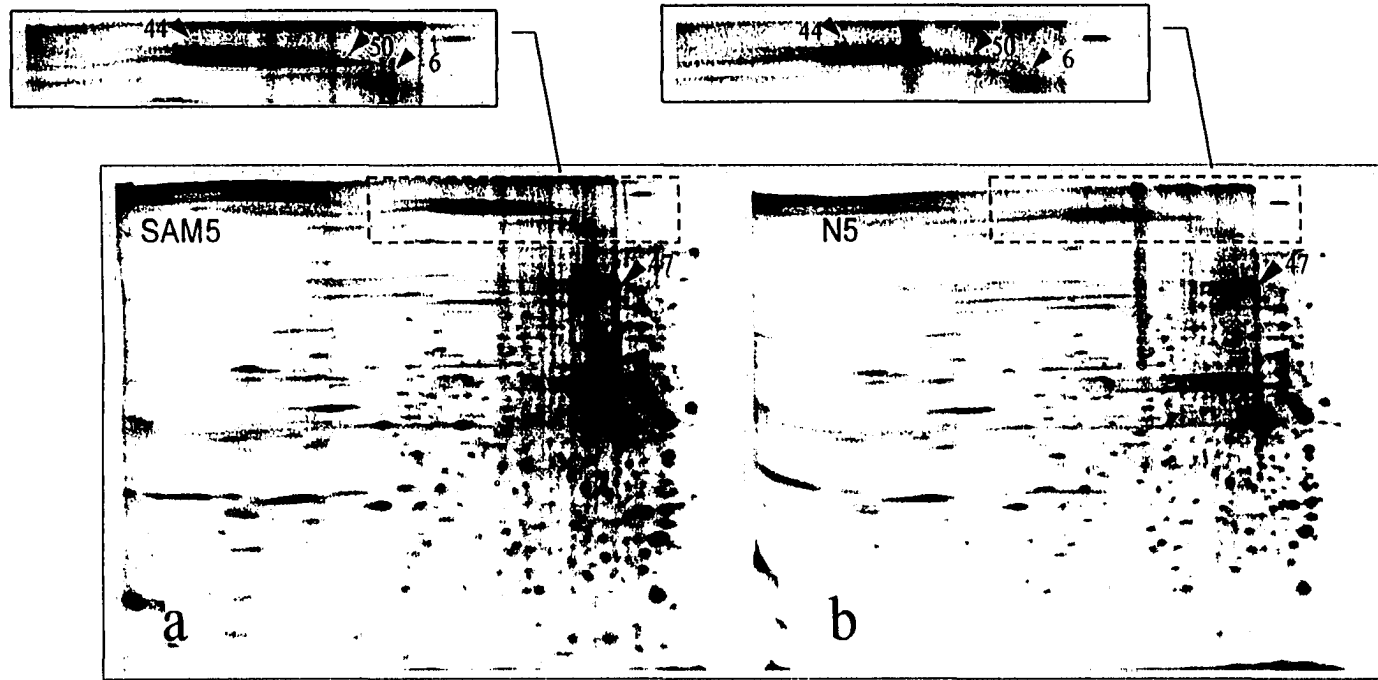
Fig.3.22. Two-dimensional gels of radiolabeled proteins in extracts collected from skin fibroblasts grown for 5 days on a) cpTi coated with SAM, b) cpTi. It appears that non muscle myosin type A (spot 6) is synthesized at slightly higher concentration on cpTi coated with SAM.

this increases on day 3 (Fig. 3.21.) to become approximately equal to that of NMMHC-A on the fifth day of incubation (Fig. 3.22.).

On the third day of incubation, the expression of cellular fibronectin appears to increase in the sample from SAM-coated titanium (Fig. 3.21a). The loading of this sample is less than the sample representing the non-coated discs (Fig. 3.21b).

Vinculin, a marker for focal adhesion sites, appears to also reach its highest level of expression on day 3, where most fibroblasts are in their log phase. However, we did not detect a notable difference in the expression of vinculin on the coated or non-coated titanium (Fig. 3.21.).

α-actinin was continuously expressed in the fibroblasts during the 5 day period. The expression of this cytoskeletal protein did not appear to be affected by the surface coating. Other major cytoskeletal proteins such as actins, vimentins, annexins, and tropomyosins did not show a notable change of expression as the result of surface coating with SAM (Fig. 3.20.- 3.22.).

3.12. Proteomic map of human skin fibroblast

Figure 3.19., represents a schematic reproduction of the proteins synthesised by human skin fibroblasts. Most of the spots were present in all samples examined but some were found in specific gels. Thirty-three spots are labelled. The majority of the protein spots were identified by comparison to the Human Skin Fibroblast 2D database (http://biosun.biobase.dk/~pdi/2Dgallery) but several proteins were identified by MALDI/MS and immunodetection (Table 3.5.).

CHAPTER 4: DISCUSSION

4.1. Surface roughness

Surface roughness is believed to play a major role in adhesion and growth of cells on various substrata and is therefore an important factor in biocompatibility. Although there is controversy as to whether surface roughness affects cell adhesion, the effect of surface topography on the orientation and morphology of cells *in vitro* and *in vivo* are well-documented (Brunette and Chehroudi, 1999). Cells align to the irregularities of a substrate, a process known as "topographic guidance". This phenomenon is well represented by Fig. 4.1. On titanium discs, fibroblasts are mostly elongated and follow the grooves (Fig. 4.1b). On tissue culture polystyrene the cells form a typical pattern of swirls (Fig. 4.1a). We suggest that the processing of polystyrene forms this particular patterning in this material.

Our results show that titanium foil had the roughest surface of all the substrates used in our study. Despite the similarities between the surface of cpTi foil and cpTi discs, the difference in surface roughness was significant (p<0.001) and resulted in approximately 8.0% increase in the surface area of the foil as compared to the discs (Table 3.1). We also found that surface roughness values of both types of TPS (wells and culture dishes) differed significantly (p<0.0001).

Wennerberg and coworkers (Wennerberg et al., 1993) have measured the surface parameters of Nobelpharma™ implants by profilometric analysis. Our experimental

Fig.4.1. Immunofluorescence labeling of vitronectin of human skin fibroblasts 1 day after seeding on a) TPS, b) cpTi disc. On TPS fibroblasts are well spread and grow in typical swirl-shaped pattern. On cpTi fibrobalst are elongated and follow the grooves which run in circles from top to bottom of the image (magnification 500 X, bar = 20μm).

titanium discs exhibited shallower (0.25 μm) but more frequent grooves as compared to the clinically relevant Nobelpharma implants (0.53 μm). The mean height of irregularities on our experimental discs was more than electropolished cpTi (0.14 μm) but lower than the same value for etched cpTi (0.41 μm) (Kononen et al., 1992). The mean height of irregularities on the surface of the experimental titanium foils (0.36 μm) was close to that of etched cpTi and Nobelpharma implants.

There is a clear difference in surface roughness of cpTi discs and TPS wells (Table 3.1.). We did not find a significant difference in the number of cells grown on these surfaces during the initial stages of growth. The slightly greater surface area of cpTi may, however, account for the higher cell density at 10 days. This suggests that there may be other factors that influence cell population per unit area, such as cell shape, cellular orientation, packing of cells, overlapping, or growth restrictions imposed by deep grooves. We believe that in our studies, the overriding factor influencing cell behavior was the difference in the surface chemistry of titanium and tissue culture polystyrene.

Profilometric surface analysis showed that cpTi discs had rougher surfaces than TPS wells. Surface geometry affects the shape and orientation of cells, subsequently altering secretion and assembly of cellular fibronectin (Chou et al., 1995). From previous studies which found a correlation between surface roughness and efficiency of cell attachment (Clark, et al., 1987) increased adhesion to cpTi compared to TPS might have been expected. This was not found but, to the best of our knowledge, our study is the first to attempt to measure the strengths of attachment to these two surfaces.

4.2. Growth of fibroblasts on tissue culture polystyrene and titanium surfaces

The growth of fibroblasts on cpTi and TPS is shown in figure 3.2. The log phase of growth (days 3 - 8), the doubling time of fibroblasts was shorter on cpTi. However, when we considered the entire culture period (day1-10), a non-linear correlation analysis showed no statistically significant difference in the rates of proliferation on the two substrates. This suggests that the fibroblasts grown on cpTi may require more time to reach the log phase but once in the log phase they grow rapidly to form confluent cultures. This may be the result of the greater surface area of cpTi. It is believed that an increase in the surface area of titanium may delay the initial growth of cells on cpTi (Noth et al., 1999). However, the enhanced rate of growth on cpTi during the log phase may be due to the lower strength of attachment of fibroblasts to titanium. Cells may be able to move and divide at a faster rate on a less adhesive surface.

The results of investigations on the rate of growth of fibroblasts on titanium and plastic have been inconsistent (Hunter et al., 1995; Degasne et al., 1999; Lincks et al., 1998; Noth et al., 1999; den Braber et al., 1998). A reason for this inconsistency may be the use of various cell types and/or surface treatments in these experiments. In particular, the length of the study-periods varies greatly among these investigations. As we have shown in section 3.2., on different substrates the rate of cell proliferation may vary significantly depending on the phase of cellular growth. In an early model of a cell-factory, Molin and Heden (1967) used titanium plates. They found that fibroblasts grew efficiently on titanium and concluded that the rate of proliferation was higher than on plastic or glass. In vitro, growth and migration of fibroblasts are interrelated. As the number of fibroblasts increases in culture, they are displaced to make room for the newly

divided cells. The rate of migration of rat dermal fibroblasts was shown to be significantly higher on untreated titanium than on tissue culture plastic (Jansen et.al., 1999). Interestingly, both substrates exhibited similar values for surface energy (contact angle).

4.3.   Detachment of fibroblasts from tissue culture polystyrene and titanium

A stable attachment is essential for viability of anchorage-dependent cells. Cell migration, however, requires co-ordination between the formation of new adhesions and subsequent release from the previous sites. For this reason, an intermediate strength of attachment is probably best suited for growth and migration of cells (Dimilla et al., 1991; Duband et al., 1991). This is also consistent with the fact that optimal cell migration occurs at intermediate substrate concentrations (Dimilla et al., 1993; Goodman et al., 1991). Indeed a strong adhesion may not release rapidly enough and result in inhibited cell movement and growth. Our results demonstrate that skin fibroblasts adhere less strongly to titanium than to tissue culture polystyrene. This is indicated by: (1) a higher rate of cellular proliferation during the log phase, (2) a higher rate of cellular detachment on centrifugation, and (3) a smaller quantity of substrate-attached material that remains behind after detachment of fibroblasts from cpTi with EGTA.

Subsequent to treatment with EGTA, fluid shear forces may easily detach cells. This may occur by two mechanisms: (1) through a breakage of ligand-receptor interaction and (2) by extraction of receptors from the cell membrane (Evans et al., 1991).   Cells with fewer and more widely separated adhesion sites can be easily detached by either mechanism.   In contrast, cells that have more receptors focalized at specific sites of

adhesion may resist detachment to the point where the cell membrane is ruptured and receptor complexes are left behind on the substrate.

Lotz and co-workers (Lotz et al., 1989) found that essentially all fibroblasts continued to adhere to microtiter wells when challenged with a maximum centrifugational force of 3.6 x 10^{-4} dynes/cell. The same force was however sufficient to detach glioma cells from fibronectin. Although in the present study we used a force that was 20-fold higher (7.85 x 10^{-3} dynes/cell), this was still not sufficient to detach a significant number of fibroblasts from TPS. As in the study by Lotz and co-workers (1989) the force required to separate the normal skin fibroblasts from TPS exceeded the integrity of the microtiter chamber. In contrast, fibroblasts readily detached from cpTi after 3 or 5 days in culture. The magnitude of the force required to detach 50% of the fibroblasts from cpTi is in good agreement with the value predicted by Ward and Hammer (1993) in their theoretical analysis. According to this model the cytoskeletal linkages at focal contacts are considered to have no mechanical rigidity and thus cells respond to centrifugational stress by peeling from the substrate through progressive bond breakage at the edge of the cells. Fracture, however, may occur when adhesive contacts form a rigid cytoskeletal linkage. Since the fracture model requires detachment forces considerably (>100 times) larger than the reported values, this may explain why fibroblasts cultured on TPS resist detachment. This is also consistent with our results, which show that the patterns of fibronectin receptors remaining on TPS after release of the fibroblasts resemble cellular imprints.

The results of the present investigation clearly demonstrate a temporal effect on the detachment of fibroblasts from titanium surfaces, the strength of attachment

decreasing with time on cpTi. Since the total number of cells at each time was measured and shown to be comparable on both surfaces, it seems unlikely that a difference in cell-cell attachment (Nagahara and Matsuda, 1996) could explain our results.

4.4. Quantification of total protein in the cells and substrate-attached material

The titanium foil and tissue culture plastic dishes were exclusively used in the experiment involving the assay for total protein (section 2.4). This was necessary since sufficient quantities of SAM could not be extracted from the small titanium discs. Despite the larger surface area of titanium foils (due to surface roughness), we found that more proteins remained in the SAM collected from tissue culture polystyrene dishes. We believe that this is mainly a consequence of the highly adhesive interactions present between fibroblasts and TPS. A rigid cytoskeletal structure resists detaching forces to the point of fracture and results in larger cell fractions remaining in SAM. In support of this idea, we demonstrated, by immunofluorescent labeling (section 3.6), that larger and more numerous cellular fragments remained in SAM on TPS. The study of morphology and content of SAM may help us gain a better understanding of the mechanical properties of the cell-substrate interface.

Surface topography is known to alter the expression of some extracellular proteins such as fibronectin, matrix metalloproteinase and collagen (Grossneir-Schrieber and Tuan, 1991; Chauo, et al., 1995; Chauo, et al., 1998). It was found that chick calvarial cells produced more collagen on rough titanium than on smooth titanium or plastic controls (Groessner-schrieber and Taun, 1991). Chou and co-workers (1995) showed that substratum topography alters cell shape and regulates expression of mRNA level of

fibronectin (1995) and matrix metalloproteinase (1998) in human fibroblasts. In the present investigation we compared the quantity of proteins present in the culture of skin fibroblasts grown on cpTi and TPS. The surface characteristics of these substrates differed not only in topographical features but also in other physical and chemical properties. We sought to find a difference in the synthesis of total-protein on the two substrates. Further investigations are necessary to determine if a single or multiple factors influence the production of proteins on each surface.

4.5. Attachment of fibroblasts to titanium coated with substrate-attached material

At times it may be clinically useful to obtain a strong seal between a biomaterial and its surrounding tissue. Attachment of the epithelium and/or dermis to the surface of percutaneous abutments may prevent onset of inflammation in peri-implant environment. Culp (1974) reported that transformed cells become less mobile and resist movement away from the colony edges when cultured on SAM. This property of SAM could not be mimicked by adsorbed serum alone. We used this concept to improve the adhesion of normal skin fibroblasts to titanium. Our results show that coating of cpTi with SAM from later cultures causes a dramatic increase in the strength of fibroblast attachment. Interestingly, adhesion of fibroblasts to SAM-coated cpTi was still not as strong as the attachment to TPS and initially fewer cells attached to this substrate. Organic surfaces possess a much lower charge density but may be ideal for cellular growth and proliferation since they may contain sites for specific adhesive interactions (Koller and Papoustsakis, 1995).

The mechanism by which SAM enhances the strength of attachment of cells to cpTi must be addressed. As SAM contains many ECM components in addition to fibrillar fibronectin, this effect may be postulated to be the result of extracellular signals affecting the cytoskeleton and focal contact formation, which in turn promote cellular stiffness. It was demonstrated that binding of fibronectin-receptor to fibronectin induces attachment of the integrin to the force-generating components of the cytoskeleton (Felsenfeld et al., 1996). In section 3.11., we show that coating of titanium with SAM induces fibroblasts to express more myosin heavy chain (type A), a major component of stress fibres. These findings are in line with the idea that cell adhesion may be promoted by strengthening the rigidity of cytoskeleton.

Regardless of the mechanism by which SAM enhances cellular attachment, precoating of cpTi with SAM is proposed as a simple biological treatment to improve the strength of attachment at the titanium-tissue interface.

4.6.   Immunofluorescence for fibronectin and fibronectin receptor

Analysis of extracts from amniotic mesenchymal cells by two-dimensional electrophoresis has demonstrated the presence of $\beta 1$-integrin receptors in SAM (Niederreiter et al., 1994). In the present study, we have fluorescently labelled fibronectin receptor ($\alpha 5/\beta 1$ or $\beta 5$) in SAM from skin fibroblasts. In contrast to the diffuse distribution of the integrins observed in SAM prepared on cpTi, a higher concentration could be detected in the SAM on TPS and these closely followed the outline of the cells. This may imply that more receptors accumulate at the cell-TPS interface. Alternatively, a rigid linkage of integrins to the cytoskeleton or cross-linking

of receptors may cause cell membranes to rupture and to leave a greater number of integrins on TPS. The latter explanation is supported by the observation that more protein was also collected from SAM on TPS and that this was made up of larger aggregations of fibronectin and other proteins.

Immobilisation of the fibronectin on the negatively charged surface of tissue culture polystyrene results in the formation of a rigid extracellular matrix indicated by dense fibrillar patches (Grinnell and Feld, 1982; McAbee and Grinnell, 1985). Stronger interaction of fibronectin with the TPS may not be favourable to dewebbing and reorganisation of the matrix (Altankov and Groth, 1994). Under physiological conditions, a surface oxide that is weakly negatively charged (Tengvall and Lundström, 1992) covers titanium. This surface may adsorb fibronectin with less affinity, thus allowing the cells to arrange the fibronectin fibres into a less compact and more uniform network. Recently it was reported that coupling of the $\alpha5/\beta1$ integrins to a rigid fibronectin matrix strengthens the integrin-cytoskeletal linkage (Choquet et al., 1997). This may account for the observed differences in the organisation of the fibrillar fibronectin on the two substrates and also explain why fewer receptors were left behind in SAM on cpTi.

4.7. Adsorbed serum proteins on titanium and tissue culture polystyrene

Initial interaction of most implant materials with the living tissues begins with the adsorption of plasma proteins onto the substrates (Grinnell, 1978; Imamoto et al., 1985; Vroman and Adams, 1986; Liu et al., 1998). The physical and chemical composition of this adsorbed biofilm ultimately determines the biocompatibility of a material.

We found that plasma proteins adsorbed to titanium surfaces are consistently present as a significant part of the extracts of whole cell lysates in both early (1 day in culture) and late cultures (5 days in culture). This is important since it suggests that fibroblasts remain in contact with the adsorbed serum proteins for the duration of our experiments (5 days). Previous investigations have demonstrated the adsorption of serum albumin (Adell et al., 1989; Liu et al., 1998), thrombospondin (Kanagaraja et al., 1996) and other serum components from blood to titanium surfaces. The results of the present study confirm these findings and add a number of additional serum proteins to this list (Table 3.3). The adsorbed serum proteins remain firmly attached to cpTi and may therefore play a major role in determining cell and tissue response to titanium. For example, titanium is shown to be a highly thrombogenic material (Hong et al., 1999) making it unfavorable for use in devices which are in direct contact with blood for a prolonged period. However, by virtue of the same property, the abundance of serum proteins on titanium provides a suitable environment for the cell growth and tissue development that is required for osseointegration.

Different physico-chemical properties of each substrate used in our studies such as its surface-chemistry, -roughness and -tension result in adsorption of the biofilm layer. When we compared the proteins in the whole serum to the proteins that adsorb to cpTi or TPS, we found that adsorption of serum proteins onto both surfaces was non-selective. However, more protein appeared to adsorb to the cpTi than to TPS. This suggests that the concentration of each protein and/or the thickness of the adsorbed biofilm may be important in the initial interaction of cells with the substrate. Some adsorbed proteins may act as targets for secondary binding by other adhesion-proteins and thus modulate

cell adhesion. For example, plasminogen and/or serotransferrin may act to inhibit cell-substrate adhesion. At higher concentrations, serotransferrin, a well-known mitogen for fibroblasts (Dawes, Gray and Laurent, 1990) may act to reduce cell attachment on cpTi.

It is important to note that next to serum albumin, fetuin and FETA appear to be the most abundant serum proteins adsorbed to the substrates. Both fetuin and FETA are major components of fetal serum. The bovine fetuin molecule contains three N– linked and two O-linked glycosides with carbohydrates accounting for nearly 30% of the total weight (Brown et al., 1992; Demetriou et al., 1996). The sialic acid accounts in part for the acidic nature of this protein. Removal of the sialic acid raises the pI to 5.25 (Nie, 1992). The amino acid sequence of fetuin includes an EF hand motif that is suggested to bind Ca^{2+}. In fact, high amounts of fetuin consistently occur in the mineralized phase of bone and teeth (Schinke et al., 1996). Moreover, the 56 kDa bone sialic acid containing protein (BSP) was shown to be the dephosphorylated form of fetuin (Ohnishi et al., 1993). It is therefore suggested that fetuin may be important in remodeling of hard tissues (Brown et al., 1992). The mean concentration of fetuin in fetal bovine serum (10 - 22 mg/mL) is considerably higher than the concentration of its human homolog (α2-HS glycoprotein) (0.4 - 0.6 mg/mL) (Brown et al., 1992; Nie, 1992). This is also evident from the result of our study comparing the adsorbed serum proteins of human and bovine origin. Since the concentration of fetuin in the adsorbed biolayer on cpTi is greater than its human homolog (α2-HS glycoprotein), this raises a concern regarding the clinical relevance of *in vitro* investigations of mineralization on titanium implants that use bovine serum as a blood substitute. It may be necessary to use human serum instead of the widely used FBS to fairly represent the clinical conditions. Interestingly, it was shown

that in vitro mineralization could be induced in periodontal ligament fibroblasts despite the lack of expression of osteopontin, bone sialic acid containing protein or alkaline phosphatase by these cells (Nohutcu et. al, 1997). For mineralization, a mineralizing medium containing ascorbic acid, beta-glycerophosphate and 10% fetal bovine serum was required.

Serum albumin and FETA are two of the most prominent members of the albuminoid gene family which also includes vitamin D-binding protein (VTDB). Albuminoid proteins are synthesized in the liver and secreted into the blood stream and are considered to have many biological activities (Gersten and Hearing, 1989). It is suggested that proteolytic cleavage of serum albumin or FETA may generate various regulatory peptides capable of eliciting a variety of biological responses (Mizejewski, 1997). Indeed, FETA has been shown to be a regulator of growth in many cell types (Mizejewski, 1997). It has also been proposed as an adhesion molecule for epithelial cells (Gersten and Hearing, 1989). This is thought to be a consequence of FETA's self-binding ability to form dimeric associations. The high degree of identity (30-47%) between the amino acid sequence of FETA and several extracellular cellular matrix (ECM) adhesion molecules such as syndecan, fibronectin, collagens and integrins (Mizejewski, 1997) implicate FETA in cell-cell and cell-ECM adhesion. Since fibronectin is a major part of the extracellular matrix collected from the substrates it may act as a binding-site for secondary interaction with FETA.

4.8. Substrate specific down regulation of fibronectin and myosin

Fibronectin and myosin heavy chain type A were the only two cellular proteins that showed a detectable substrate specific change in our studies. Chou and co-workers (1996) studied the expression of fibronectin in early and late cultures of fibroblasts grown on titanium coated silicon wafers and tissue culture plastic. They found that after 16 hours in culture the expression of fibronectin was higher on titanium but this was reversed in the late cultures (90 hours). In the present study, we could not detect a difference in the expression of fibronectin on the first day of incubation on cpTi and TPS. This may be due to the sparse amount of fibronectin relative to the other major cellular proteins in the early cultures of fibroblasts. In our 2D SDS-PAGE system, the optimal quantity for loading in the first dimension was determined to be approximately 5 µg of the complex protein mixture. A higher loading may have been required to detect fibronectin in the 2D gels of the early cultures. However, the result of the 2D SDS-PAGE analysis of the extracts on the fifth day of incubation is in agreement with the results of Chou and co-workers (1996) which showed an increase in the expression of fibronectin in the late cultures of gingival fibroblasts grown on tissue culture polystyrene. In addition, we described a dense network of fibrillar fibronectin at the interface of fibroblasts and TPS (section 3.6), whereas we found that fibroblasts growing on cpTi organize a less dense matrix of cellular fibronectin. We also found a higher expression of fibronectin in the substrate-attached material collected from the 5 day cultures extracted from TPS.

A denser fibrillar matrix of fibronectin is also seen in fibroblasts under mechanical strain *in vitro* (Meazzini et al., 1998). It is conceivable that the thick biofilm

of serum proteins adsorbed to cpTi results in a decrease in the affinity of cellular fibronectin to the substrate thus causing a decrease in intracellular tension. This resembles the behavior of fibroblasts grown on floating collagen gels (Halliday and Tomasek, 1995). Cells on the stabilized gels can produce tension and assemble fibronectin into fibrils while fibroblasts cultured on floating gels do not.

It is known that mechanical tension leads to an increase in synthesis of fibronectin and a coordinated change in cytoskeleton (Meazzini et al., 1998). A reduction in cellular contractility may in turn cause a down regulation of fibronectin and the formation of a less dense fibrillar matrix on cpTi. An increase in the rigidity of the extracellular matrix may conversely result in a strengthening of the cytoskeletal linkages (Choquet et al., 1997). Cells respond to stiffness of extracellular matrix by increasing the amount of tension they apply to the substrate. In experiments where synthetic fibronectin ligands (RGD peptides) were coated onto the substrate, magnetically twisting the peptides resulted in an increase in the cellular stiffness (Wang et al., 1993).

In the present investigation we found that modulation in the expression of cellular fibronectin is accompanied by a change in the expression of myosin heavy chain (NMMHC-A). This cytoskeletal protein is well known for its role in stress fiber contractility. Its down-regulation on cpTi could conceivably reduce cellular contractility and promote fibroblasts to organize a less dense fibrillar matrix of fibronectin. This, in turn, may result in the observed decrease in the strength of cell adhesion to titanium relative to tissue culture polystyrene. These findings are in line with the results presented in section 3.3., where we demonstrated that fibroblasts adhere less strongly to cpTi than to TPS surfaces. We propose that the assembly of a less dense fibrillar matrix of

fibronectin by fibroblasts cultured on cpTi may be a consequence of a reduction in the cytoskeletal stiffness caused by a reduction in myosin heavy chain type A. It remains to be seen if a difference in the adsorbed biofilm alone can explain the observed down regulation of myosin heavy chain in cells grown on cpTi.

There is evidence that SAM promotes adhesion in fibroblasts (Murray and Culp, 1980). This is suggested to be the result of the high concentration of adsorbed serum proteins, heparan sulfate proteoglycans and fibronectin in SAM (Lark and Culp 1984; Culp et al., 1978). The cellular content of SAM is a network of focal contact and close contact material rigidly coupled to the substrate (Lattera, Silbert and Culp 1983; Hsieh and Chen, 1983; Neideritter et al., 1990). Stress fibres containing filamentous actin and myosin II interact with the extracellular matrix at focal adhesions (Burridge, 1996). On adhesive substrata, stress fibres provide the contractile strength that is necessary to facilitate cell movement within a rigid matrix (Burridge, 1996). Clustering of integrins into focal adhesions and focal complexes is required for the assembly of filopodia, lamellipodia and stress fibres. There is a close relationship between the organization of the ECM and the actin cytoskeleton. For example, the formation of focal adhesions occur at high density of RGD peptides while at very low density cells attach but do not spread (Massia and Hubble, 1991). Clustering may occur when integrins bind to high density fibronectin matrix and/or by the tensile force exerted through the actinomyosin complex . Since the fibronectin in SAM is formed by living cells, it is both stretched and contracted in a manner that more new binding sites may be exposed, thus increasing the accessibility of RGD peptides (Krammer et al., 1999). In fact, it was demonstrated that cellular contractility exposes a cryptic binding site in fibronectin (Zhong et al., 1998). The

fibrillar fibronectin in SAM may be more inductive to receptor clustering and formation of stress fibres.

In the present study, we demonstrated that coating of titanium with SAM enhances the expression of myosin heavy chain type A. Myosin may positively contribute to the tension transmitted to the cell membrane by actin filaments and thus increase cellular stiffness. A higher expression of NMMHC-A was also observed in fibroblasts grown on tissue culture polystyrene. Interestingly, fibroblasts on TPS and SAM-coated cpTi were more resistant to detachment than those uncoated cpTi. This raises a question: Do highly adhesive substrates upregulate expression of myosin heavy chain type A?

Synthesis of both isoforms of myosin II (IIA and IIB) appear to be inversely affected by SAM-coating. A similar finding was reported by Kawamoto and Adelstein (1991) who found that stimulation of fibroblasts with serum resulted in an increase in the myosin IIA mRNA expression whereas the level of mRNA for myosin IIB was proportionately declined. Both values approached a similar level at a later stage of incubation. The isoforms of myosin II also show a spatial specificity within the bovine aortic endothelial cells (Kolega, 1998). Both isoforms distribute along stress fibres within lamellipodia and around the nucleus (Kolega, 1998). The A isoform appears more rapidly in the newly formed cellular structures, in particular in the leading edges, and is also lost more rapidly when the structures are disassembled. The B isoform appears later and is mostly found around the nucleus and the trailing edges.

In migrating fibroblasts, myosin II localises preferentially at the posterior region of the cell and serves to release adhesions at this end by exerting a contractile force. The observed increase in myosin IIA synthesis on SAM-coated discs and tissue culture plastic

may be the result of the enhanced adhesiveness of these surfaces over the cpTi. Another explanation for the upregulation of myosin heavy chain type A may be that fibroblasts form more new adhesive structures on SAM-coated cpTi than on cpTi alone.

4.9. Expression of other major proteins was not affected by the substrata

We found no evidence to implicate a change in the expression of other abundant proteins detected in the 2D SDS-PAGE gels, however, it is possible that changes in the synthesis of less prominent proteins were undetected. In a larger 2D gel system, it is possible to obtain a better resolution of the protein spots in both dimensions. A larger gel also makes it possible to load more of the sample in the first dimension. Another method to improve the resolution of the gels is by using immobilized pH gradient gels in the first dimension (Berkelman and Stenstedt, 1998). Nevertheless, we were able to produce 2D gels of high standard with excellent reproducibility.

Since composition and topography of the substrate is known to influence cytoskeletal organization (Oakley, Jaeger and Brunette, 1997) we were surprised to find no evidence of change in the expression of the major cytoskeletal proteins such as vinculin, vimentin, tubulin or actin. However, a change in the expression of these major housekeeping proteins may not be required since a change in their structural organisation may be adequate to elicit a response to a particular substrate topography. For example, formation of focal adhesions and the accumulation of vinculin at these sites are known to be the hallmark of stable cell adhesion to a substrate (Burridge and Chrzanowska-Wodnicka, 1988). Despite a stronger attachment of fibroblasts to SAM coated cpTi, we found no evidence of an increase in the expression of vinculin in fibroblasts grown on

this substrate. However, other cell-matrix contacts, such as close contacts, are abundantly present in fibroblasts and they may be more numerous than focal adhesion sites (Singer et al., 1988). Close contacts follow the pattern of the fibrillar fibronectin. Immunohistological studies may help visualise the distribution of cell-matrix contacts and myosin in cells grown on SAM coated cpTi.

Our results imply that a subtle change in the production of a contractile protein (NMMHC-A) may be adequate to influence behavior of fibroblasts in culture.

4.10. Proteomic map of human skin fibroblasts

One of the major goals of our investigations is to map substrate specific proteomic response of fibroblasts. We believe that this is a novel approach to studying biocompatibility. It provides a global view of the changes that may occur when cells come in contact with various biomaterials. A 2D database is required to provide the names and positions of the hundreds of proteins detectable by two-dimensional electrophoresis. Such a database could potentially be useful in prescreening for compatibility of various materials or surface treatments. Furthermore, this may help to understand and unravel the biochemical basis of biocompatibility.

A database of biocompatibility must identify the major cellular and extracellular proteins. To this end, we have taken the first steps in establishing such a database for human skin fibroblasts grown on titanium and tissue culture polystyrene.

4.11. Conclusion

The purpose of the present study was to gain a better understanding of the adhesion of dermal fibroblasts to titanium and to ultimately develop a method to improve the attachment of these cells to titanium implants. To this end we have shown that:

1) Skin fibroblasts attach less strongly to cpTi than to TPS. In support of this observation, we provided physical, morphological and biochemical evidence of the intact extracellular matrix on each substrate and on the remaining interface after detaching the cells from each surface. From these results we hypothesized a possible role for cytoskeleton in determining the material property of the fibroblast-substrate interface.

2) Upregulation of myosin heavy chain type A and fibronectin on the more adhesive TPS substrate is in line with our finding that the fibronectin matrix is more tightly packed on the tissue culture treated polystyrene surface. This also provides further evidence that fibroblasts may require higher contractility to organize and rearrange this sticky extracellular matrix. We suggested that the adsorbed serum proteins on each substrate influence the rigidity of the extracellular matrix.

3) Despite the nonselectivity of protein adsorption onto cpTi and TPS, considerably more protein adsorbs to titanium. We proposed that the difference in the quantity of the adsorbed proteins and the thickness of this biofilm might render the surface of titanium less adhesive to fibroblasts. However, it is also possible that cell adhesion on cpTi or TPS may be influenced by the concentration of one or more potent component(s) of this biofilm.

4) Coating with SAM enhances the adhesion of fibroblasts to titanium. Substrate-attached material contains many membrane, cytoskeletal, extracellular matrix and serum

components. One or more component of SAM may be responsible for this effect. The fibrillar fibronectin formed by living cells may be suggested as a strong candidate for this property of SAM.

5) Biocompatibility is a multifaceted phenomenon. It is the combined effect of surface property, protein adsorption, and cell adhesion and protein synthesis that produce an overall biological response to a foreign material. A global approach to study biocompatibility may be essential in unraveling the relations between these factors. We believe that the most important contribution of the present study is to introduce the potential for such an approach to future investigations.

4.12. Future directions

4.12.1. Proteomic mapping of biocompatibility

Current trends in developing new dental and craniofacial implant systems are directed towards improvement of host tissue responses by modifying the properties of presently available or the use of new materials. This will require the continued acquisition of knowledge of cell behavior and cell response to a growing number of "biomaterials" that will be available commercially.

The ultimate test of biocompatibility of an implant material is a long-term clinical trial. Regrettably, it is become common practice to commercially launch modified copies of clinically successful implant systems prior to proper *in vivo* assessments. Since *in vitro* models are convenient and inexpensive, many investigations have relied on their use to rationalize the application of a particular implant material or a modality of surface treatment. Presently there are no global identification markers for biocompatibility *in*

vitro other than attachment, spreading and growth of cells. Proteins coordinate most of the cell functions including cellular responses to various substrates. It is therefore of importance to identify possible changes in the composition of the total protein pool when cells encounter various implants and these may reveal the common links to molecular biocompatibility. Thanks to the many advances in proteome analysis, it is now possible to simultaneously study complex patterns of protein expression comprising of thousands of proteins. This will greatly facilitate the investigation of biocompatibility at the molecular level.

To this end, 2D-SDS-PAGE databases of different cell types such as fibroblasts, osteoblasts, keratinocytes, etc. grown on a specific implant material may be used to compare proteomic responses of various cells to a single biomaterial. Similarly, databases could be established to analyze the change(s) in composition of proteins of a particular cell line grown on different implant materials. This is in line with our present study but it is possible to extend the scope of these studies to include the effects of surface-topography and chemistry on the expression of cellular proteins on titanium. More specifically, we are interested in the proteomic changes that occur as the result of alterations in cell shape and morphology on various grooved substrates. The most apparent influence of surface topography on cell behavior is changes that occur in the form and orientation of cells, which are mainly regulated by cytoskeletal structures. For example, convexity or concavity of cell sized grooves may influence the production of compression resistant or tension resistant components of cytoskeleton such as microtubules or microfilaments respectively.

4.12.2. Adsorption of serum proteins and biocompatibility

Another aspect of biocompatibility that requires more attention is the nature and composition of the adsorbed biofilm. The results of the present study showed a dramatic difference in the amount of adsorbed serum proteins to titanium and tissue culture plastic. To explain this observation we must devise experiments that will determine the effect of various surface characteristics such as surface-roughness and surface-tension on the adsorption of serum proteins. An interesting question is whether there is a relationship between surface roughness and quantity of adsorption of serum proteins. It is conceivable that more proteins adsorb to rough surfaces due the presence of micropockets filled with adsorbed proteins. The thickness of the adsorbed biolayer may be important in how cells organize the extracellular matrix. On a thicker adsorbed biolayer it may be easier to reorganize the fibronectin matrix by webbing and dewebbing. The concentration of bioactive proteins, such as fetuin (a dephosphorylated form of bone sialic acid containing protein) in the adsorbed protein layer may also play a role in the specific biological response to a particular material.

4.12.3. Fibrillar fibronectin and cell adhesion to titanium

The results of the present study raised some questions regarding the role of fibronectin in adhesion of fibroblasts to titanium and tissue culture treated polystyrene. Immunoflourescent labeling suggests that the organization of fibronectin matrix by fibroblasts differ on the two substrates. We propose that the variation in the structure of fibronectin matrix may be the result of the difference in surface roughness.

Fibronectin in tissues forms disulphide crosslinked fibrils. A fragment from the first type-III repeat of fibronectin binds to fibronectin and induces spontaneous disulphide crosslinking. Treatment of soluble fibronectin with this inducing fragment converts the monomeric fibronectin into fibrillar structures which resemble and behave much like cellular fibronectin matrix (Morla et al., 1994). This in vitro-derived, commercially available polymerized form of fibronectin (superfibronectin) is highly adhesive to fibroblasts and has been shown to suppress cell migration (Morla et al., 1994). Immunofluorescent labeling and confocal microscopy of superfibronectin on different surface topographies may provide information on the influence of surface topography and patterning in the initial stage of organization of fibronectin. Furthermore, it would be interesting to study the rate of cell migration on titanium coated with superfibronectin.

The serum-adsorbed layer may also be important in how fibroblasts reorganize the fibrillar web of fibronectin. Serum-treated and non-treated titanium may be coated with FITC conjugated superfibronectin and fibroblasts may be added to study the webbing and dewebbing process at various time intervals.

4.12.4. In vivo study of titanium coated with substrate-attached material and superfibronectin

Miniature titanium implants and abutments have been used in rats to study the peri-implant soft tissues around percutaneous devices (Chehroudi, Gould and Brunette, 1989). This rat model can be used to study the attachment of the dermis to abutments that are coated with substrate-attached material or superfibronectin. An improved attachment of the dermis to the abutment may inhibit the downward migration of epithelial cells.

What distinguishes this proposed study from the other investigations on the effect of fibronectin in cell adhesion to implants is the influence of <u>fibrillar</u> and <u>non-soluble</u> form of fibronectin present in SAM and in superfibronectin. Furthermore, the fibrillar fibronectin provides the cells with a natural patterning and RGD spacing of the cell-binding sites. This may be important to elicit the proper outside-in signaling for the formation of stress fibers and focal adhesions.

4.12.5. Morphological study of myosin heavy chain type A and B in fibroblasts grown on various substrates

In the present study, the result of two dimensional electrophoresis and peptide mapping suggest that myosin heavy chain plays a role in the response of fibroblasts to their substrate. Immunofluorescence labeling of this molecule in cells grown on various substrates should further aid to confirm these findings. We expect that the expression of myosin heavy chain type A is upregulated on more adhesive substrates. Since surface topography is known to affect the shape and orientation of cells, we believe it may also modulate the expression of myosin heavy chain in fibroblasts.

REFERENCES

Adell R, Eriksson B, Lekholm U, Branemark PI, Jemt T. A long-term follow-up study of osseointegrated implants in the treatment of totally edentulous jaw. Int J Oral Maxillofac Implants 1990;5:347-59.

Adell R, Lekholm U, Rockler B, Brånemark P-I. A 15 year study of osseointegrated implants in the treatment of the edentulous jaw. Int J Oral Surg, 1981:10:387-416.

Albrektsson T, Brånemark PI, Hamsson HA, Ivarsson B, Jönsson U. Ultrastructural analysis of the interface zone of titanium and gold implants. In: Clinical application of biomaterials, Lee AJC (editor). John Wiley & Sons, New York, 1982, p.167.

Altankov G, Grinnell F, Groth T. Studies on the biocompatibility of materials: fibroblast reorganization of substratum-bound fibronectin on surfaces varying in wettability. J Biomed Mater Res 1996; 30: 385-3991.

Altankov G, Groth TH. Reorganization of substratum-bound fibronectin on hydrophilic and hydrophobic materials is related to biocompatibility. J Mater Sci: Mater Med 1994;5:732-737.

Baier RE, Dutton RC. Initial events in interaction of blood with foreign surfaces. J Biomed Mater Res 1969; 3: 191-193.

Baier RE, Meyer AE. Future directions in surface preparation of dental implants. J Dent Educ 1988; 52 : 788-791.

Ben-Ze'ev A, Robinson GS, Bucher NL, Farmer SR. Cell-cell and cell-matrix interactions differentially regulate the expression of hepatic and cytoskeletal genes in primary cultures of rat hepatocytes. Proc Nat Acad Sci USA. 1988; 85: 2161-2165.

Berkelman T, Stenstedt T. 2-D electrophoresis using immobilized pH gradients principles and methods. Amersham Pharmacia Biotech Inc., Piscataway, NJ, USA, 1998.

Bonding P, Ahlgren P, Dige-Petersen H. Permanent, skin penetrating, bone-anchored titanium implants. A clinical study of host-reaction in bone and soft tissue. Acta Otolaryngol (Stockh) 1992;112:455-461.

Botha SJ. Physical, mechanical, chemical, biological and optimal surface characteristics for bio-acceptability. J Dent Assoc S Afr 1997; 52: 273-282.

Brown WM, Saunders NR, Møllgård K, Dziegiewska KM. Fetuin - an old friend revisted. Bioessays 1992;11:749 - 755.

Brånemark PI, Albrektsson T. Titanium implants permanently penetrating human skin. Scand J Plast Reconstr Surg 1982;16:17-21.

Brånemark P-I, Hansson BO, Adell R, Breine U, Lindström J, Hallen O, Öhman A. Osseointegrated implants in the treatment of the edentulous jaw. Experience from a 10-year period. Scand J PlastReconstr Surg 1977; 16: 1-132.

Britch M, Allen TD. The modulation of cellular contractility and adhesion by trypsin and EGTA. Exp Cell Res. 1980; 125: 221-31.

Britland S, Clark P, Connolly P, Moores GR. Micropatterned substratum adhesiveness: A model for morphogenetic cues controlling cell behaviour. Exp Cell Res 1992; 198: 124-129.

Brunette DM. The effects of implant surface topography on the behavior of cells. The Int J Oral Maxillofac Implants 1988; 3: 231-246.

Brunette DM, Chehroudi B. the effects of the surface topography of micromachined titanium substrata on cell behavior in vitro and in vivo. J Biomech Eng 1999:121:49-57.

Brunette DM, Kenner G S, Gould TRL. Titanium surface orient growth and migration of cells from human gingival explants. J Dent Res 1983; 62: 1045-1048.

Bundy KJ, Roberts OC, O'Connor, McLeod V, Rahn B. Quantification of fibroblast adhesion to biomaterials using a fluid mechanics approach. J Mater Sci Mater Med 1994; 5: 500-502.

Burridge K. Crosstalk between Rac and Rho [comment]. Science 1999; 283: 2028-2029.

Burridge K, Nuckolls G, Otey C, Pavalko F, Simon K, Turner C. Actin-membrane interaction in focal adhesions. Cell Diff Dev 1990; 32: 337-342.

Burridge K, Chrzanowska-Wodnicka M. Focal adhesions, contractility, and signaling. Annu Rev Cell Dev Biol 1996; 12: 463-519.

Burridge K, Turner CE, Romer LH. Tyrosine phosphorylation of paxillin and pp125[FAK] accompanies cell adhesion to extracellular matrix: a role in cytoskeletal assembly. J Cell Biol 1992; 119: 893-903.

Carsson L, Röslund T, Albreksson B, Albreksson T. Implant fixation improved by close fit: cylindrical implant-bone interface studied in rabbits. Acta Orthop 1988; 272.

Cathcart MK, Culp LA. Phospholipid composition of substrate adhesion sites of normal, virus-transformed, and revertant murine cells. Biochemistry 1979; 18: 1167-1176.

Celis JE, Østergaard M, Jensen NA, Gromova. Human and mouse proteomic databases: novel resources in the protein universe. FEBS Letts 1998; 430: 64-72.

Celis JE. Cell biology a laboratory handbook (second edition). Academic Press 1997, volume 4, pp. 367-368.

Chehroudi B, Gould TRL, Brunette DM. The role of connective tissue in inhibiting epithelial downgrowth on titanium-coated percutaneous implants. J Biomed Mater Res 1992;26:493-515.

Chehroudi, B. and Brunette, D.M. Effects of surface topography on cell behavior. In Encyclopedic Handbook of Biomaterials and Bioengineering, ed. D. L. Wise, D. J. Trantolo, D. E. Altobelli, M. J. Yaszemski, J.D. Gresser and E. R. Schwartz. Part S. Materials. 1991, New York, pp. 813-842.

Choquet D, Felsenfeld DP, Sheetz MP. Extracellular matrix rigidity causes strengthening of integrin-cytoskeleton linkages. Cell 1997;88:39-48.

Chou L, Firth JD, Uitto VJ, Brunette DM. Effects of titanium substratum and grooved surface topography on metalloproteinase-2 expression in human fibroblasts. J Biomed Mater Res 1998;39:437-45.

Chou L, Firth JD, Uitto VJ, Brunette DM. Substratum surface topography alters cell shape and regulates fibronectin mRNA level, mRNA stability, secretion and assembly in human fibroblasts. J Cell Sci 1995; 108: 1563-1573.

Chun JS, Jacobson BS. Spreading of HeLa cells on a collagen substratu requires a second messenger formed by lipoxygenase metabolism of arachidonic acid released by collagen receptor clustering. Mol Biol Cell 1992; 3: 481-492.

Clark EA, Brugge JS. Integrins and signal transduction pathways: the road taken. Science 1995; 268: 233-239.

Clark P, Connolly P, Curtis ASG, Dow JAT, Wilkinson CDW. Cell guidance by ultrafine topography in vitro J Cell Sci 1991; 99: 73-77.

Clark P, Connolly P, Curtis ASG, Dow JAT, Wilkinson CDW. Topographical control of cell behaviour. I. Simple step cues. Development, 1987; 99: 439-448.

Clark P, Connolly P, Curtis ASG, Dow JAT, Wilkinson CDW. Topographical control of cell behaviour II. Multiple grooved substrata. Development 1990; 108: 635-644.

Clark P, Connolly P, Moores GR. Cell guidance by micropatterned adhesiveness in vitro. J Cell Sci 1992; 103: 287-292.

Cramer LP, Mitchison TJ. Myosin is involved in postmitotic cell spreading. J Cell Biol 1995;131(1):179-89.

Culp LA. Substrate-attached glycoproteins mediating adhesion of normal and virus-transformed mouse fibroblasts. J Cell Biol 1974; 63: 71-83.

Culp LA, Murray BA., Rollins BJ. Fibronectin and proteoglycans as determinants of cell-substratum adhesion. J Supramol Struct. 1979; 11: 401-427.

Culp LA, Rollins BJ, Buniel J, Hitri S. Two functionally distinct pools of glycosaminoglycan in the substrate adhesion site of murine cells. J Cell Biol 1978;79:788-801.

Curtis A, Wilkinson C. Topographical control of cells. Biomaterials 1997; 18: 1573-1583.

Dai Y. Whittal RM. Bridges CA. Isogai Y. Hindsgaul O. Li. Matrix-assisted laser desorption ionization mass spectrometry for the analysis of monosulfated oligosaccharides. Carbohydr Res 1990;304(1):1-9.

Davies JE, Lowenberg B, Shiga A. The bone-titanium interface *in vitro*. J Biomed Mat Res 1990; 24: 1289-1306.

Davies JE, Ottensmyer P, Shen X, Hashimoto M, Peel SAF. Early extracellular matrix synthesis. In: The bone –biomaterial interface, Davies JE (editor). University of Toronto Press, Toronto, Canada, 1992, pp. 214-228.

Dawes KE, Gray AJ, Laurent GJ. Thrombin stimulates fibroblast chemotaxis and replication. Eur J Cell Biol 1990;61:126-130.

De Bruijan JD, Flach FS, De Groot K, Van Blitterswijk CA, Davies JE. Analysis of the bony interface with various types of hydroxyapatite in vitro. Cells Mater 1993; 3: 115-127.

Defillipi, P, Bozzo C, Volpe G, Romano G, Venturino M, et al. Integrin-mediated signal transduction in human endothelial cells: analysis of protein phosphorylation events. Cell Adhes Commun 1994; 2: 75-86.

Degasne I, Basle MF, Demais V, Hure G, Lesourd M, Grolleau B, Mercier L, Chappard D. Effects of roughness, fibronectin and vitronectin on attachment, spreading, and proliferation of human osteoblast-like cells (Saos-2) on titanium surfaces. Calc Tiss Int 1999; 64:499-507.

Demetriou M, Binkert C, Sukhu B, Tenebaum HC. Fetuin/α2-HS glycoprotein is a transforming growth factor-β type II receptor mimic and cytokine antagonist. J Biol Chem 1996;271:2755-1276.

den Braber ET, Jansen HV, de Boer MJ, Croes HJ, Elwenspoek M, Ginsel LA, Jansen JA. Scanning electron microscopic, transmission electron microscopic and confocal laser scanning microscopic observation of fibroblasts cultured on microgrooved surfaces of bulk titanium substrata. J Biomed Mater Res 1998;40:425-33.

Dimilla P, Barbee K, Lauffenburger D. Mathematical model for the effects of adhesion and mechanics on cell migration speed. Biophys J 1991;60:15-37.

Dimilla PA, Stone JA, Quinn JA, Albelda SM, Luffenburger DA. Maximal migration of human smooth muscle cells on fibronectin and type IV collagen occurs at an intermediate attachment strength. J Cell Biol 1993; 122: 729-737.

Donely TG, Gillette WB. Titanium endosseous implant-soft tissue interface: A literature review. J Periodontol 1991;62:153-160.

Doolittle KW, Reddy I, McNally JG. 3D analysis of cell movement during normal and myosin-II-null cell morphogenesis in dictyostelium. Dev Biol (Orlando)1995;167(1):118-29.

D'Souza SE, Haas TA, Piotrowicz RS, Byers-Ward V, McGrath DE, Soule HR, Cierniewski C, Plow EF, Smith JW. Ligand and cation binding are dual functions of a

discrete segment of the integrin beta 3 subunit: cation displacement is involved. Cell 79(4):659-67, 1994.

Duband J, Dufour S, Yamada S, Yamada K. Neural crest cell migration induced by antibodies to beta-1 integrins. A tool for studying the roles of substratum molecular avidity and density in migration. J Cell Sci 1991;98:517-532.

Dunn MJ. Quantitative two-dimensional gel electrophoresis: from proteins to proteomes. Biochem Soc Trans 1997; 25: 248-254.

Edwards JG, Hameed H, Campbell G. Induction of fibroblast spreading by Mn2+: a possible role for unusual binding sites for divalent cations in receptors for proteins containing Arg-Gly-Asp. J Cell Sci 1988; 89: 507-13.

Ellingsen JE. A study on the mechanism of protein adsorption to TiO2. Biomaterials 1991; 12: 593-596.

Evans E, Berk D, Leung A. Detachment of agglutinin-bonded red cells: Forces to rupture molecular point attachments. Biophys J 1991;59: 838-848.

Felsenfeld DP, Choquet D, Sheetz MP. Ligand binding regulates the directed movement of β1 integrins on fibroblasts. Nature 1996;383:438-440.

Feneselau C. MALDI MS and strategies for protein analysis. Analyt Chem 1997; 69: 661A-665A.

Fukui Y, De Lozanne A, Spudich JA. Structure and function of the cytoskeleton of a Dictyostelium myosin-defective mutant. J Cell Biol 1990;110(2):367-78.

Garcia JG, Verin AD, Schaphorst K. Regulation of endothelial cell myosin light chain kinase by Rho, cortactin, and p60 (src). Am J Physiol 1999; 276: L989-998.

Garvey B, Bizios R. A method for transmission electron microscopy examination of the osteoblast/hydroxyapatite interface. J Appl Biomater 1994; 5: 39-45.

Gersten DM, Hearing VJ. Albuminoid molecules: a novel variability generating cell-surface receptor system. Med Hypoth 1989;30:135-40.

Gibbs J. Immobilization principles-selecting the surface. In: ELISA techniques bulletin No.1, Corning Incorporation, 1995, pp. 1-11.

Ginsberg MH, Du X, Plow EF. Inside-out integrin signalling. Curr Opin Cell Biol 1992; 4: 766-771.

Goodman S, Risse G, von der Mark K. The E8 subfragment of laminin promotes locomotion of myofibroblasts over extracellular matrix. J Cell Biol 1991;109:799-809.

Gould TRL, Brunette DM, Westburg L. The attachment mechanisms of epithelial cell attachment to implant surfaces in vitro. Int J Periodontics Restorative Dent 1990;10:68-79.

Grinnell F, Feld M. Fibronectin adsorption on hydrophilic and hydrophobic surfaces detected by antibody binding and analysed during cell adhesion in serum-containing medium. J Biol Chem 1982;257:4888-4893.

Grinnell F. Cellular adhesiveness and extracellular substrata. Int Rev Cytol 1978;53: 65-44.

Grossner-Schreiber B, Tuan RS. The influence of the titanium implant surface on the process of osseointegration. Dtsch Zahnarliche Zeitschrift 1991;46:691-3.

Gumbiner BM. Cell Adhesion: The molecular basis of tissue architecture and morphogenesis. Cell 1996; 84: 345–357.

Hagert CG, Branemark P-I, Albrektsson T, Strid KG, Irstam L. Metacarpophalangeal joint replacement with osseintegrated endoprostheses. Scand J Plast Reconstr Surg 1986;20:207-218.

Hakansson B, Liden G, Tjellstrom A. Ten years of experience with the swedish bone-anchored hearing system. Ann Otol Rhinol Laryngol 1990;99 (suppl 151):1-16.

Hall A. Small GTP-binding proteins and the regulation of actin cytoskeleton. Annu Rev Cell Biol 1994; 10: 31-54.

Halliday N, Tomasek J: Mechanical properties of the extracellular matrix influence fibrobectin assembly in vitro. Exp Cell Res 1995;217:107-117.

Hay ED. Interaction of migrating embryonic cells with extracellular matrix. Exp Biol Med 1985; 10: 174-193.

Hench LL. Bioceramics and the origin of life. J Biomed Mat Res 1989; 23: 685-703.

Hobo S, Ichida E, Garcia LT. Osseointegration and Occlusal Rehabilitation, Quintessence, Chicago, 1989, pp. 3-104.

Hochstrasser DF. Harrington MG. Hochstrasser AC. Miller MJ. Merril CR.Methods for increasing the resolution of two-dimensional protein electrophoresis. Analyt Biochem 1988;173(2):424-35.

Holgers KM. Soft tissue reaction around clinical skin-peneterating titanium implants (Ph.D. Thesis), University of Göteborg, Sweden, 1994.

Holgers KM, Tjellström A, Bjursten LM, Erlandsson BE. Soft tissue reactions around percutaneous implants: a clinical study on skin-penerating titanium implants used for bone –anchored auricular prostheses. Int J Oral Maxillofac Imp 1987;2:35-39.

Holgers KM, Tjellström A, Bjusten LM, Erlandsson BE. Soft tissue reactions around percutaneous implants: a clinical study of soft tissue conditions around skin-peneterating titanium implants for bone-anchored hearing aids. Am J Otol 1988;9:56-59.

Hong J, Andersson J, Ekdahl KN, Elgue G, Axen N, Larsson R, Nilsson B. Titanium is a highly thrombogenic biomaterial: possible implications for osteogenesis. Thromb Haemost 1999;82:58-64.

Hoogland C, Sanchez JC, Tonella L, Bairoch A. The SWISS-2D PAGE database: what has changed during the last year. Nucleic Acids Res 1999; 27: 289-291.

Hotchin NA, HallA. The assembly of integrin adhesion complexes requires both extracellular matrix and intracellular rho/rac GTPases. J Cell Biol 1995; 131: 1857-1865.

Hsieh P, Chen LB. Behavior of cells seeded in isolated fibronectin matrices. J Cell Biol 1983;96:1208-17.

Hubbe MA. Adhesion and detachment of biological cells *in vitro*. Prog Surf Sci 1981; 11: 65-138.

Hunter A, Archer CW, Walker PS, Blunn GW. Attachment and proliferation of osteoblasts and fibroblasts on biomaterials for orthopaedic use. Biomaterials 1995; 16:287-95.

Huttenlocker A, Sandborg RR, Horwitz AF. Adhesion in cell migration. Curr Opin Cell Biol 1995; 7: 697-706.

Imamoto GK, Winterton LC, Stoker RS, Van Wagner RA, Andradem JD, Moser DF. Fibronectin adsorption detected by interfacial fluorescence. J Colloid Interface Sci 1985;106:459-464.

Ingber DE. Cellular tensegrity: defining new rules of biological design that govern the cytoskeleton. J Cell Sci 1993; 104: 613-627.

James RA. The support system and pregingival defense mechanism of oral implants. J Oral Implantol 1976;6:270-279.

Jansen JA, den Braber ET, Walboomers XF, De Ruijter JE. Soft tissue and epithelial models. Adv Dent Res 13:57-66, 1999.

Jay PY, Pham PA, Wong SA, Elson EL. A mechanical function of myosin II in cell motility. J Cell Sci 1995; 108: 387-393.

Jimenez CR, Huang L, Qiu Y, Burlingame AL. Searching sequence databases over the internet: protein identification using MS-Fit. Current protocols in protein science, John Wiley & Sons Inc., 1998: (Supplement 14), pp. 16.5.1-16.5.6.

Jones BM. A unifying hypothesis of cell adhesion. Nature 1966; 212: 362-365.

Jungblut P, Thiede B. Protein identification from 2-DE gels by MALDI mass spectrometry. Mass Spectrometry Rev 1997; 16: 145-162.

Kanagaraja S, Lundstrom I, Nygren H, Tengvall P. Platelet binding and protein adsorption to titanium and gold after short time exposure to heparinized plasma and whole blood. Biomaterials 1996;17:2225-2232.

Kasemo B. Biocompatibility of titanium implants: surface science aspects. J Prosthet Dent 1983; 49: 832-837.

Kasemo B, Lausmaa J. The biomaterial-tissue interface and its analogues in surface science and technology. In: Davies, JE (editor), The bone-biomaterial interface. Part I: the material surface. Toronto University Press, 1991, pp. 19-32.

Kawamoto S., Adelstein RS. Chicken nonmuscle myosin heavy chains: differential expression of two mRNAs and evidence for two different polypeptides. J Cell Biol 1991;112:915-24.

Keller JC, Dougherty WMJ, Grotendorst GR, Wightman GP. In vitro cell attachment to characterized cp titanium surfaces. J Adhesion 1989; 28: 115-133.

Klinger MM, Rahemutulla F, Prince CW, Lucas LC, Lemons JE. Proteoglycans at the bone-implant interface. Crit Rev Oral Biol Med 1998; 9: 449-463.

Kolega J. Cytoplasmic dynamics of myosin IIA and IIB: spatial 'sorting' of isoforms in locomoting cells. J Cell Sci 1998;111 (Pt 15):2085-95.

Koller MR, Papoutsakis ET. Cell adhesion in animal cell culture: physiological and fluid-mechanical implications. Bioproc Technol 1995;20:61-110.

Kononen M, Hormia M, Kivilahti J, Hautaniemi J, Thesleff I. Effect of surface processing on the attachment, orientation, and proliferation of human gingival fibroblasts on titanium. J Biomed Mat Res 1992;26:1325-41, 1992.

Kornberg LJ, Earp Hs, Turner CE, Prockop C, Juliano RL. Signal transduction by integrins: increased protein tyrosine phosphorylation caused by clustering of beta 1 integrins. Proc Natl Acad Sci USA 1991; 88: 8392-8396.

Krammer A, Lu H, Isralewitz B, Schulten K, Vogel V: Forced unfolding of the fibronectin type III module reveals a tensile molecular recognition switch. Proc Natl Acad Sci USA 1999:96;1351-1356.

Laemmli U.K.Cleavage of structural proteins during the assembly of the head of bacteriophage T4. Nature 1970;227(259):680-5.

Landegren U. Measurement of cell numbers by means of endogenous enzyme hexosaminidase: Applications to detection of lymphokines and cell surface antigens. J Immunol Methods 1984;67:379-385.

Lark MW, Culp LA. Modification of proteoglycans during maturation of fibroblast substratum adhesion sites. Biochemistry 1983; 22: 2289-2296.

Lark MW, Culp LA. Multiple classes of heparan sulfate proteoglycans from fibroblast substratum adhesion sites. Affinity fractionation on columns of platelet factor 4, plasma fibronectin, and octyl-sepharose. J Biol Chem 1984;259:6773-82.

Laterra J, Silbert JE, Culp LA. Cell surface heparan sulfate mediates some adhesive responses to glycosaminoglycan-binding matrices, including fibronectin. J Cell Biol 1983;96:112-23.

Lauffenburger, DA, Horwitz, AF. Cell migration: A physically integrated molecular process. Cell 1996; 84: 359-369.

Lincks J, Boyan BD, Blanchard CR, Lohmann CH, Liu Y, Cochran DL, Dean DD, Schwartz Z. Response of MG63 osteoblast-like cells to titanium and titanium alloy is dependent on surface roughness and composition. Biomaterials 1998;19:2219-32.

Liu F, Zhou M, Zhang F. ^{125}I labelling of human serum albumin and fibrinogen and a study of protein adsorption properties on the surface of titanium oxide. Appl Rad Isotopes 1998; 49: 67-72.

Lotz MM, Bursdal CA, Erickson HP, McClay DR. Cell adhesion to fibronectin and tenascin: Quantitative measurements of initial binding and subsequent strengthening response J Cell Biol 1989; 109: 179⋅5-1805.

Malawista SE, De Boisfleury Chevance A. The cytokineplast: purified, stable, and functional motile machinery from human blood polymorphonuclear leukocytes. J Cell Biol 1982; 95: 960-973.

Martin JY, Schwartz Z, Hummert TW, Schraub DM, Simpson J, Lankford J Jr, Dean DD, Cochran DL, Boyan BD. Effect of titanium surface roughness on proliferation, differentiation, and protein synthesis of human osteoblast-like cells (MG63). J Biomed Mat Res 1995; 29:389-401.

Massia Sp, Hubble JA. An RGD spacing of 440 nm is sufficient for integrin $\alpha_v\beta_3$-mediated fibroblast spreading and 140 nm for focal contact and stress fiber formation. J Cell Biol 1991; 114: 1089-1100.

Masuda Y, Yliheikkilä PK, Felton DA, Cooper LF. Generalizations regarding the process and phenomenon of osseointegration. Part I. In vivo studies. Int J Oral Maxillofac Implants 1998;13:17-29.

McAbee DD, Grinnell F. Binding and phagocytosis of fibronectin-coated beads by BHK cells: Receptor specificity and dynamics. J Cell Physiol 1985;124:240-246.

McKinney RV, Steflick DE, Koth DL, Singh B. The scientific basis for dental implant therapy. J Dent Educ 1988;52:696-705.

McKinney RV, Steflik DE, Koth DL. Evidence for junctional epithelial attachment to ceramic dental implants: A transmission electron microscopic study. J Periodontol 1985;56:579-591.

Meazzini MC, Toma CD, Schaffer JL, Gray ML, Gerstenfeld LC. Osteoblast cytosleletal modulation in response to mechanical strain *in vitro*. J Orthop Res 1998;16:170-180.

Microsoft Encarta Encyclopidia 99 (CD-ROM). Titanium. Microsoft Inc., 1998.

Miyamoto S, Akiyama SK, Yamada KM. Synergistic roles for receptor occupancy and aggregation in integrin transmembrane function . Science 1995; 267: 883-885.

Mizejewski GJ. α-Fetoprotein as a biological response modifier: relevance to domain and subdomain structure. Proc Soc Exp Biol Med 1997;25:353-362.

Molin O, Hedén CG. Large scale cultivation of human diploid cells on titanium discs in a special apparatus. Proceedings of the 10th Inernational Congress for Microbiological Standardization, Prague 1967. Progress in Immunobiological Standardization, vol 3. Regamey RH, Hennessen W, Ungar D. Karger, Basel/New York, 1967, pp.106-110.

Moriatory J, Fox S, Dmytryk J, Kusy R. Scaling of a titanium implant surface with metal and plastic instruments. J Dent Res 1990; 69: 370.

Morla A, Zhang Z, Ruoslahti E. Superfibronectin is a functionally distinct form of fibronectin. Nature 1994;367:193-6.

Murray BA. Ansbacher R. Culp LA. Adhesion sites of murine fibroblasts on cold insoluble globulin-adsorbed substrata. J Cell Physiol 1980;104:335-48.

Nagahara S, Matsuda T. Cell-substrate and cell-cell interactions differently regulate cytoskeletal and extracellular matrix protein gene expression. J Biomed Mat Res 1996;32:677-686.

NakanoT, Scott PG. Purification and characterization of a gelatinase produced by fibroblasts from human gingiva. Biochem Cell Biol 1986; 64:387-393.

Nanci A, McCarthy GF, Zalzal S, Clockie CML, Warshawsky H, McKee MD. issue response to titanium implants in the rat tibia: Ultrastructural, Immunoytochemical and lectin-cytochemical characterization of the bone-titanium interface. Cell Mater 1994;4: 1-30.

Neiderreiter M, Gimona M, Steichsbier F, Celis JE, Small JV. Complex protein composition of isolated focal adhesions: A two-dimensional gel and database analysis. Electrophoresis 1994;15:511-519.

Nie Z. Fetuin: its enigmatic property of growth promotion. Am J Physiol 1992;263 (Cell Physio.):C55-C562.

Nohutcu RM, McCauley LK, Koh AJ, Somerman MJ. Expression of extracellular matrix proteins in human periodontal ligament cells during mineralization in vitro. J Periodontol 1997;68:320-7.

Noth U, Hendrich C, Merklein F, Altvater T, Rader CP, Schutze N, Eulert J, Thull R. Standardized testing of bone implant surfaces with an osteoblast cell culture system. II. Titanium surfaces of different degrees of roughness. Biomed Tech 1991;44:6-11.

Nyfakh AA, Svitkina TM. Isolation of focal contact membrane using saponin. Exp Cell Res 1983; 149: 582-586.

Nygren H, Tengvall P, Lundstrom I. The initial reactions of TiO2 with blood. J Biomed Mater Res 1997; 34: 487-92.

O'Farrell PH. High resolution two-dimensional electrophoresis of proteins. J Biol Chem 1975; 250: 4007-4021.

Oakely C, Brunette DM. The sequence of alignment of microtubules, focal contacts and actin filaments in fibroblasts spreading on smooth and grooved titanium substrata. J Cell Sci 1993; 106: 343-354.

Oakley C, Jaeger NA, Brunette DM. Sensitivity of fibroblasts and their cytoskeletons to substratum topographies: topographic guidance and topographic compensation by micromachined grooves of different dimensions. Exp Cell Res 1997;234:413-24.

Oegema K, Mitchison TJ. Rappaport rules: cleavage furrow induction in animal cells. Proc Nat Acad Sci USA 1997;94(10):4817-20.

Ohnishi T, Nakamura O, Ozawa M, Arakaki N, Muramatsu T, Daikuhara, "Molecular cloning and sequence analysis of cDNA for a 59 kD bone sialoprotein of the rat: demonstration that it is a counterpart of human alpha 2-HS glycoprotein and bovine fetuin. J Bone Miner Res 1993;8:367-377.

Palecek, SP, Schmidt, CE, Lauffenburger, DA, Horwitz, AF. Integrin dynamics on the tail region of migrating fibroblasts. J Cell Sci 1996; 109: 941-952.

Parel SM, Branemark P-I, Tjellstrom A, Gion G. Osseointegration in maxillofacial prosthetics. Part II. Extraoral applications. J Prosthet Dent 1986;55:600-606.

Parsegian VA. Molecular forces governing tight contact between cellular surface and substrates. J Prosthet Dent 1983; 49: 838-842.

Pritchard DI, Morgan H, Cooper JM. Micro-scale patterning of biological molecules. Angew Gem 1995; 34: 91-93.

Regen, CM, Horwitz AF. Dynamics of B1 integrin-mediated adhesive contacts in motile fibroblasts. J Cell Biol 1992; 119: 1347-1359.

Revel JP, Wolken K. Electronmicroscope investigations of the underside of cells in culture. Exp Cell Res 1973; 78: 1-14.

Revel JP, Hoch P, Ho D. Adhesion of culture cells to their substratum. Exp Cell Res 1974; 84: 207-218.

Ridley AJ, Hall A. The small GTP-binding protein rho regultea the assembly of focal adhesions and actin stress fibers in response to growth factors. Cell 1992; 70: 389-399.

Rollins BJ, Culp LA. Glycosaminoglycans in the substrate adhesion sites of normal and virus-transformed murine cells. Biochemistry 1979; 18: 141-148.

Ruoslahti E, Öbrink B. Common principles in cell adhesion. Exp Cell Res 1996;227:1-11.

Sastry SK, Horwitz AF. Integrin cytoplasmic domains: mediators of cytoskeletal linkages and extra- and intracellular initiated transmembrane signaling. Curr Opin Cell Biol 1993; 5: 819–831.

Scarborough DE, Mason RG, Dalldorf FG, Brinkhous KM. Morphologic manifestation of blood-solid interfacial interactions. Lab Invest 1969; 20: 146.

Schaller MD, Otey CA, Hilderbrand JD, Parsons TJ. Focal adhesion kinase and paxillin bind to peptides mimicking beta integrin cytoplasmic domains. J Cell Biol 1995; 130: 1181-7.

Schevchenko A, Jensen ON, Podtelejnikov AV, Sagliocco F, Wilm M, Vorm O, Mortensen P, Shevchenko A, Boucherie H, Mann M. Proc Natl Acad Sci USA 1996; 93:14440.

Schevchenko A, Wilm M, Vorm O, Mann M. Mass spectrometric sequencing of proteins from silver-stained polyacrylamide gels. Analyt Chem 1996; 68: 850-858.

Schinke T, Amendt C, Trindl A, Pöscke O, Müller-Esterl W, Jahen-Dechent W. The serum protein α2-HS glycoprotein/fetuin inhibits apatite formation *in vitro* and in mineralizing calvaria cells. J Biol Chem 1996;271:20789-20796.

Schwartz MA, Schaller MD, Ginsberg MH. Integrins: emerging paradigms of signal transduction. Annu Rev Cell Dev Biol 1995 ; 11: 549-599.

Sevastianov VI. Interaction of protein adsorption and blood compatibility of biomaterials in High Performance biomaterials, Szcher, M., (editor). Technomic Publishing, Lancaster, PA, 1991.

Sharpe PT. Laboratory Techniques in Biochemistry and Molecular Biology: Methods of cell separation, Elsevier, Amsterdam, 1988, pp. 18-69.

Singer II, Scott S, Kawka DW, Kazazis DM, Gailit J, Ruoslahti E. Cell surface distribution of fibronectin and vitronectin receptors depends on substrate composition and extracellular matrix accumulation. J Cell Biol 1988;106:2171-82.

Standford CM, Keller JC. The concept of osseointegration and bone matrix expression. Crit Rev Oral Biol Med 1991;2:83-101.

Tengvall P, Lundström I. Physico-chemical consideratiions of titanium as a biomaterial. Clin Mater 1992;9:115-134.

Thode K, Luck M, Schroder W, Blunk T, Muller RH, Kresse M. The influence of the sample preparation on plasma protein adsorption patterns on polysaccharide-stabilized iron oxide particles. J Drug Target 1998; 5: 459-469.

Tilney GL. The role of actin in nonmuscle cell motility. Soc Gen Physiol Ser 1975;30:339-88.

Tjellstrom A, Yontchev E, Lindstom J, Branemark PI. Five years' experience with bone-anchored auricular prostheses. Otolaryngol Head Neck Surg 1985;93:366-72.

Turner CE, Burridge K. Transmembrane molecular assemblies in cell-extracellular matrix interactions. Curr Opin Cell Biol 1991; 3: 849-53.

Vesely P, Boyde A, Jones S. Behaviour of osteoclasts in vitro-contact behaviour of osteoclasts with osteoblast-like cells and networking of osteoclasts for 3D orientation. J Anat 1992; 181: 277-291.

Vessey AR, Culp LA. Contact-inhibited revertant cell lines isolated from SV40-transformed cells. VIII. Membrane protein and glycoprotein. Virology 1978; 86: 556-561.

Vroman L, Adams AL. Adsorption of proteins out of plasma and solutions in narrow spaces. J Colloid Interface Sci 1986;11:391-402.

Walivaara B, Askendal A, Lundstrom I, Tengvall P. Blood protein interactions with titanium surfaces. J Biomater Sci Polym Ed 1996; 8: 41-48.

Wang N, Butler J, Ingber D: Mechanotransduction across the cell surface and through the cytoskeleton. Science 1993:260:1124-1127.

Ward MD, Hammer DA. A theoretical analysis for the effect of focal contact formation on cell-substrate attachment strength. Biophys J 1993; 64: 936-959.

Wennerberg A, Albrektsson T, Andersson B. Design and surface characteristics of 13 commercially available oral implant systems. Int J Maxillofac Implants 1993:8:622-33.

Whittal RM, Li L. High-resolution matrix-assisted laser desorption/ionization in a linear time-of-flight mass spectrometer. Analyt Chem 1995;67(13):1950-4.

Wilson K, Goulding KH. Principles and Techniques of Biochemistry, third edition. Cambridge University Press, New York, 1992, pp. 45-79.

Williams DF. Titanium as a metal for implantation, part 1: physical properties. J Med Eng Tech 1977;1:195-203.

Wojciak-Stothard B, Curtis A, Monaghan W, Macdonald K, Wilkinson C. Guidance and activation of murine macrophages by nanometric scale topography. J Cell Res 1996:223: 426-435.

Zhong C, Chrzanowska-Wodnicka M, Brown J, Shaub A, Belkin AM, Burridge K. Rho-mediated contractility exposes a cryptic site in fibronectin and induces fibronectin matrix assembly. J Cell Biol 1998; 141: 539-551.

Zweymüller KA, Lintner FK, Semlitsch MF. Biologic fixation of a press-fit titanium hip joint endoprostheses. Clin Orthop 1988; 235: 195-206.